Geomorphometric regularities of the spatial distribution of colluvial deposits

Dissertation

in fulfilment of the requirements for the degree “Dr. rer. nat.”

of the Faculty of Mathematics and Natural Sciences

at the Christian-Albrechts-University of Kiel

Submitted by

Andrey V. Mitusov

Kiel, 2014

First referee:	Prof. Dr. Hans-Rudolf Bork
Second referee:	Prof. Dr. Johannes Müller
Date of oral examination:	February 17, 2015
Approved for publication:	December 12, 2014
Dean:	Prof. Dr. Wolfgang J. Duschl

I dedicate this work to my children:

Semjon and Liza

Content

Abstract	4
Zusammenfassung	5
1. Introduction	6
2. Key area locations	8
3. Methods	9
3.1. Digital elevation models	9
3.2. Morphometric variables	9
3.3. Landforms described by signs of curvatures	11
3.4. Determination of colluvial deposits	13
3.5. Indicator of the spatial variability of the colluvial accumulation rate (CAR)	13
3.6. Statistics	14
3.7. Determination of the potential role of main local landforms for the processes of soil erosion or colluvial accumulation	14
4. Results	14
4.1. Statistical properties of the indicator of the colluvial accumulation rate (CAR) and the thickness of colluvial deposits	14
4.2. Statistical relationships in the dataset	15
4.3. Distributions of the thickness of colluvial deposits and the indicator of the colluvial accumulation rate (CAR) on main local landforms	16
5. Discussion	18
5.1. Relationship of the thickness of colluvial deposits with the MCA	18
5.2. Relationship of the indicator of the colluvial accumulation rate (CAR) with the MCA	19
5.3. Relationship between the thickness of colluvial deposits and the indicator of the colluvial accumulation rate (CAR)	19
5.4. Spatial distribution of orographic attributes related with colluvial deposits	21
5.5. Geomorphometric quantitative descriptor of erosion and accumulation processes for terrains considered as one unit	23
5.6. Phases of transformation of the local landforms	24
6. Conclusions	6
6.1. The spatial antagonism between land surface portions with a maximal colluvial storage and a high colluvial accumulation rate (CAR)	26
6.2. Application of the occurrence frequency of main local landforms for the assessment of the erosion/accumulation status of a terrain	27
6.3. Phases of land surface transformation on the local level	27
Acknowledgements	28
References	28
List of abbreviations	32
Affidavit	33
Appendix I	34
Appendix II	44
Appendix III	56
Appendix IV	68

Abstract

The general objective of the investigation is to examine the basic relationships between quantitative characteristics of the modern land surface and the distribution of colluvial deposits on a fine spatial resolution. For a description of the colluvial deposits, thicknesses and accumulation rates were used. The experimental part was exemplarily conducted on two key areas located in Northern Germany. The land surface was characterized by a system of 17 morphometric variables and 12 types of landforms described by curvatures. Curvatures describe land surface segments at the local level, whereas at the regional level land surface portions are described by maximal catchment area.

Land surface segments characterized by a high volume of colluvial deposits as well as land surface segments with a high colluvial accumulation rate (CAR) were identified. The spatial antagonism between these land surface segments was experimentally detected at local and regional levels. A hypothesis on the dual system of the land surface memory was suggested for the conceptual understanding of this result. A high CAR can be associated with the function of short-term memory, whereas the storing of a large volume of colluvial deposits can be associated with the function of long-term memory. In conditions of the key areas, land surface portions responsible for short-term memory had a CAR approximately 20 times higher and colluvial thickness approximately two times smaller than land surface portions responsible for long-term memory.

Two groups of landforms (described by curvatures) related with soil erosion and colluvial accumulation were experimentally identified. The proportion of occurrence frequency between these groups of landforms indicates potential domination of the erosion or accumulation processes in the region. The intensity of these processes can be assessed by comparison of the occurrence frequency of a chosen group of landforms for the real land surface and for an artificial random surface. The more the deviation the more intensive the backbone process is manifested. Based on this approach, the potential erosion/accumulative status at sampling points and in the surrounding terrain was assessed. At sampling points of the key area of Perdoel, the land surface is potentially suitable for intensive accumulation; at sampling points of the key area of Bornhoeved the land surface is potentially suitable for accumulation with medium intensity, and for the surrounding terrains of both key areas for erosion with low intensity. The results coincided with the existing information obtained by traditional methods. Hence, the approach can be used as an additional method of the assessment of the potential erosion/accumulative status of a terrain from a geomorphometric point of view.

Three phases of land surface transformation during colluviation were experimentally distinguished. The phases were identified according to the correlations between the thicknesses of colluvial layers among each other and correlations of the thicknesses of colluvial layers with curvatures. Each phase is characterized by a group of four landform types described by curvatures. The first phase is associated with the beginning of accumulation processes. The second phase is indicated by the beginning of a detectible transformation of the land surface due to long-term sedimentation. The third phase is characterized by the largest differences between modern and buried surfaces. At the end of this phase, the sedimentation processes on the local level were terminated.

Therefore, a new quantitative approach based on methods of geomorphometry and statistics was developed for investigations of erosion/accumulation processes on fine spatial resolution. This new approach allowed the explanation of regularities of spatial distribution of colluvial deposits on fine spatial resolution.

Zusammenfassung

Das Ziel des Forschungsvorhabens ist die Untersuchung grundlegender Beziehungen zwischen den quantitativen Charakteristika heutiger Landoberflächen und der räumlich hochaufgelösten Verteilung kolluvialer Ablagerungen. Für die Beschreibung der kolluvialen Ablagerungen wurden die Parameter Mächtigkeit und Akkumulationsrate verwendet. Die Feldarbeiten zu der vorgestellten Analyse wurden in zwei Schwerpunktgebieten in Norddeutschland durchgeführt. Die Charakterisierung der Landoberfläche wurde mit Hilfe eines Systems von 17 morphometrischen Variablen sowie 12 Landformtypen, die durch positive und negative Krümmungen differenziert werden, vorgenommen. Krümmungen beschreiben Bereiche von Landoberflächen auf lokaler Ebene, wohingegen Landoberflächen auf regionaler Ebene durch die maximale Einzugsgebietsgröße beschrieben werden.

Landoberflächen, die durch ein hohes Volumen kolluvialer Ablagerungen charakterisiert sind, sowie Landoberflächen mit hohen kolluvialen Akkumulationsraten (CAR) wurden identifiziert. Der räumliche Antagonismus zwischen diesen Landoberflächen auf lokaler und regionaler Ebene wurde experimentell nachgewiesen. Für das konzeptuelle Verständnis der Ergebnisse wird die Hypothese des dualen Systems des „land surface memory“ vorgeschlagen. Hohe kolluviale Akkumulationsraten können mit der Funktion des „short-term memory“ verknüpft werden, wohingegen die Ablagerung großer Volumina kolluvialer Sedimente mit der Funktion des „long-term memory“ verbunden werden kann. Es hat sich gezeigt, dass Bereiche von Landoberflächen, die für das „short-term memory“ verantwortlich sind, 20-fach höhere kolluviale Akkumulationsraten und zweifach geringere kolluviale Mächtigkeiten aufweisen, verglichen mit Landoberflächen, die für das „long-term memory“ verantwortlich sind.

Zwei Gruppen von Landformen (beschrieben durch positive und negative Krümmungen), die in Beziehung mit Bodenerosion und kolluvialer Akkumulation stehen, wurden experimentell identifiziert. Das Verhältnis der Auftrittshäufigkeit zwischen diesen Gruppen von Landformen deutet auf potentiell dominierende Erosions- oder Akkumulationsprozesse in der Region hin. Die Intensität dieser Prozesse kann mit Hilfe eines Vergleichs der Auftrittshäufigkeit einer bestimmten Gruppe von Landformen zwischen der realen und einer künstlichen Oberfläche ermittelt werden. Je größer die Abweichung desto intensiver ist der dahinterliegende Prozess ausgeprägt. Basierend auf diesem Ansatz wurde die potentielle Erosion/Akkumulation an den Probenahmestellen und deren Umgebung bewertet. Die Probenahmestellen des Untersuchungsbereiches Perdoel deuten auf eine intensive Akkumulation hin; die des Untersuchungsbereiches Bornhoeved weisen auf eine mittlere Akkumulation hin. Die umgebenden Bereiche beider Untersuchungsgebiete zeigen eine Erosion mit geringer Intensität. Die Ergebnisse stimmen mit den existierenden Informationen überein, die mit klassischen Methoden ermittelt wurden. Aus geomorphometrischer Sicht kann das Vorgehen daher als eine zusätzliche Methode zur Bewertung des potentiellen Erosion-/Akkumulationsstatus eines Gebietes verwendet werden.

Drei Phasen der Transformation der Landoberfläche während der Ablagerung von Sedimenten wurden experimentell differenziert. Die Phasen wurden identifiziert, basierend auf der Korrelation zwischen der Mächtigkeit der kolluvialen Schichten untereinander sowie der Korrelation zwischen der Mächtigkeit der Kolluvien und negativen und positiven Krümmungen. Jede Phase konnte durch eine Gruppe von vier Landformtypen beschrieben werden. Die erste Phase ist verbunden mit dem Beginn eines nachweisbaren Akkumulationsprozesses. Die zweite Phase ist gekennzeichnet durch den Beginn einer nachweisbaren Transformation der Landoberfläche durch langfristige Sedimentation. Die dritte Phase ist charakterisiert durch die größte Differenz zwischen der modernen und der begrabenen Oberfläche. Am Ende dieser Phase waren die Sedimentationsprozesse auf lokaler Ebene abgeschlossen.

Demzufolge wurde ein neuer quantitativer Ansatz basierend auf den Methoden der Geomorphologie und der Statistik für die Untersuchung von kleinräumigen Erosions- und Akkumulationsprozessen entwickelt. Dieser neue Ansatz ermöglicht die Beschreibung von Regelmäßigkeiten der räumlichen Verteilung kolluvialer Ablagerungen.

1. Introduction

Colluvial (slope) deposits are among the main indicators of human-triggered soil erosion during the Holocene (*e.g.* Bork, 1983; Lang, 2003; Kaiser et al., 2007; Dotterweich, 2008; Brown, 2009; Dreibrodt et al., 2010; Fuchs et al., 2010). Investigations about the spatial distribution of colluvial deposits are based on a well-known concept. Runoff accumulates over remote areas and transports colluvial matter over relatively local distances during heavy rain events (*e.g.* Lang et al., 1999). This is linked to the low output of colluvial matter from slopes into fluvial systems (*e.g.* de Moor and Verstraeten, 2008; Houben et al., 2012). Another factor influencing the low output of colluvial deposits is the disconnectivity of sediment cascades caused by different types of natural and artificial borders in a catchment (*e.g.* Walling, 1983; Fryirs, 2013).

The application of information derived from colluvial deposits for palaeo-reconstructions is very common. Only in Germany more than a hundred excavated key areas exist (Dreibrodt et al., 2010). However, quantitative regularities of the distribution of colluvial deposits with detailed spatial resolution are still not clear. Mapping of colluvial deposits is mainly based on the interpolation between a large number of samplings that is linked with a large amount of fieldwork (*e.g.* Rommens et al., 2005; Houben, 2008; Reiß et al., 2009). Moreover, such interpolation does not indicate situations in which a buried surface is characterised by high spatial heterogeneity. The problem can be solved with the help of predictive models, although only several investigations have been published in this direction (*e.g.* Dietrich et al., 1995; Mitasova et al., 1997; Mitas and Mitasova, 1998; Follain et al., 2006).

In comparison with pedometrics, the application of spatial predictive models for colluvial deposits is limited by the deficit of quantitative predictors. Many of them cannot be measured precisely with high spatial resolution. However, if the main triggers of soil erosion are land use and climate, the spatial distribution of colluvial deposits in the slope/valley system depends mainly on the land surface. In this context, the modern methods of geomorphometry provide an extended system of morphometric variables (MVs) for the quantitative description of the land surface (Shary et al., 2002). These MVs can be precisely calculated based on high definition measurements of the modern topography (*e.g.* Florinsky, 2012). One group of MVs describes the modern land surface, another group can be used for a determination of buried landforms (Shary et al., 2002; Mitusov et al., 2013, appendix I).

Most relationships of the spatial distribution of colluvial deposits with MVs are not known. Hence, the **general objective** of this investigation is to establish the basic relationships between quantitative characteristics of the modern land surface and distribution of colluvial deposits on a fine spatial resolution. The **specific objectives** to be pursued include:

– ***a comprehension of spatial relationships between colluvial thickness and accumulation rate***

The thickness or storage of colluvial deposits is a traditional object for mapping. However, the spatial distribution of another important parameter, such as the colluvial accumulation rate (CAR), is often not considered. This parameter is only determined at several sampling points and extrapolated for the whole valley. Theoretical antagonism between these parameters is known. However, the practical consequences from this fact are not discussed in the literature. For an understanding of the spatial interaction between these parameters, different types of land surface portions should be compared according to maximal values of colluvial thickness and CARs.

– ***an assessment of erosion and accumulation intensity from a point of view of geomorphometry***

The reconstruction of processes based on a landform shape is one of the backgrounds of geomorphology. Hence, it is assumed that the size of area occupied by landforms of one type reflects the scale of related processes. The role of landforms in erosion and accumulation processes can be determined on the basis of their material content such as thickness of colluvia. In this case, the total area and occurrence frequency of different landforms can be used for a geomorphometric description of the spatial proportion between erosion and accumulation processes on a large terrain.

– ***the quantification of transformation phases of the land surface under long-term sedimentation***

The spatial distribution of colluvial deposits is duly linked with the transformation of the land surface. In comparison with geological processes, the mechanisms of colluvial distribution are characterised by low energy input. Hence, the results of these processes are often not clearly visible without special techniques. The reconstruction of transformation phases of landforms is based on statistical comparisons between MVs and the thickness of colluvial layers. The known sequences of the phases enable the automatic reconstruction or prediction of the land surface shape in the past or the future.

2. Key area locations

The data were obtained from two key areas located in Northern Germany approximately 35 – 40 km south of Kiel (Fig. 1). The key area of "Perdoel" is located in the lower part of a dry subcatchment of Lake Belau near the farm Perdoeler Muehle. The key area of "Bornhoeved" is located in the upper part of a dry subcatchment of Lake Bornhoeved. The dataset of colluvial deposits consists of 64 points at the key area of Perdoel (Fig. 1B) and 71 points at the key area of Bornhoeved (Fig. 1C). Present and past ecological conditions in the region are shown in previous publications (Mitusov et al., 2013, appendix I; 2014, appendix II).

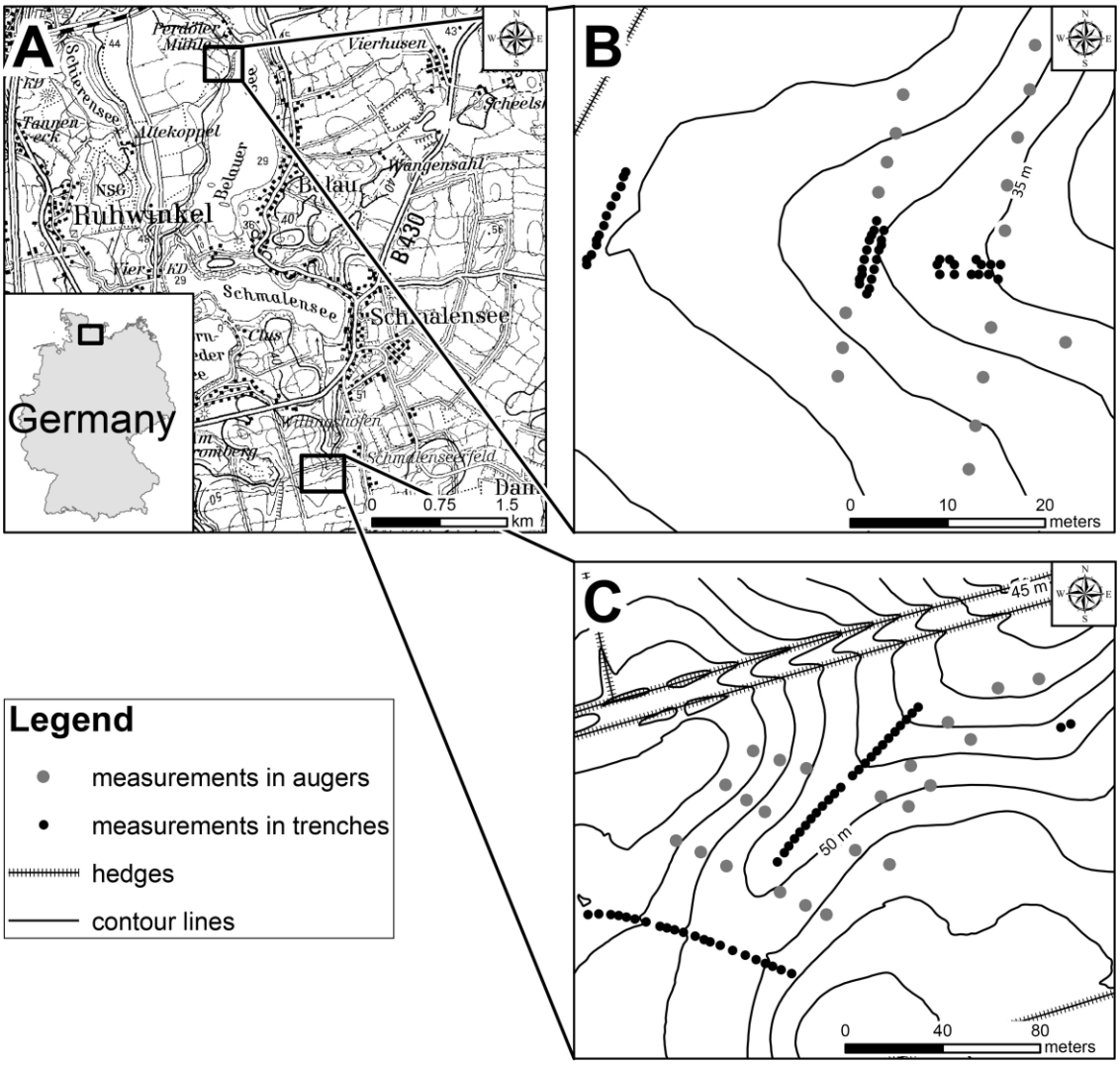

Fig. 1. Locations of the key areas and sampling points. A: Area overview. B: Key area of Perdoel. C: Key area of Bornhoeved.

3. Methods

3.1. Digital elevation models

A digital elevation model (DEM) with 1 m resolution from the State Bureau of Surveying and Geoinformation, Schleswig-Holstein (Landesvermessungsamt Schleswig-Holstein, 2012) was used during investigations at the key area of Perdoel (Mitusov et al., 2013, appendix I) and surrounding terrain. For the investigations at the key area of Bornhoeved a DEM with a resolution of 5 m was prepared based on field measurements by a differential GPS (Mitusov et al., 2014, appendix II). A terrain around the key area of Bornhoved was analysed based on the DEM from the State Bureau of Surveying and Geoinformation, Schleswig-Holstein (Landesvermessungsamt Schleswig-Holstein, 2012) that was generalised up to 5 m resolution.

The modern land surface of the key areas includes many artificial macro- and microstructures. The macrostructures are hedges and ditches around arable lands. Some of these macrostructures are clearly visible in their natural settings; others are destroyed and their remnants are only visible after geomorphometrical analysis. The microstructures were established due to arable soil treatment. However, these structures were not detected at the sampling point locations. Moreover, the artificial structures do not have a strong impact on the catchment borders of the key areas. Hence, the maximal catchment area calculated at every sampling point, based on the modern land surface, will not strongly differ from former topography. This coincidence depends on the topography and long-term development of an individual catchment of the land surface and might not be observed for other terrains.

3.2. Morphometric variables

The land surface was characterized by the system of 17 morphometric variables (MVs) described by Shary et al. (2002). These MVs are divided into four groups according to their physical meaning (Table 1). Additionally, based on different calculation methods, local and regional MVs can be distinguished (*e.g.* Shary, 1995). Regional MVs are a maximal catchment area (MCA) and a maximal dispersal area (MDA). For the calculation of regional MVs, extended terrain portions have to be taken into account (*e.g.* Tarboton, 1997). Local MVs are curvatures and slope steepness (*GA*). For the calculation of local MVs, only a small number of grid cells around a sampling point have to be considered (Shary et al., 2002).

The correct equations for local MVs that are used in this investigation were given by Shary (2012). The mathematical theory explains statistical relationships among MVs and links every MV with physical processes on the land surface (Shary et al., 2002). The MVs used are free from specific coefficients. As a result, these MVs can be comparably applied to different landscapes. This gives the selected MVs an advantage over other MVs. For the calculation of all MVs, the analytical GIS Eco developed by P. Shary was used (Wood, 2009). The maps of basic MVs for the key areas are shown in previous publications (Mitusov et al., 2013, appendix I; 2014, appendix II).

Investigations of the land surface on different scales are usual in geosciences. In this context, the definition of "scale" traditionally means an area size and data resolution. Nowadays, methods of remote surveying of the land surface enable investigations of large terrains with a fine spatial resolution. Hence, in the following text the terms "regional level" and "local level" are used. These terms are used for identifying the size of areas around sampling points and are not linked with the resolution of DEMs.

Table 1. System of morphometric variables (based on Shary et al., 2002).

Variable name, Unit	Description
Vertical zonation	
Altitude (*Z*), m	Vertical changes in climate conditions
Morphometric pre-requisites of surface runoff and soil throughflow generation	
Slope steepness (*GA*), degrees	Flow velocity
Maximal catchment area (MCA), m^2	Maximum area from which material moving downslope may be collected
Maximal dispersal area (MDA), m^2	Maximal area at which materials moving downslope may be diffused
Horizontal (tangential) curvature (*kh*), m^{-1}	Flow convergence/divergence
Vertical (profile) curvature (*kv*), m^{-1}	Relative flow deceleration/acceleration
Difference curvature (*E*), m^{-1}	Compares *kh* (in plan) and *kv* (in profile)
Total accumulation curvature (*KA*), m^{-2}	Reveals relative accumulation zones
Characteristics of land surface dissection	
Rotor (*rot*), m^{-1}	Flow line rotation direction
Total ring curvature (*KR*), m^{-2}	Flow line twisting
Vertical excess curvature (*kve*), m^{-1}	Describes to what extent *kv* is larger than minimal curvature (*kmin*)
Horizontal excess curvature (*khe*), m^{-1}	Describes to what extent *kh* is larger than minimal curvature (*kmin*)
Characteristics of geometrical landforms	
Maximal curvature (*kmax*), m^{-1}	Geometrical ridge forms
Minimal curvature (*kmin*), m^{-1}	Geometrical valley forms
Total Gaussian curvature (*K*), m^{-2}	Separated elliptic and saddle landforms
Mean curvature (*H*), m^{-1}	Connected to "equilibrium" surface condition
Unsphericity (*M*), m^{-1}	Surface deviation from spherical form

3.3. Landforms described by signs of curvatures

The land surface has four main directions (Shary et al., 2002). Two main directions of a surface itself are determined by normal sections with minimal (*kmin*) and maximal (*kmax*) curvatures. The gravity field produces such definitions as “up” and “down”. The shape of the land surface in direction from top to down as well as in perpendicular direction is defined by “gravitational” curvatures *kv* and *kh*. Other curvatures mainly describe different relationships between these four curvatures. Shary (1995) developed a theory for the identification of twelve types of main local landforms by signs of curvatures (Fig. 2). The set of these landforms is given in Table 2.

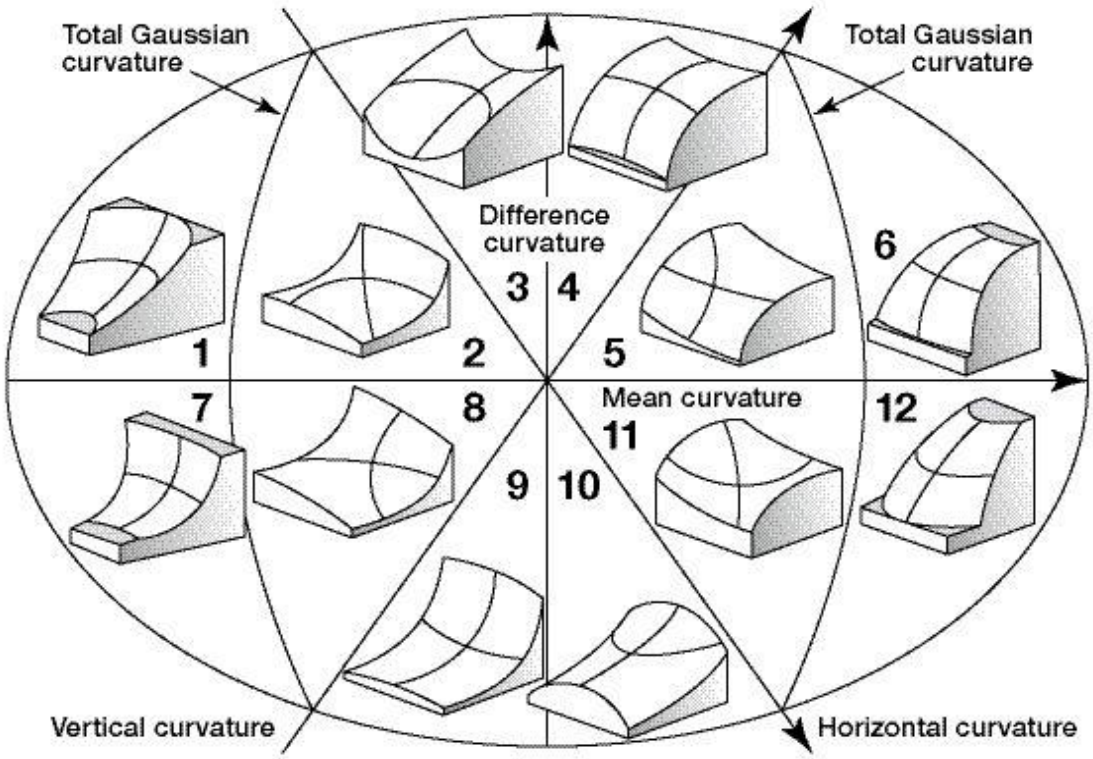

Fig. 2. Distribution of twelve types of main local landforms in coordinates of five curvatures (Shary et al. 2005).

The number of main local landforms cannot be extended by the introduction of other curvatures. Hence, 12 main local landforms can be considered as elementary segments of the land surface. A curvature = 0 is very rare for the land surface. Landforms that include at least one curvature = 0 are entitled as rare local landforms (Shary, 1995). Such rare landforms were not observed in the DEMs used for the investigations.

Table 2. Signs of curvatures for identification of twelve types of main local landforms (based on Shary et al. 2005).

N	Title of landform types	*K*	*H*	*kh*	*kv*	*E*	*kmin*	*kmax*
1	C-depressions with positive difference curvature	+	–	–	–	+	–	–
2	C-saddles mean-concave, convergent-decelerating, with positive difference curvature	–	–	–	–	+	–	+
3	C-saddles mean-concave, convergent-accelerating, with positive difference curvature	–	–	–	+	+	–	+
4	C-saddles mean-convex, convergent-accelerating, with positive difference curvature	–	+	–	+	+	–	+
5	C-saddles mean-convex, divergent-accelerating, with positive difference curvature	–	+	+	+	+	–	+
6	C-hills with positive difference curvature	+	+	+	+	+	+	+
7	C-depressions with negative difference curvature	+	–	–	–	–	–	–
8	C-saddles mean-concave, convergent-decelerating, with negative difference curvature	–	–	–	–	–	–	+
9	C-saddles mean-concave, divergent-decelerating, with negative difference curvature	–	–	+	–	–	–	+
10	C-saddles mean-convex, divergent-decelerating, with negative difference curvature	–	+	+	–	–	–	+
11	C-saddles mean-convex, divergent-accelerating, with negative difference curvature	–	+	+	+	–	–	+
12	C-hills with negative difference curvature	+	+	+	+	–	+	+

According to the statistical hypothesis of Shary (1995), the occurrence of each of the main local landforms has approximately equal probability (≈ 1/12) for a random surface. In nature, a deviation from this probability depends on the type of terrain. The accumulative landforms occur more often within mountainous terrains and less often on flatlands. This can be explained by the development of the land surface under impaction of tectonics in mountains and denudation of local concavities on flatlands. Other properties of the main local landforms are considered by Shary et al. (2005). In the following text, instead of the long term “main local landforms” the short term “landforms” will be used.

3.4. Determination of colluvial deposits

The thickness of colluvial deposits (M) was measured in trenches and auger cores. Locations and depths of trenches were defined so that all sequences of colluvial layers could be investigated at the bottoms of both valleys. Auger cores were distributed on slopes. Sequences and characteristics of different colluvial layers were described using conventional field methods (Ad-hoc-Arbeitsgruppe Boden, 2005). The mean thickness of a colluvial layer was calculated for each cell of a DEM that was crossed by the trenches. For auger cores, this procedure was unnecessary. The average bulk density of colluvial deposits was taken as 1.5 g cm^{-3}. Other properties of colluvial layers at the key areas are considered in previous publications (Dreibrodt et al., 2009, appendix III; Dreibrodt and Wiethold, *submitted*). The total duration of colluvial deposition at the key area of Bornhoved can be assumed to span approximately 2800 years and at the key area of Perdoel approximately 3000 years.

3.5. Indicator of the spatial variability of the colluvial accumulation rate (CAR)

The absolute value of a CAR is calculated with the commonly known equation (I):

$$CAR = S/C/D \qquad (I),$$

where:
CAR – colluvial accumulation rate, t m^{-2} a^{-1};
S – storage of colluvial deposits, t;
C – catchment area, m^2;
D – duration of accumulation, years.

Primarily, this equation is used for the determination of a CAR at one or several points. The number of points of precise calculation of the CAR is limited by expensive procedures to determine the age of colluvial layers. However, the spatial variability of a CAR is defined by the storage of colluvial deposits and the catchment area. Hence, the ratio between them can be used as an indicator of the spatial variability of the CAR. The storage of colluvial deposits and the catchment area can be measured at every sampling point. It has to be noted that the values of the catchment area are much larger than the values of colluvial storage. Hence, spatial variability of the CAR stands in high negative dependence to the MCA.

The investigation focuses on the spatial distribution of the thickness of colluvial layers and the CAR. A CAR cannot be measured with high spatial resolution. Hence, instead of absolute values of a CAR, the indicator of the CAR was used in the following work.

3.6. Statistics

Well-known statistical methods were used for data analysis (StatSoft Inc., 2013). An overview was made using basic descriptive statistics. For the determination of normality, the tests of Shapiro-Wilk and Anderson-Darling were performed. Quantitative comparisons were made with the help of the non-parametric rank correlation coefficient of Spearman (r_S). Correlation coefficients with a significance level (p) of $p > 0.05$ were not considered.

3.7. Determination of the potential role of main local landforms for the processes of soil erosion or colluvial accumulation

The role of landforms for processes of soil erosion or colluvial accumulation was determined according to the variability of the thickness of colluvial deposits (Mitusov, *submitted*, appendix IV). For every group of landforms of one type, the median thickness of colluvium (M_{group}) was calculated. Afterwards, values of M_{group} were compared with the median thickness of colluvium for a whole key area (M_{key}). If M_{group} was equal to or higher than M_{key}, such a landform type was accepted as potentially related with the colluvial storage. These types of main local landforms were denoted by the abbreviation LLF^M, where "M" stands for colluvial deposits. If M_{group} was smaller than M_{key}, such landform types were accepted as potentially related with the processes of soil erosion. A determination of the role of landforms based on material content enables the assessment of geomorphometric prerequisites of these processes on large terrains. For example, outside of the sampling points, LLF^M may not contain colluvial deposits at all. However, in case of the activation of erosion and accumulation processes, colluviation will take place at LLF^M in the first order.

4. Results

4.1. Statistical properties of the indicator of the colluvial accumulation rate (CAR) and the thickness of colluvial deposits

The statistical distribution of the indicator of the CAR is close to the logarithmic type for both key areas (Fig. 3A). The most often occurring values are small and distributed over a narrow interval. This type of statistical distribution is caused by the MCA that is one of the components of the CAR. The statistical distribution type of the thickness of colluvial deposits varies depending on the key area (Fig. 3B). The bar chart of the thickness of colluvial deposits from the key area of Bornhoeved has no well expressed peak in the data except for several outliers. It might be caused by the location of this key area in a relatively flat valley. Thick peaks are clearly visible on the bar chart of the data from the key area of Perdoel. Two main peaks within the intervals 49 – 92 cm and

145 – 176 cm are caused by the distribution of sampling points on slopes and at the bottom of the relatively steep valley. A small peak in the interval 6 – 27 cm indicates that several sampling points are located in the former arable area and reflects the thickness of the former ploughing layer.

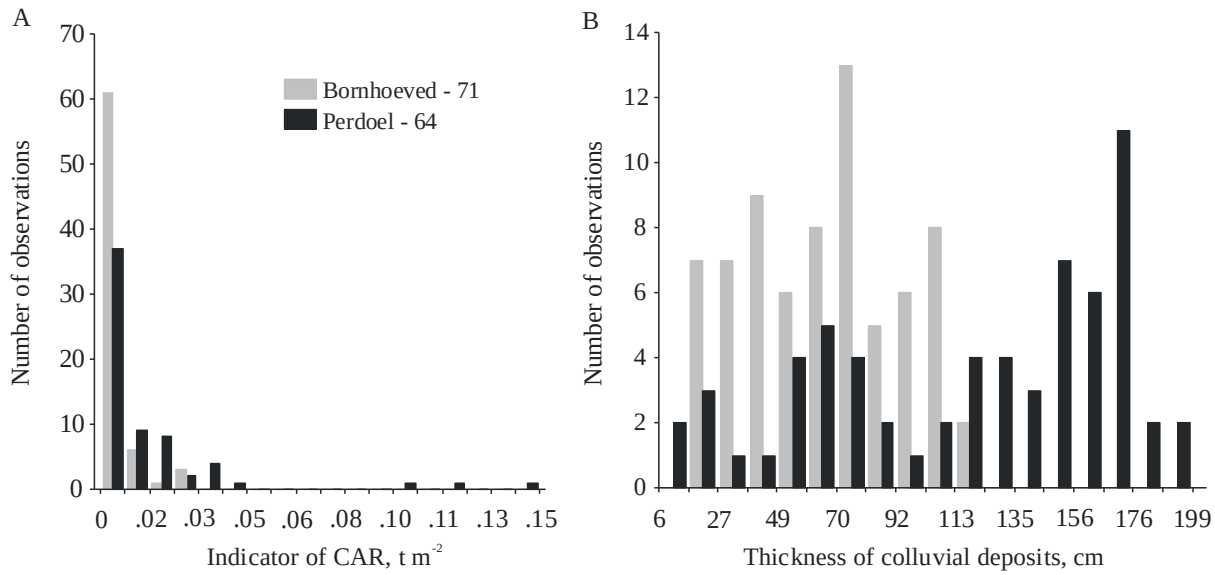

Fig. 3. Statistical distribution of the indicator of the colluvial accumulation rate (CAR) (A) and the thickness of colluvial deposits (B).

4.2. Statistical relationships in the dataset

The thickness of colluvial deposits and the indicator of the CAR are statistically dependent parameters. The correlation coefficients $r_S = –0.41$ at the key area of Bornhoeved and $r_S = –0.75$ at the key area of Perdoel were obtained between these parameters. The relationships between the thickness of colluvial deposits and the MCA are relatively strong and positive: $r_S = 0.69$ at the key area of Bornhoeved (Mitusov et al., 2013, appendix I) and $r_S = 0.85$ at the key area of Perdoel (Mitusov et al., 2014, appendix II). The strong negative relationship between the MCA and the indicator of the CAR is the result of the disproportion between components in the equation for the CAR.

The specifics of the correlations of individual colluvial layers with curvatures were well described in previous articles (Mitusov et al., 2013, appendix I; 2014, appendix IV). Here, only the results for the total thickness of colluvial deposits will be considered (Fig. 4). Signatures of r_S with curvatures indicate the concentration of the thickest colluvial deposits at convergent areas ($kh < 0$) and at the zones of relative deceleration of surface flows ($kv < 0$) with a more twisted section for kv in comparison with kh ($E > 0$). These land surface portions are characterised by a tendency to concave geometry ($kmin < kmax < 0$) with a more twisted section for $kmin$ in comparison with $kmax$ ($H < 0$).

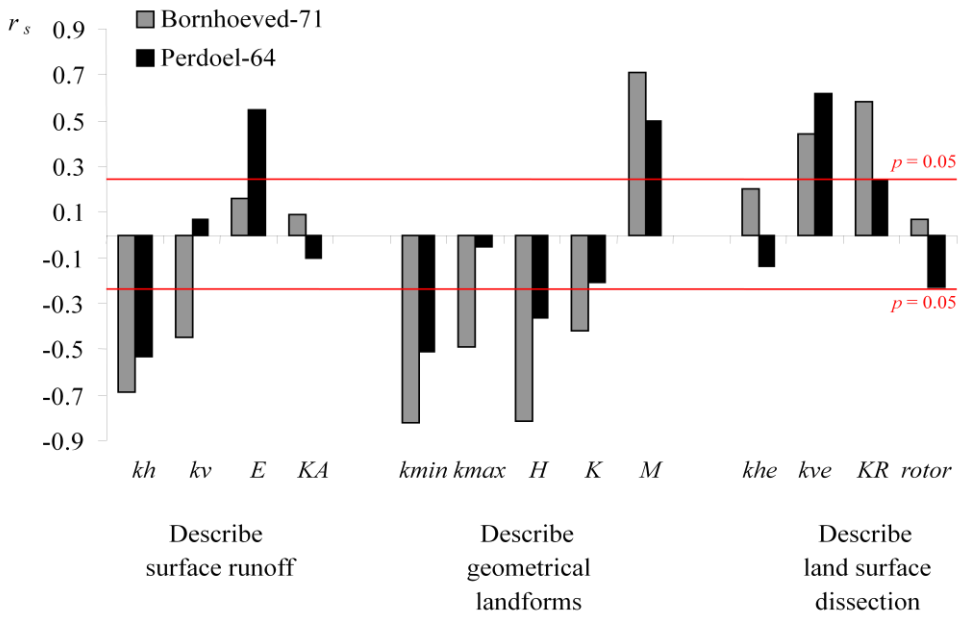

Fig. 4. Spearman correlations (r_S) between total thickness of colluvial deposits and curvatures. Based on data from Mitusov et al. (2013, appendix I; 2014, appendix II).

An interpretation of correlations with *K* is more difficult because values of $K < 0$ describe both convex and concave landforms. This terminates a meaningful interpretation of correlations in the interval of $K < 0$. A distribution of the thickness of colluvial deposits on land surface portions with $K > 0$ is defined by proportions between values of two geometrical (*kmin*, *kmax*) and gravitational (*kh*, *kv*) pairs of curvatures with different signatures. A correlation with *KR* (Fig. 4) indicates that the thickest colluvial deposits are concentrated at land surface portions with maximal radial asymmetry. Correlation with *M* indicates that the thickest colluvial deposits are concentrated at points with maximal differences between *kmax vs. kmin*. A correlation with *kve* indicates that the thickest colluvial deposits are concentrated at points with maximal differences between *kv vs. kmin.*

4.3. Distributions of the thickness of colluvial deposits and the indicator of the colluvial accumulation rate (CAR) on main local landforms

Correlations with curvatures (Fig. 4) indicate that land surface portions with the thickest colluvial deposits have complex shapes. This is an argument for the analysis of the spatial distribution of the thickness of colluvial deposits and the indicator of the CAR at main local landforms defined by signs of curvatures (Table 3).

Table 3. The total thickness of colluvial deposits and the indicator of the colluvial accumulation rate (CAR) at main local landforms.

Type of landform	*n*	Thickness of colluvium, cm			Indicator of CAR, t m^{-2}		
		Q_1	Median	Q_3	Q_1	Median	Q_3
The key area of Bornhoeved							
1	3	69.1	76.3	80.9	0.00010	0.00011	0.00010
2	7	88.4	92.0	103.3	0.00013	0.00014	0.00013
3	10	67.0	75.2	101.3	0.00012	0.00017	0.00012
4	2	55.5	64.4	73.4	0.00342	0.00574	0.00342
5	3	26.2	27.0	28.8	0.00334	0.00376	0.00334
6	6	27.1	37.2	62.0	0.00601	0.00703	0.00601
7	9	77.3	80.7	94.0	0.00172	0.00281	0.00172
8	7	66.6	100.7	101.8	0.00030	0.00057	0.00030
9	11	48.3	55.0	61.5	0.00544	0.00653	0.00544
10	7	34.0	44.0	62.0	0.00146	0.00442	0.00146
12	6	27.5	35.5	44.8	0.00505	0.00572	0.00505
Entire dataset	71	44.3	67.0	88.3	0.00030	0.00364	0.00030
The key area of Perdoel							
1	8	146.5	169.3	175.0	0.00004	0.00006	0.00004
2	7	91.8	133.0	167.3	0.00005	0.00008	0.00005
3	18	92.5	160.3	169.8	0.00007	0.00009	0.00007
4	8	88.8	146.0	163.6	0.00046	0.00121	0.00046
5	2	157.3	162.5	167.8	0.00601	0.00680	0.00601
6	5	63.0	83.0	105.5	0.01148	0.02390	0.01148
7	4	39.8	82.5	125.0	0.00769	0.01086	0.00769
8	2	134.3	140.5	146.8	0.00256	0.00506	0.00256
9	4	57.5	65.0	72.3	0.01249	0.01567	0.01249
10	3	88.5	109.0	118.0	0.02955	0.03288	0.02955
12	3	50.5	80.0	99.8	0.02121	0.03940	0.02121
Entire dataset	64	71.1	133.0	136.9	0.00007	0.00306	0.00007

Note: Q_1 and Q_3 – first and third quartiles.

The reproducible results were found for both key areas (Table 3). The landforms described as $kmin < kh < 0$ (types 1, 2, 3 and 8) are characterized by relatively thick colluvial deposits. The landforms described as $0 < kh < kmax$ (types 6, 9, 10 and 12) are characterized by relatively thin colluvial deposits. A low indicator of the CAR is found at the landform types 1, 2 and 3; a high indicator at the landform types 5, 6, 9, 10 and 12 (Table 3). At other local landforms, the thickness of colluvial deposits and the indicator of the CAR are varied depending on the key area.

5. Discussion

5.1. Relationship of the thickness of colluvial deposits with the MCA

A positive relationship between the thickness of colluvial deposits and the MCA is described by a logarithmic trend (Fig. 5). This indicates that accumulation is more intensive than erosion at the same sampling points. On the regional level, positive relationships with the MCA mean that spatial variability of the thickness of colluvial deposits is caused by remote orographic factors. Probably, this situation is most often observed in small dry valleys without gully formation, coinciding with similar investigations (*e.g.* Tunnickliffe and Church, 2011; Schneider et al., 2011).

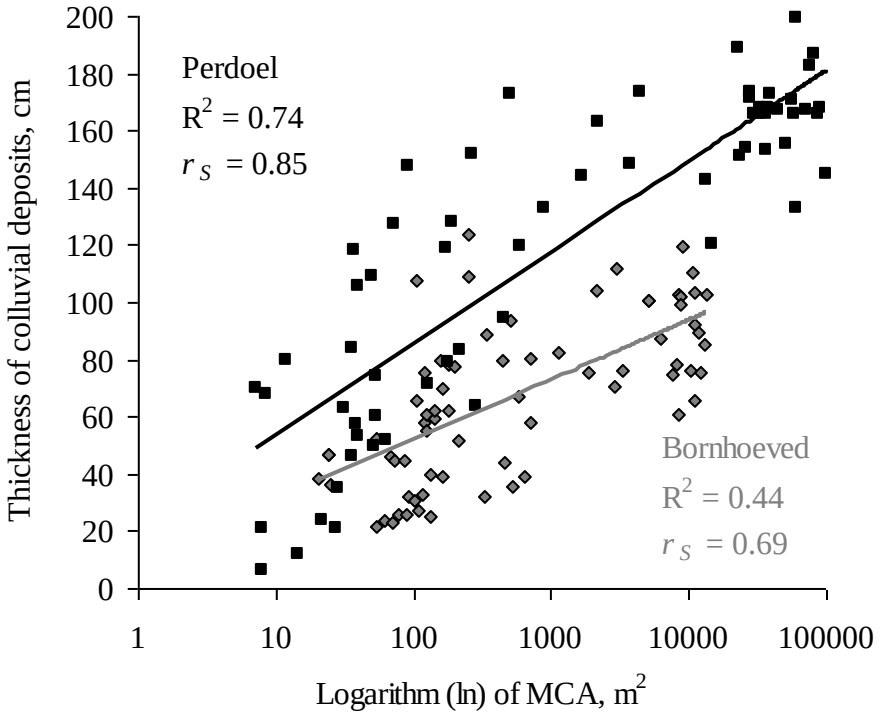

Fig. 5. Relationship between the thickness of colluvial deposits and the maximal catchment area (MCA). Grey dots are the data from the key area of Bornhoeved. Black dots are the data from the key area of Perdoel.

5.2. Relationship of the indicator of the colluvial accumulation rate (CAR) with the MCA

Manual techniques for the calculation of a catchment area provide only one value for the whole valley. This is the main restrictor for experimental investigations of the spatial variability of the CAR in conditions of small dry valleys. Measurements of colluvial storage and catchment area at every sampling point allow the construction of an experimental trend between these two parameters (Fig. 6).

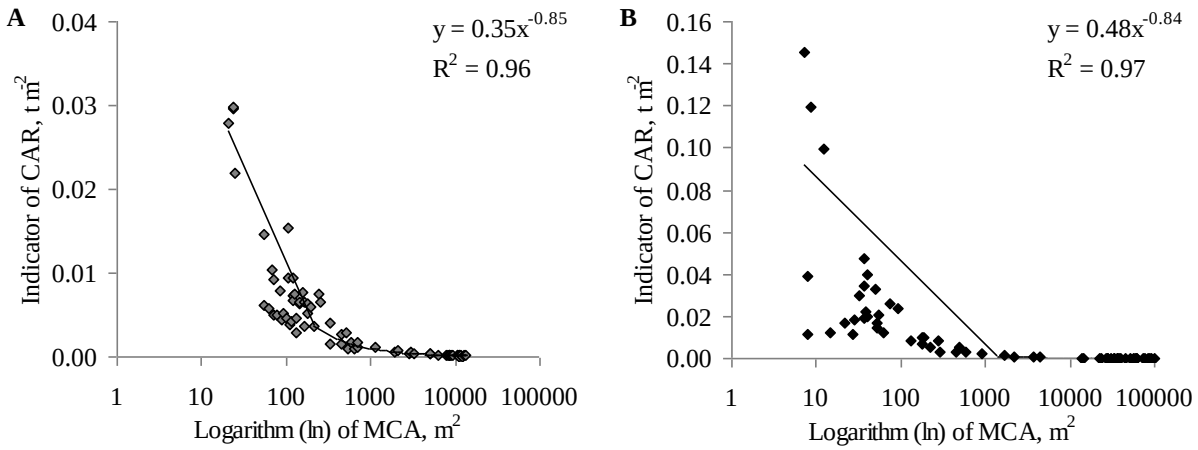

Fig. 6. Negative relationship between the indicator of the colluvial accumulation rate (CAR) and the maximal catchment area (MCA). A: The key area of Bornhoeved. B: The key area of Perdoel.

A strong negative relationship between a catchment area and the CAR is the result of the equation for the calculation of the CAR. This relationship is described by a power trend (Fig. 6). A curve of the trend indicates a sharp change from conditions of a relatively small catchment (*e.g.* slopes) to conditions of a relatively large catchment (*e.g.* valley bottom). The measurements show that the CAR tends to zero values (but $\neq 0$) at the valley bottom. Relatively large values of a CAR are only observed on slopes with thin colluvial deposits and small catchment areas.

5.3. Relationship between the thickness of colluvial deposits and the indicator of the colluvial accumulation rate (CAR)

Absolute values of the thickness of colluvial deposits and the indicator of the CAR are higher at the key area of Perdoel compared to the key area of Bornhoeved. This can be caused by the position of the key areas in the lower or upper parts of a catchment. Due to such differences, it can be assumed that the power of sediment delivery processes at the key area of Perdoel is higher than at the key area of Bornhoeved.

A descending logarithmic trend is the best monotonic descriptor of the relationship between the thickness of colluvial deposits and the indicator of the CAR (Fig. 7). At Bornhoeved, the determination coefficient is relatively low (Fig. 7). This is probably caused by the noise linked with the relatively low intensity of erosion and accumulation processes at this key area. The generalisation of the data by median values in groups of landforms reduced this noise. The derived trends show relatively equal coefficients of determination (Fig. 7).

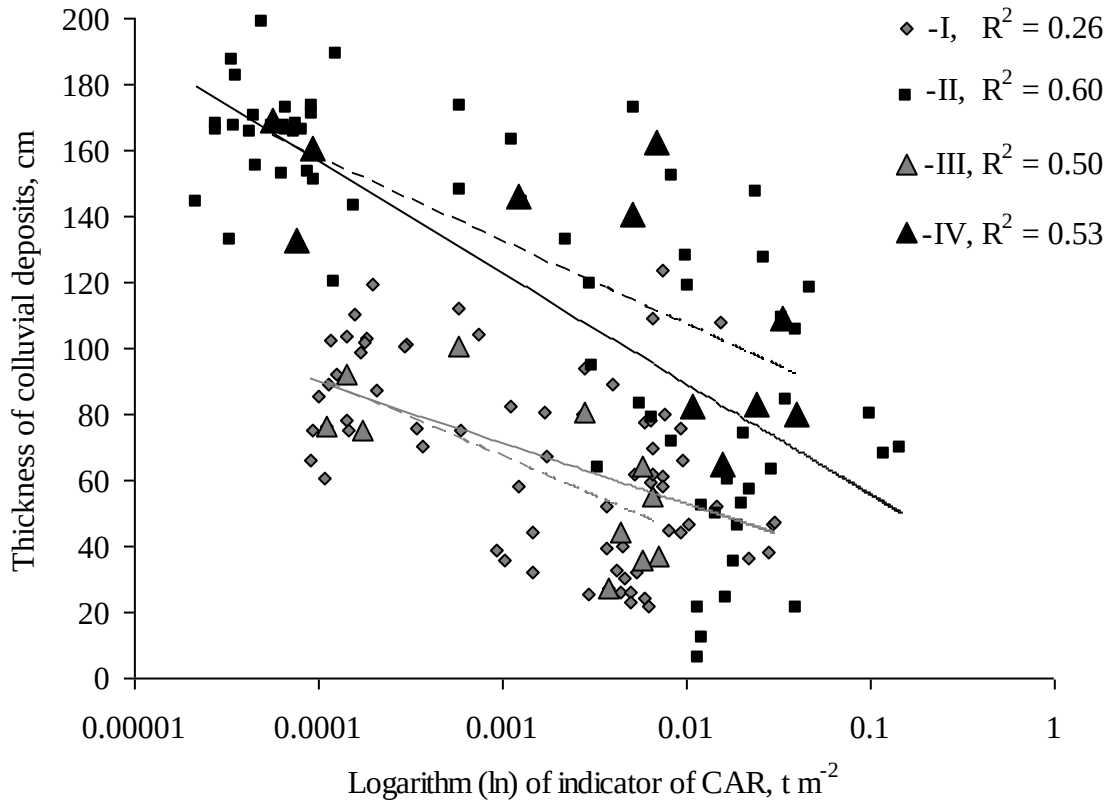

Fig. 7. Relationship between the thickness of colluvial deposits and the indicator of the colluvial accumulation rate (CAR). I: Data from the key area of Bornhoeved, all sampling points. II: Data from the key area of Perdoel, all sampling points. III: Median values in groups of landforms, key area of Bornhoeved. IV: Median values in groups of landforms, key area of Perdoel. The continuous lines are the logarithmic trends through all datasets. The dotted lines are the logarithmic trends through datasets generalised by median values in groups of landforms from Table 3.

The direction of trends (Fig. 7) as well as negative correlations between the thickness of colluvial deposits and the indicator of the CAR show statistical distribution of the highest values of these parameters at different land surface portions. The same results are obtained by comparisons of the median data (Table 3). On the regional level, these observations are in agreement with relationships of the thickness of colluvial deposits and the indicator of the CAR with the MCA.

5.4. Spatial distribution of orographic attributes related with colluvial deposits

It is expected if a landscape parameter has strong correlations with MVs, then the maps of these MVs can be used for the spatial assessment of this parameter. Such maps reflect a potential pattern of the response variable. In the present investigation, the maps of the MCA and main local landforms can be used for these purposes. Landforms described by curvatures are not sensitive to landscape position on a regional level. The MCA as well as such regional terms as “slope” and “valley” cannot be defined on a local level. Hence, the maps of the MCAs are linked with the distribution of colluvial deposits on a regional level (Fig. 8A and C); maps of main local landforms on a local level (Fig. 8B and D).

Relationships with the MCA show that colluvial deposits are concentrated in the areas of high values of the MCA (Fig. 5). In landscapes, high values of the MCA are observed at valley bottoms and in closed depressions. This is also relevant for the spatial distribution of colluvial deposits. Hence, light cells of the gridded map of the MCA show areas with potential soil erosion, dark cells with colluvial accumulation (Fig. 8A and C). The space between these areas can be characterised as transit zones on slopes. These areas have no sharp borders because the map of the MCA represents a continuous surface.

Relationships with curvatures (Fig. 4) show that colluvial deposits accumulated on several types of landforms (Table 3). The size of an individual landform duly coincides with the grid spacing of a DEM. However, most of the landforms are incorporated into larger patches with a systematic spatial structure (Fig. 8B and D). The pattern of these patches approximately coincides with large structures existing on the MCA maps: light areas potentially indicate areas of soil erosion at uphills; dark areas of colluvial accumulation at valley bottoms. The patches of landforms have sharp borders at certain grid spaces. This is caused by the fact that a map of main local landforms represents a discrete surface.

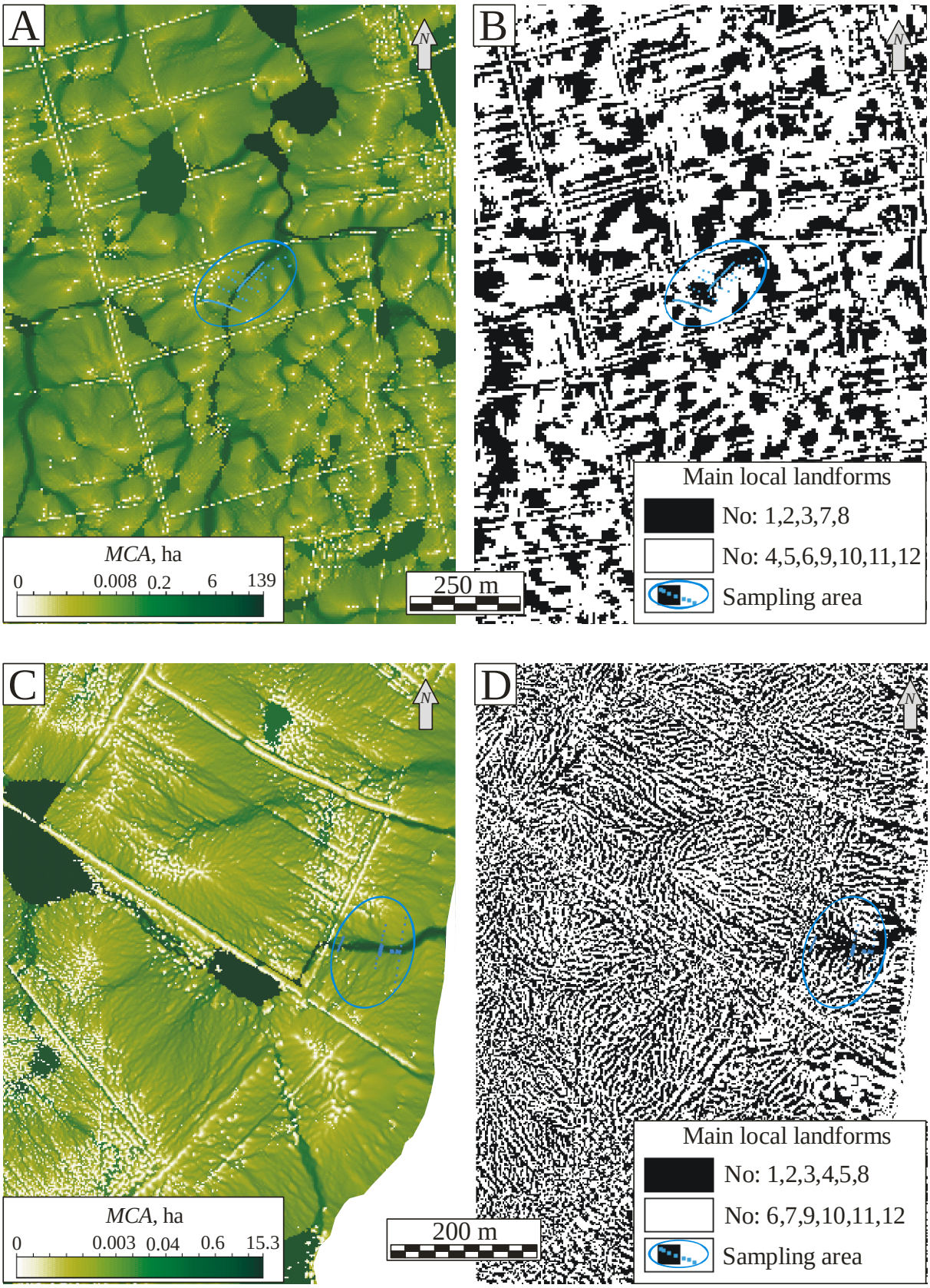

Fig. 8. Maps of orographic attributes that reflected land surface portions with potential soil erosion (light areas) and colluvial accumulation (dark areas) on regional (maps of the MCA) and local (maps of main local landforms) levels. A and B: The key area of Bornhoeved, grid spacing 5 m. C and D: The key area of Perdoel, grid spacing 1 m.

Applications of maps of MVs for the description of the potential pattern of colluvial deposits are not in competition with the application of statistical predictive models, but are able to extend them. The simultaneous application of models and maps of MVs can be considered on the example of the determination of a hydrological network. The map of the MCA is only calculated on the basis of a DEM and reflects a potential hydrological network. It may also be constructed for dry regions where this potential cannot be realised in form of surface water flows. Hydrological models duly take into account the volume of water in surface flows and other criteria. Hence, the model is focused on the description of the real situation. However, statistical modelling can be restricted by the deficit of initial data and is sensitive to the distance from samplings.

5.5. Geomorphometric quantitative descriptor of erosion and accumulation processes for terrains considered as one unit

The material content of landforms (*e.g.* volume of colluvium) reflects processes related with these landforms (*e.g.* erosion or accumulation). Hence, the size of an area occupied by these landforms and/or their occurrence frequency indicates the scale of the related processes. For the investigations in this direction, a relatively large set of landforms should be considered. Regional orographic structures have no fixed size. A DEM of key areas may include only a small number of such structures. As opposed to regional structures, the size of local landforms duly coincides with the size of grid cells of a DEM. Hence, mainly all DEMs have a sufficient number of local landforms for the analysis of their occurrence frequency.

At both key areas, several types of main local landforms with a large storage of colluvial deposits (LLF^M) were identified (Table 3). Therefore, an analysis of their occurrence frequency may reflect the erosion/accumulation status of the land surface at sampling points and the surrounding terrain. It is assumed that the occurrence of LLF^M at the level of 50 % indicates equilibrium between potential erosion and potential accumulation. The occurrence frequency of LLF^M at sampling points at both key areas is more than 50 % (Fig. 9). It indicates the domination of accumulative processes at sampling points on the local level. This coincides with the positive correlation between the thickness of colluvium and the MCA (Fig. 5), which indicates the domination of accumulative processes at sampling points on the regional level as well. The occurrence of LLF^M in the areas around sampling points is stable at approximately 40 % and is not sensitive to the size of terrain around the key areas (Fig. 9). These results show a potential domination of erosion processes around the key areas on the local level.

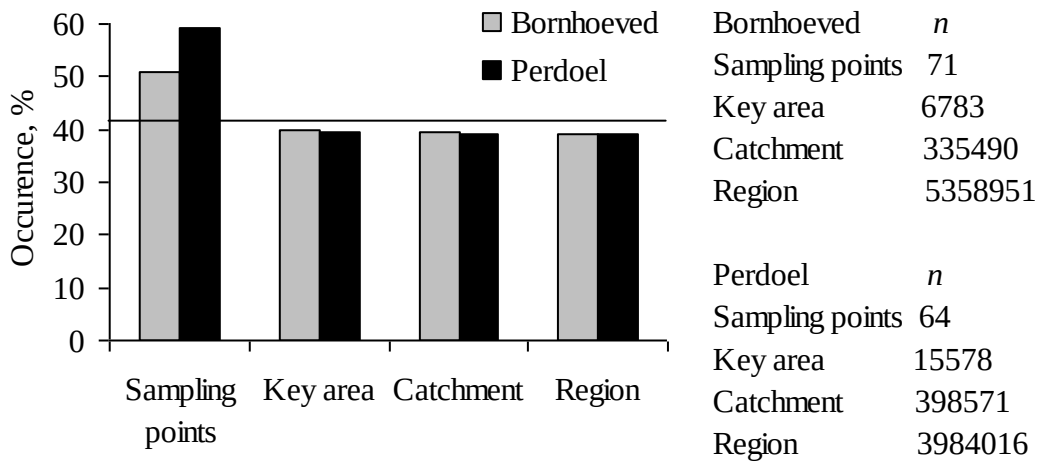

Fig. 9. The occurrence frequency of the group of main local landforms with colluvial deposits thicker than the median for a whole key area (LLF^M). The horizontal line shows the theoretical occurrence frequency of LLF^M (= 41.67 %).

The approach reflects a potential domination of soil erosion or colluvial accumulation. However, a direct comparison of the occurrence frequency does not indicate the intensity of these processes. For this purpose, experimental results have to be compared with the theoretical distribution of landforms for a random surface. The random surface is free of traces of any systematic processes. In case of activation of erosion or accumulation processes on such a surface, the number of landforms related with the dominant process will be increased. Hence, the more the deviation between random and natural surfaces, the more intensive the backbone process is manifested.

The group of LLF^M at the key areas consists of five types of landforms. The theoretical occurrence frequency of this number of landforms is 41.67 % (probability 5/12). The maximal difference from this level was observed for data from sampling points of Perdoel. It shows an intensive transformation of the land surface due to accumulation. At sampling points of Bornhoeved, the land surface transformation is also caused by accumulation and its intensity can be assessed as medium. For terrains around the differences between the experimental and the theoretical occurrence frequency of LLF^M, it is shown that processes of land surface transformation were caused by erosion. The intensity of the erosion can be assessed as low.

5.6. Phases of transformation of the local landforms

The fragmentation of the process of land surface transformation during colluvial sedimentation into several phases is useful for scientific reasons. These phases take turn at the same point of the land surface in duration of long-term colluviation. Direct observations on this time scale are not possible. However, in large spatial datasets all phases of land surface transformation can be determined at different sampling points by surveying both modern and buried surfaces during one

field campaign. Precise information on buried landforms at sampling points can be extracted from the thickness of colluvial layers, correlations among them as well as with the curvatures of modern land surface. Based on this three phases can be determined.

Local landforms 1, 2, 7 and 8 can be associated with the first phase of land surface transformation. This phase is characterized by *kmin* < *kh* < 0 and *kmin* < *kv* < 0 (Fig. 10A). Initially, such a surface shape is formed due to erosion. As a result of environmental condition changes, colluvial accumulation can occur at these types of landforms. On the local level, the accumulation processes during this phase can be determined by positive correlations between the thickness of colluvial layers and negative correlations of the thickness of colluvial layers with curvatures (*kh*, *kv*, *kmin* and *kmax*).

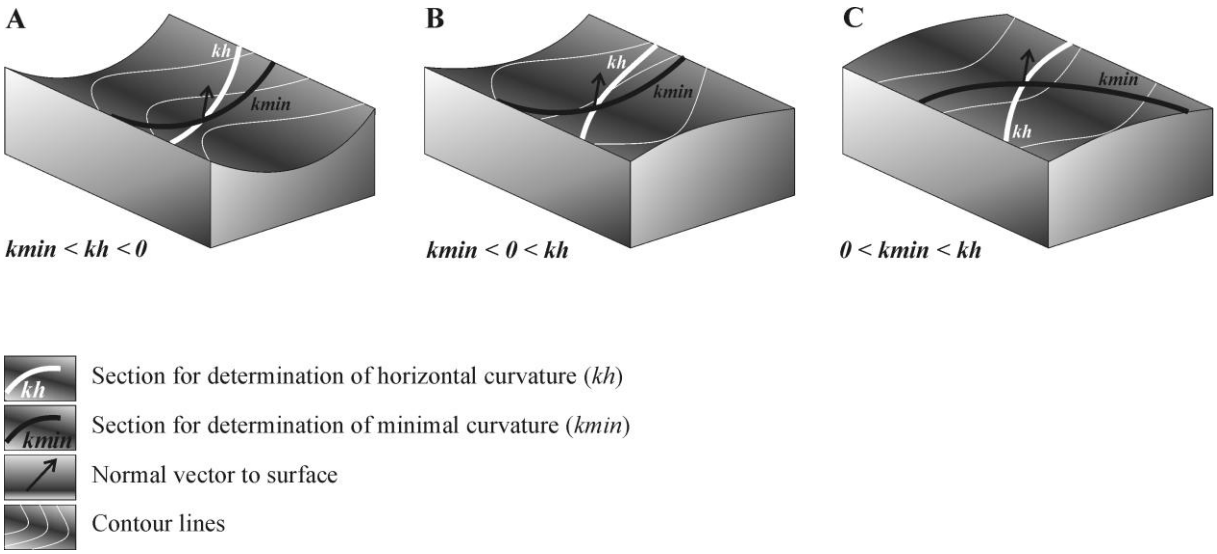

Fig. 10. Three phases of land surface transformation described by the combination of signatures of curvatures on the example of *kh* and *kmin*.

Local landforms 3, 4, 9 and 10 can be associated with the second phase of land surface transformation. This phase is characterized by *kmin* < *kh* < 0 < *kv* or *kmin* < *kv* < 0 < *kh* and can be entitled as "transit" (Fig. 10B). During this period, the geometry of the surface itself is still concave, but accumulation is already restricted by the positive signature of *kh* or *kv*. This phase can be determined by positive correlations between the thickness of colluvial layers and negative correlations of the thickness of colluvial layers with one of curvatures *kh*, *kv*, *kmin* and *kmax*. However, the correlation with *kmin* or *kmax* can be stronger than with *kh* or *kv* (Mitusov et al., 2013, appendix I).

Local landforms 5, 6, 11 and 12 can be associated with the third phase of land surface transformation. This phase is characterized by *kmin* < 0 < *kh* (and *kv*) or 0 < *kmin* < *kh* (and *kv*) and can be denoted as "inversion" (Fig. 10C). The result of such a transformation is characterized by a completely inverted surface and the absence of local colluvial accumulation. The following colluvial accumulation at these landforms may be caused only by the influence of remote factors.

The orographic component of these remote factors is described by the MCA. This phase can be determined by negative correlations between thicknesses of colluvial layers as well as by positive correlations of the thickness of colluvial layers with one of curvatures *kh*, *kv*, *kmin* and *kmax* (Mitusov et al., 2014, appendix II).

6. Conclusions

6.1. The spatial antagonism between land surface portions with a maximal colluvial storage and a high colluvial accumulation rate (CAR)

The positive relationship between the MCA and the thickness of colluvial deposits is described by a logarithmic trend. This indicates a monotonic impact of remote areas on the colluvial accumulation at sampling points. The strong negative relationship between the MCA and the CAR is also described by the logarithmic trend. This relationship is mainly caused by a disproportion between the absolute values of the MCA and colluvial storage that are components of the equation of the CAR. Previous relationships affect the formation of the negative relationship between the thickness of colluvial deposits and the CAR, which is described by the logarithmic trend too. The MCA is the regional MV. Hence, spatial antagonism between the thickness of colluvial deposits and the CAR is expressed on a regional level of consideration.

Spatial antagonism between zones of maximal colluvial storage and the fastest CAR was also found on the local level of consideration. Maximal values of the thickness of colluvial deposits were observed at four main local landforms (types 1, 2, 3 and 8). The highest CAR was observed at five other main local landforms (types 5, 6, 9, 10 and 12). These results are representative for both key areas. It has to be pointed out that the MCA and the indicator of the CAR have no formal mathematical relationships with local landforms. Hence, the relationships obtained on the local level are the obligatory function of erosion and accumulation processes on the land surface.

The strong spatial antagonism between land surface portions with maximal colluvial storage and a maximal CAR needs a conceptual understanding. Slopes and bottoms of valleys as well as groups of main local landforms have two different functions for the distribution of colluvial deposits. These functions can be associated with a dual system of the land surface memory. A fast CAR on a slope can be understood as the function of short-term land surface memory. The storing of a large volume of colluvial deposits at the bottom of a valley can be interpreted as the function of long-term land surface memory.

6.2. Application of the occurrence frequency of main local landforms for the assessment of the erosion/accumulation status of a terrain

A new geomorphometric approach for the potential erosion/accumulation assessment of the terrain was developed. The specific of this approach is that the whole terrain is considered as one unit disregarding internal variability. An example of such internal variability is the occurrence frequency of landforms at the sampling points. Finally, it is shown that the occurrence frequency of main local landforms is a quantitative criterion for the assessment of the scale of different processes of land surface transformation. Intensity of land surface modification can be assessed according to differences between the occurrence frequency of main local landforms on natural and random surfaces. This pure geomorphometric criterion is free of any subjective manipulations and can be used for the comparison of different terrains.

In the present investigation, approximately 40 % of the terrain around the key areas is covered by landforms which potentially store colluvial deposits. Other landforms, covering approximately 60 % of the terrain, can be considered as zones of potential erosion. This proportion reflects that the area around the key areas is potentially characterized by the domination of weak erosion processes.

6.3. Phases of land surface transformation on the local level

Correlations between the thickness of colluvial layers as well as with curvatures of the modern land surface reflect the shape of the former landforms buried by colluvial deposits. This provides an instrument for the investigation of land surface transformation under long-term sedimentation on the local level. Four types of local landforms characterize every phase of land surface transformation. The beginning of accumulation processes took place during the first phase (types 1, 2, 7 and 8). The beginning of a sensitive transformation of the land surface due to long-term sedimentation took place during the second phase (types 3, 4, 9 and 10). The third phase (types 5, 6, 11 and 12) is characterized by the strongest land surface transformation relative to the initial buried surface. In the end of this phase, sedimentation processes on the local level terminate.

The phases can be detected by objective methods of geomorphometry and statistics. The transformation sequence of main local landforms in time enables an automatic prediction (or reconstruction) of the land surface in the future (or past) at sampling points.

Acknowledgements

I wish to express my sincere gratitude and profound appreciation to everyone who has made this thesis possible. I am very thankful to my supervisor, Hans-Rudolf Bork, for allowing me to join his team, for his wise guidance and solid support during the entire research period. I am grateful to my second supervisor for kindly agreeing to supervise. Special thanks go to Peter Shary, Ian Evans and Takashi Oguchi for the very helpful revision of the articles and important consultations.

Furthermore, I would like to acknowledge the Graduate School "Human Development in Landscapes" of Christian-Albrechts University Kiel and personally Johannes Müller for financial support of the investigations.

In addition, I would like to thank Stefan Dreibrodt as well as other former and present colleagues, Olga E. Mitusova, Iraj Emadodin, Jann Wendt, Svetlana V. Khamnueva, Jürgen Zahrer, Piotr Jamrog, Annegret Larsen, Carolin Lubos, Sandra Kiesow, Doris Kramer, Andreas Mieth, Sophia Dazert and Markus Schütz, for research discussions and an excellent climate in our team.

I am grateful to the group of archaeologists led by Ingo Lütjens for successful cooperation in the field work at the key area of Bornhoeved and to the owners of the farm "Perdöler Mühle", family Overath, for allowing excavations at the key area of Perdoel. I am also indebted to the students of the Master's program "Environmental management" of Kiel University, to Mathias Bahns for excavations and assistance during the field campaign and to Eileen Küçükkaraca for English language editing.

My utmost gratitude is addressed to my family and parents for their love, understanding and strong support.

References

Ad-hoc-Arbeitsgruppe Boden (Ed.), 2005. Bodenkundliche Kartieranleitung, 5th edition. Bundesanstalt für Geowissenschaften und Rohstoffe in Zusammenarbeit mit den Staatlichen Geologischen Diensten, Hannover. 438 p.

Bork, H.-R., 1983. Die holozäne Relief- und Bodenentwicklung in Löβgebieten. Catena Suppl. 3, 1–93.

Brown, A.G., 2009. Colluvial and alluvial response to land use change in Midland England: An integrated geoarchaeological approach. Geomorphology 108, 92–106.

de Moor, J.J.W., Verstraeten, G., 2008. Alluvial and colluvial sediment storage in the Geul River catchment (The Netherlands) – Combining field and modelling data to construct a Late Holocene sediment budget. Geomorphology 95, 487–503.

Dietrich, W.E., Reiss, R., Hsu, M.-L., Montgomery, D.R., 1995. A process-based model for colluvial soil depth and shallow landsliding using digital elevation data. Hydrological Processes 9 (3-4), 383–400.

Dotterweich, M., 2008. The history of soil erosion and fluvial deposits in small catchments of central Europe: Deciphering the long-term interaction between humans and the environment — A review. Geomorphology 101, 192–208.

Dreibrodt, S., Lubos, C., Terhorst, B., Damm, B., Bork, H.-R., 2010. Historical soil erosion by water in Germany: Scales and archives, chronology, research perspectives. Quaternary International 222, 80–95.

Dreibrodt, S., Nelle, O., Lütjens, I., Mitusov, A., Clausen, I., Bork, H.-R., 2009. Investigations on buried soils and colluvial layers around Bronze Age burial mounds at Bornhöved (northern Germany): an approach to test the hypothesis of 'landscape openness' by the incidence of colluviation. The Holocene 19, 487–497. Appendix III.

Dreibrodt, S., Wiethold, J., *submitted*. Lake Belau and its catchment (northern Germany) – a northern central Europe key site of human impact on the landscape since the onset of agriculture. The Holocene.

Florinsky, I.V., (Ed.), 2012. Digital Terrain Analysis in Soil Science and Geology. Elsevier, Amsterdam, Boston, Heidelberg, London, New York, Oxford, Paris, San Diego, San Francisco, Singapore, Sydney, Tokyo. 379 p.

Follain, S., Minasny, B., McBratney, B.A., Walter, C., 2006. Simulation of soil thickness evolution in a complex agricultural landscape at fine spatial and temporal scales. Geoderma 133, 71–86.

Fryirs, K., 2013. (Dis)Connectivity in catchment sediment cascades: a fresh look at the sediment delivery problem. Earth Surface Processes and Landforms 38, 30–46.

Fuchs, M., Fischer, M., Reverman, R., 2010. Colluvial and alluvial sediment archives temporally resolved by OSL dating: Implications for reconstructing soil erosion. Quaternary Geochronology 5, 269–273.

Houben, P., 2008. Scale linkage and contingency effects of field-scale and hillslope scale controls of long-term soil erosion: Anthropogeomorphic sediment flux in agricultural loess watersheds of Southern Germany. Geomorphology 101, 172–191.

Houben, P., 2012. Sediment budget for five millennia of tillage in the Rockenberg catchment (Wetterau loess basin, Germany). Quaternary Science Reviews 52, 12–23.

Kaiser, K., Schoch, W.H., Miehe, G., 2007. Phases of soil erosion-derived colluviation in the loess hills of South Germany. Catena 69, 91–102.

Landesvermessungsamt Schleswig-Holstein, http://www.schleswig-holstein.de/LVERMGEOSH/DE/LVERMGEOSH_node.html 2012.

Lang, A., 2003. Phases of soil erosion-derived colluviation in the loess hills of South Germany. Catena 51, 209–221.

Lang, A., Hönscheidt, S., 1999. Age and source of colluvial sediments at Vaihingen–Enz, Germany. Catena 38(2), 89–107.

Mitas, L., Mitasova, H., 1998. Distributed erosion modeling for effective erosion prevention. Water Resources Research 3, 505–516.

Mitasova, H., Mitas, L., Brown, W.M., Johnston, D., 1997. GIS tools for erosion/deposition modeling and multidimensional visualization. Part IV: Processed based erosion simulation for spatially complex conditions and its applications to installations. Part V: Impact of transport capacity and terrain structures on erosion simulations. Report for USA CERL. Urbana-Champaign: University of Illinois, 30 p. Website: http://www4.ncsu.edu/~hmitaso/gmslab/reports/cerl97/rep97.html]

Mitusov, A.V., *in revision*. Assessment of potential erosion/accumulation based on local landforms related with colluvial deposits. Geomorphology, Appendix IV.

Mitusov, A.V., Dreibrodt, S., Mitusova, O.E., Khamnueva, S.V., Bork, H.-R., 2013. Detection of land surface memory by correlations between thickness of colluvial deposits and morphometric variables. Geomorphology 191, 109–117, Appendix I.

Mitusov, A.V., Mitusova, O.E., Wendt, J., Dreibrodt, S., Bork, H.-R., 2014. Correlation of colluvial deposits with the modern land surface and the problem of slope profile description. Geomorphology 220, 30–40, Appendix II.

Reiß, S., Dreibrodt, S., Lubos, C.C.M., Bork, H.R., 2009. Land use history and historical soil erosion at Albersdorf (northern Germany)—Ceased agricultural land use after the pre-historical period. Catena 77(2), 107–118.

Rommens, T., Verstraeten, G., Lang, A., Poesen, J., Govers, G., Van Rompaey, A., Peeters, I., 2005. Soil erosion and sediment deposition in the Belgian loess belt during the Holocene: establishing a sediment budget for a small agricultural catchment. The Holocene 15(7), 1032–1043.

Schneider, A., Gerke, H.H., Maurer, T., 2011. 3D initial sediment distribution and quantification of mass balances of an artificially-created hydrological catchment based on DEMs from aerial photographs using GOCAD. Physics and Chemistry of the Earth 36, 87–100.

Shary, P.A., 1995. Land Surface in Gravity Points Classification by a Complete System of Curvatures. Mathematical Geology 27(3), 373–390.

Shary, P.A., 2012. The mathematical basis of local morphometric variables. In: Florinsky, I. V. (Ed.), Digital terrain analysis in soil science and geology. Appendix a. Elsevier, Amsterdam, Boston, Heidelberg, London, New York, Oxford, Paris, San Diego, San Francisco, Singapore, Sydney, Tokyo, pp. 289–313.

Shary, P.A., Sharaya, L.S., Mitusov, A.V., 2002. Fundamental quantitative methods of land surface analysis. Geoderma 107, 1–35.

Shary, P.A., Sharaya, L.S., Mitusov, A.V., 2005. The problem of scale-specific and scale-free approaches in geomorphometry. Geografia Fisica e Dinamica Quaternaria. Volume devoted to 32 International Geological Congress (December, 2005). 28 (1), 81–101.

StatSoft, Inc., 2013. Electronic Statistics Textbook. Tulsa, OK: StatSoft. WEB: http://www.statsoft.com/textbook/.

Tarboton, D.G., 1997. A new method for the determination of flow directions and upslope areas in grid digital elevation models. Water Resources Research 30, 9–17.

Tunnicliffe, J.F., Church, M., 2011. Scale variation of post-glacial sediment yield in Chilliwack Valley, British Columbia. Earth Surface Processes and Landforms 36, 229–243.

Walling, D.E., 1983. The sediment delivery problem. Journal of Hydrology 65, 209–237.

Wood, J., 2009. Overview of software packages used in geomorphometry. In: T. Hengl and H.I. Reuter (Eds.). Geomorphometry: Concepts, Software, Applications. Developments in Soil Science, Volume 33. Amsterdam, etc.: Elsevier, Chapter 10, 257–267.

List of abbreviations

General

CAR	colluvial accumulation rate
DEM	digital elevation model
LiDAR	light detection and ranging
LLF^{M}	main local landforms potentially related with the storage of colluvium
M	colluvial deposits
M_{group}	median thickness of colluvium in group of landforms of one type
M_{key}	median thickness of colluvium for whole key area
MVs	morphometric variables
p	significance level
R^2	determination coefficient
r_S	non-parametric rank correlation coefficient of Spearman

Morphometric variables

Z	altitude
GA	slope steepness
MCA	maximal catchment area
MDA	maximal dispersal area
kh	horizontal (tangential) curvature
kv	vertical (profile) curvature
E	difference curvature
KA	total accumulation curvature
rot	rotor
KR	total ring curvature
kve	vertical excess curvature
khe	horizontal excess curvature
kmax	maximal curvature
kmin	minimal curvature
K	total Gaussian curvature
H	mean curvature
M	unsphericity

Affidavit

I, Andrey V. Mitusov confirm the following:

- that apart from the supervisor's guidance the content and design of the essay all is my own work;

- that the material of the thesis has been published and submitted for publications in international journals:

Mitusov, A.V., Dreibrodt, S., Mitusova, O.E., Khamnueva, S.V., Bork, H.-R., 2013. Detection of land surface memory by correlations between thickness of colluvial deposits and morphometric variables. Geomorphology 191, 109–117. **Appendix I**

Mitusov, A.V., Mitusova, O.E., Wendt, J., Dreibrodt, S., Bork, H.-R., 2014. Correlation of colluvial deposits with the modern land surface and the problem of slope profile description. Geomorphology 220, 30–40. **Appendix II**

Dreibrodt, S., Nelle, O., Lütjens, I., Mitusov, A., Clausen, I., Bork, H.-R., 2009. Investigations on buried soils and colluvial layers around Bronze Age burial mounds at Bornhöved (northern Germany): an approach to test the hypothesis of 'landscape openness' by the incidence of colluviation. The Holocene 19, 487–497. **Appendix III**

Mitusov, A.V. Assessment of potential erosion/accumulation based on local landforms related with colluvial deposits. Geomorphology (*submitted*). **Appendix IV**

- that the thesis has been prepared subject to the Rules of Good Scientific Practice of the German Research Foundation.

Andrey V. Mitusov

Appendix I

Mitusov, A.V., Dreibrodt, S., Mitusova, O.E., Khamnueva, S.V., Bork, H.-R., 2013. Detection of land surface memory by correlations between thickness of colluvial deposits and morphometric variables. Geomorphology 191, 109–117.

Geomorphology 191 (2013) 109–117

Contents lists available at SciVerse ScienceDirect

Geomorphology

journal homepage: www.elsevier.com/locate/geomorph

Detection of land surface memory by correlations between thickness of colluvial deposits and morphometric variables

A.V. Mitusov *, S. Dreibrodt, O.E. Mitusova, S.V. Khamnueva, H.-R. Bork

Institute for Ecosystem Research, Christian-Albrechts-University of Kiel, Olshausenstrasse 40, D-24098 Kiel, Germany

ARTICLE INFO

Article history:
Received 6 April 2012
Received in revised form 5 March 2013
Accepted 11 March 2013
Available online 16 March 2013

Keywords:
Colluvial deposits
Morphometric variables
Memory effects
Land surface
Geomorphometry

ABSTRACT

Some morphometric variables store information about past land surfaces longer than others. This property of morphometric variables is recognised as land surface memory. Slope deposits, soils, and vegetation also have this memory. In this study, a memory effect was quantitatively detected by Spearman correlations between thickness of colluvium and morphometric variables of the modern land surface.

During long-term sedimentation, the sign of horizontal curvature (*kh*) may be inverted from minus to plus, suggesting that locations with positive *kh* values are not accumulation zones. However, the thickness of colluvial deposits at such locations in our study area indicates sediment accumulation. The sign of minimal curvature (*kmin*) tends to be more stable and remains negative. This difference provides the stronger correlation of colluvial layer thickness with *kmin* than with *kh*. The strongest correlation was found for total thickness of the colluvial deposits of the Neolithic and Iron Age with *kmin* (−0.84); the correlation with *kh* was weaker (−0.71).

1. Introduction

The fact that the modern land surface stores information about the past is a basic principle of geomorphology. In geomorphometry it is known that one group of morphometric variables (MVs) can store information about past land surfaces longer than others (Shary, 1991; Shary et al., 2002). Comparisons of these MVs enable quantitative description of the land surface memory. Unfortunately, such investigations are not common in geomorphometry. However, investigations of soil memory are popular in classical soil science (Targulian and Sokolova, 1996; Targulian, 1999; Targulian and Goryachkin, 2008; Lin, 2011) and are used for quantitative palaeoenvironment reconstructions (e.g. Mitusov et al., 2009).

To understand land surface memory from a geomorphometrical point of view, one example of interaction between memory effects in soil and the land surface will be considered (Shary et al., 2002). MVs that depend on the gravity field potentially affect the present surface flow. These MVs are known as "morphometric pre-requisites of surface runoff" (Shary, 1995). The direction, pattern or other properties of flow will be changed where the land surface changes, e.g. due to tilting. At the same time, changes in the morphometric pre-requisites of surface runoff will take place, implying that this group of MVs will reflect new information about the land surface. However, some landforms that were formed in the past can be resistant to land surface transformation. These old forms are described by MVs that are not dependent on the gravity field. These MVs are known as "characteristics of geometrical landforms" (Shary, 1995). In the case of land surface transformation, the characteristics of soils (sediments and vegetation) that formed under the long-term impact of flows will also change at different rates. In this situation, such landscape properties will show stronger correlations with characteristics of geometrical landforms rather than with morphometric pre-requisites of surface runoff: i.e. with field-invariant rather than with gravity-field-specific MVs.

The above example considers relatively fast transformation of a large part of the land surface as a whole body without changes in the local geometry of the surface. Such events are more likely in tectonically active regions. For relatively stable geological regions, land surface transforms are mainly due to erosion–accumulation processes. For example, a pattern of surface flows varies in time due to deposition of sediments in an old channel; hence the location of sediments indicates the past pattern of surface flows. The location of the sediments can be determined by material measurements (sampling) and by the analysis of land surface features.

The general idea of land surface memory detection in conditions of long-term sedimentation in tectonically stable regions is clear. Many features of spatial distribution of colluvial (slope) deposits, however, cannot be described in general terms. Methods of geomorphometry and statistical comparisons have to be used for quantitative description of land surface memory, with a detailed geomorphometrical explanation of the memory. Generation of such an explanation is the goal of the present investigation.

The research is based on consideration of correlations between MVs of the modern land surface and thickness of colluvial deposits

* Corresponding author. Tel.: +49 431 880 7444; fax: +49 431 8804083.
E-mail address: a_mitusov@mail.ru (A.V. Mitusov).

0169-555X/$ – see front matter © 2013 Elsevier B.V. All rights reserved.
http://dx.doi.org/10.1016/j.geomorph.2013.03.006

of different ages, in conditions of a relatively small dry valley located in a tectonically stable area with unindurated surface materials.

2. Study area and methods

2.1. Region

The study area (54° 04′ N; 10° 15′ E) is located in northern Germany approximately 40 km south of Kiel (Fig. 1). The main morphological elements of the surrounding landscapes, as well as the substrate (outwash sands at the study site), result from the Weichselian Glaciation (Piotrowski, 1991). After some alteration of the land surface during the Late Glacial, natural soil formation proceeded until the Neolithic settlers cleared the forests around 4300 cal BC (Hoika, 1993, 1994; Hartz, 2004). The area has been under extensive agricultural land use since the Slavonic Period of Early Medieval Times (Dreibrodt et al., 2009). Today, Cambisols and Luvisols (FAO, 1998) are the dominant soil types in the region (Schleuss, 1991). At many sites these soils are developed in the remnants of capped pristine soils on upper slopes, or in the associated colluvia downslope. The land use and soil erosion history of the region are well investigated (e.g. Garbe-Schönberg et al., 1998; Lütjens and Wiethold, 1999; Dreibrodt and Bork, 2005).

2.2. Study area

The study area is situated in the uppermost part of a small dry valley. Trenches up to 3 m deep and up to 200 m long were excavated in the thalweg area; 23 cores up to 2 m depth were made on slopes (Fig. 1). A digital elevation model (DEM) with a 5 m grid mesh was made based on a differential GPS survey. The thickness of colluvial layers was measured every 20 cm along the trenches. Mean thickness of colluvial layers was calculated for each DEM cell that was crossed by the trenches. For auger cores, however, this procedure was unnecessary. As a result, the data set consisted of the 71 points shown in Fig. 2.

2.3. Colluvial deposits

The sequences of colluvial layers and soil horizons were identified and described using conventional methods (FAO, 1998; Munsell, 2000; Ad-hoc-Arbeitsgruppe Boden, 2005). Colluvial layers were denoted with the abbreviation M for "*migrare*" (lat.) according to Ad-hoc-Arbeitsgruppe Boden (2005). Detailed description of the soils and colluvial deposits was made by Dreibrodt et al. (2009).

Colluvial deposits were considered because their spatial distribution is strongly dependent on erosion–accumulation processes caused by surface flow. An important advantage of the investigation of colluvial deposits is the possibility of determining their age. Sequences of colluvial deposits are mainly used for the assessment of palaeoerosion during the Holocene and palaeorelief reconstruction (e.g. Dotterweich, 2008; Dreibrodt et al., 2010). Quantitative models of spatial distribution of colluvial deposits (e.g. Ries, 2002; Follain et al., 2006; Reiss et al., 2008; Mitusova, 2010) are based on geomorphometric analysis of the modern land surface and on methods of predictive soil mapping (e.g. Moore et al., 1993; McBratney et al., 2000, 2003; Scull et al., 2003).

2.4. Morphometric variables

During recent decades many MVs calculated from DEMs have been introduced to geomorphometry (e.g. Shary, 1995; Zhou et al., 2008; Hengl and Reuter, 2009). In our investigation the land surface was described by 17 MVs of general geomorphometry (Table 1). These MVs were combined by the physical–mathematical theory of Shary (1995) into one system, with clear internal relationships (e.g. Evans, 1980; Shary, 1995; Evans and Cox, 1999; Shary et al., 2002; Sharaya and Shary, 2003; Shary et al., 2005), which is important for the correct interpretation of correlations between thickness of colluvial deposits and the MVs.

The MVs were divided into three groups: i) morphometric pre-requisites of surface runoff; ii) characteristics of land surface dissection; and iii) characteristics of geometrical landforms. Depending on the situation, one group of MVs or another can show the best correlations with landscape properties (e.g. Mitusov, 2001; Mitusov and Mitusova, 2005; Shary, 2005). Maps of the basic MVs are depicted in Fig. 2. For the calculation of the MVs, Analytical GIS Eco was used.

According to the statistical hypothesis of Shary (1995), the frequency of occurrence of signs of any curvatures can be predicted in a statistical sense for large data sets. Based on this hypothesis, positive and negative signs of *kh* (horizontal curvature), *kv* (vertical curvature) and *H* (mean curvature) occur in equal proportions, *kmin* (minimal curvature) < 0 or *kmax* (maximal curvature) > 0 occurs in the two-thirds of observations, and *kmin* > 0 or *kmax* < 0 in the one-third. The statistical hypothesis can also predict combinations of the signs of different curvatures. Hence, in the one-third of observations the sign of *H* does not coincide with

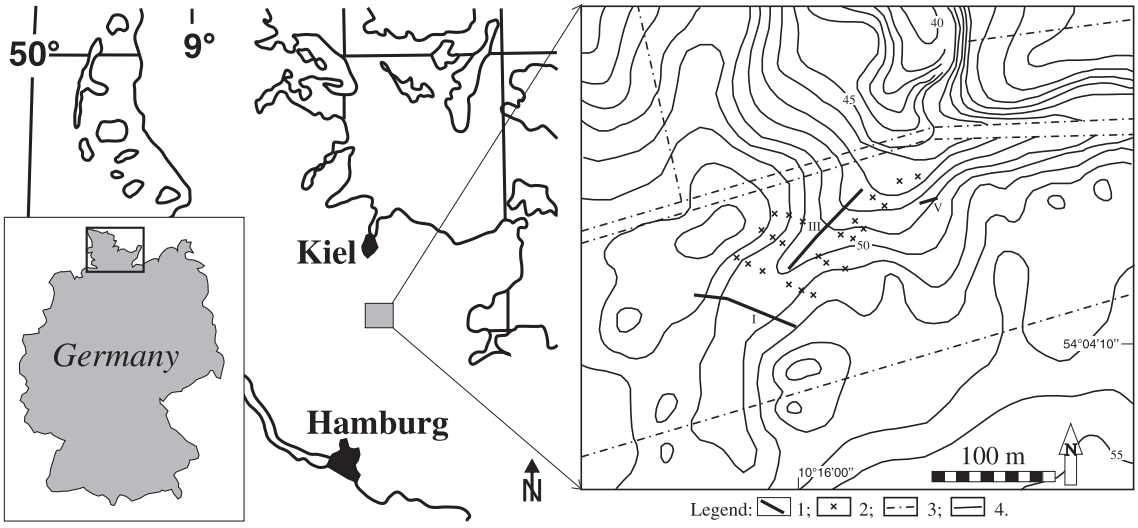

Fig. 1. Study area. Legend: 1 — trenches (I, III and V), 2 — auger sites; 3 — hedgerows; 4 — contour lines (contour lines have 1 m vertical interval).

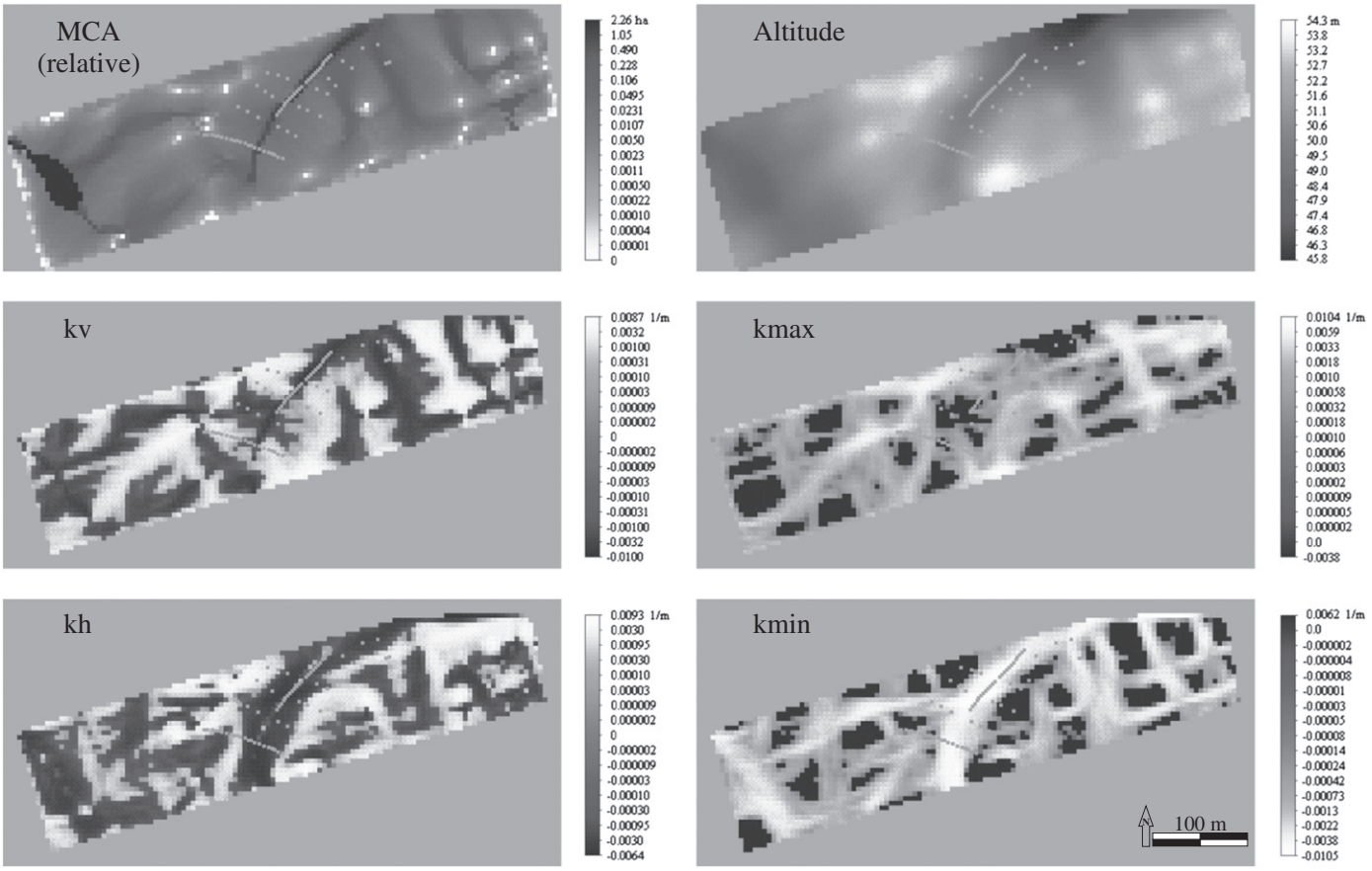

Fig. 2. Maps of basic morphometric variables, also showing the 71 sampling points.

those of *kh* or *kv*. Therefore, *H* as well as the Laplacian of altitude cannot be considered as universal descriptors of relative accumulation or deflection zones. This contradiction has not been well understood until now. In a relatively small data set, disagreement between signs of *H* and *kh* or *kv* can occur only at a few points; it can be sensed as a random error and may be excluded from the data set. In a large data set such exclusion can significantly impact the results of modelling and interpretation.

2.5. Statistical methods

Statistical analysis of the data was made using the conventional methods described in StatSoft (2010). For the detection of normality, the Kolmogorov–Smirnov test was applied. Quantitative comparisons were made by means of Spearman's non-parametric rank correlation coefficient (r_s). The non-parametric method was used because it is not dependent on a normal distribution of the data.

Table 1
Morphometric variables of general geomorphometry.

Variable name, unit	Description	Reference
Altitude (*Z*), m	Altitude zonality	Shary et al., 2002
Morphometric pre-requisites of surface runoff		
Slope steepness (*GA*), degrees	Flow rate	Shary et al., 2002
Maximal catchment area (*MCA*), m^2	Maximum area from which material moving down slope may be collected	Speight, 1968
Maximal dispersal area (*MDA*), m^2	Maximal area at which materials moving down slope may be diffused	Speight, 1974
Horizontal (tangential) curvature (*kh*), m^{-1}	Flow convergence/divergence	Krcho, 1983
Vertical (profile) curvature (*kv*), m^{-1}	Relative flow deceleration/acceleration	Evans, 1972
Difference curvature (*E*), m^{-1}	Compares *kh* (in plane) and *kv* (in profile)	Shary, 1995
Total accumulation curvature (*KA*), m^{-2}	Reveals relative accumulation zones	Shary, 1995
Characteristics of land surface dissection		
Rotor (*rot*), m^{-1}	Flow line rotation direction	Shary, 1995
Total ring curvature (*KR*), m^{-2}	Flow line twisting	Shary, 1995
Horizontal excess curvature (*khe*), m^{-1}	Describes to what extent *kv* (*kh*) is larger than minimal curvature (*kmin*) at the same point	Shary, 1995
Vertical excess curvature (*kve*), m^{-1}		Shary, 1995
Characteristics of geometrical land forms		
Maximal curvature (*kmax*), m^{-1}	Geometrical ridge forms	Gauss, 1827
Minimal curvature (*kmin*), m^{-1}	Geometrical valley forms	Gauss, 1827
Total Gaussian curvature (*K*), m^{-2}	Separated elliptic and saddle landforms	Gauss, 1827
Mean curvature (*H*), m^{-1}	Connected to “equilibrium” surface condition	Gauss, 1827
Unsphericity (*M*), m^{-1}	Surface deviation from spherical form	Shary et al., 2005

As colluvial layers have a fragmentary spatial distribution, the data set was modified for r_s computation. At points where a layer was not found, the thickness was marked as zero. For binary consideration of the existence of colluvial deposits, zero means the logic variable "NO", and other values mean "YES".

3. Properties of the data obtained

3.1. Relationships among morphometric variables at sampling points

MVs are not independent parameters (e.g. Shary, 1995). For large territories correlations between curvatures can be predicted based on Shary's statistical hypothesis (e.g. Shary, 1995; Sharaya and Shary, 2003). However, experimental plots for landscape investigations are often relatively small and restricted to one landscape element, e.g., an arable field, slope or catchment. Because the spatial distribution of sampling points is generally non-random, deviations from the statistical hypothesis are likely. In the current investigation, the positive correlation between *kh* and *kv* that can be expected for large data sets (Evans, 1980) was not found. At the same time, abnormally strong correlations were established among *kh*, *kmin* and *H* (Table 2) because the study area is small and covers only one valley.

In our data set strong relationships among maximal catchment area (*MCA*), maximal dispersal area (*MDA*) and altitude were found (Table 2). That is typical for small plots as well as for a catena along one slope (e.g. Mitusov, 2001; Shary, 2005). Between this group of MVs and the group of curvatures (mainly *kh*, *kmin*, and *H*) strong correlations were also observed (Table 2). This is due to extreme values of these MVs in the floor of the valley studied. Because the area studied here does not cover a whole catchment, only relative values of *MCA* and *MDA* could be calculated. However, the DEM covered a sufficiently large area to minimize the border effects in sampling points.

3.2. Stratigraphy of colluvial layers

The chronology of colluvial deposits was based on 18 AMS (Accelerator Mass Spectrometry) radiocarbon dates of charcoal (Dreibrodt et al., 2009). Errors in the determination of colluvial layer thickness can arise due to the similarity of deposits of different ages. A sum of layers always contains less random variations than an individual layer. However, during the combination of several individual layers, the temporal resolution decreases and important information can be lost. Thus, the precision of colluvial layer determination is always a balance between the number of errors and the temporal resolution of the final data set.

Colluvial layer M1 was deposited during the Middle Neolithic (~3500–3000 cal. BC) and Late Neolithic (~2500–2200 cal. BC) times. The first period is related to the Funnel Beaker Culture. The layer M1 has the greatest thickness and occurs most often in the data set. At 22 points M1 is associated with a buried soil. In this article only the sum of M1 and buried soil thickness was considered. This sum was labelled M1fA.

During the Bronze Age the area was protected against erosion and colluvial deposits of this period were not found. Layer M2 contained charcoals from the Iron Age (396–212 cal. BC and ~AD 250–400 cal.). Beginning in this period, agricultural land use of the landscape probably intensified. Layers M3 and M4 were deposited during Medieval (~AD 600–1400 cal.) and Modern times. At many points the border between M3 and M4 was not clear. The sum of M3 and M4 was thus considered and labelled MAp. The maximum thickness of MAp was 40 cm, coinciding with the maximal depth of elevated content of heavy metals (Dreibrodt et al., 2009).

Basic descriptive statistics of the thickness of the colluvial layers are given in Table 3. The criteria of normality (Kolmogorov–Smirnov test) showed no deviations from the normal statistical distribution for any colluvial layer. Standard deviation (*SD*) was low for the individual layers and increased for the sum of layers, coinciding with statistical theory. Information about *MCA* allows spatially distributed sampling points to be aggregated into one profile. This aggregate profile permits visualization of the short- and long-wave variations in the data. Often this operation helps to detect random errors in the data set before statistical analysis.

A generalised profile of the sequence of colluvial layers MAp–M2–M1fA was built in the coordinates of *MCA* (Fig. 3). This bar chart shows the depth and thickness of the individual colluvial layers at all points of the data set (Fig. 3A). The highest values of *MCA* were found in the valley bottom, and the lowest values were on divides (Fig. 3B). At 17 points in the sequence of colluvial layers, layer M2 was absent and the sequence MAp–M1fA was found. This indicates that if M2 had been present at these points, it was destroyed, probably by ploughing. In the valley bottom, where values of *MCA* are relatively higher, the layer M2 was preserved continuously.

Thus, erosion–accumulation processes were the dominant factor for the spatial distribution of colluvial deposits. Ploughing was able to destroy older deposits and the youngest layer that was still in development. The morphology of the deposits did not reflect any traces of geological transformation of the area during approximately the last 5000 years.

4. Relationships between thickness of colluvial layers and modern land surface

4.2. Mean thickness of colluvial deposits in different geomorphometric positions

Signs of r_s between curvatures and thickness of colluvium (Table 5) indicate that the deposits concentrate in concave locations. Fig. 4 shows

Table 2
Spearman correlations among morphometric variables ($n = 71$).

	Z	*GA*	*MCA*	*MDA*	*kh*	*kv*	*E*	*KA*	*kmin*	*kmax*	*H*	*K*	*M*	*rot*	*KR*	*khe*
GA	0.29															
MCA	−0.88	−0.50														
MDA	0.63	0.69	−0.79													
kh	0.74	0.55	−0.89	0.75												
kv	0.24	0.27	−0.25	0.57	*											
E	−0.30	−0.23	0.42	*	−0.63	0.67										
KA	*	−0.27	*	*	*	*	*									
kmin	0.69	0.70	−0.82	0.91	0.80	0.53	*	*								
kmax	0.52	0.25	−0.61	0.64	0.58	0.58	*	−0.26	0.53							
H	0.71	0.64	−0.84	0.92	0.80	0.60	*	*	0.96	0.71						
K	0.36	0.27	−0.36	0.34	0.35	*	*	0.57	0.53	*	0.35					
M	−0.50	−0.73	0.63	−0.74	−0.66	−0.30	0.27	*	−0.89	*	−0.74	−0.70				
rot	*	*	*	*	*	*	*	*	*	*	*	*	*			
KR	−0.48	−0.58	0.60	−0.62	−0.59	*	0.27	0.35	−0.69	*	−0.62	−0.39	0.68	*		
khe	*	*	*	−0.28	0.27	−0.84	−0.83	*	−0.27	*	−0.26	*	*	*	*	
kve	−0.47	−0.55	0.61	−0.44	−0.77	0.36	0.84	*	−0.54	*	−0.44	−0.32	0.63	*	0.67	−0.49

* Correlation not significant at $p \leq 0.05$.

Table 3
Descriptive statistics of colluvial layer thickness (in cm).

	MAp	M2	M1fA	M1fA + M2	M total
Number (n)	71	42	50	59	71
Min	20.2	7.2	0.8	5.0	22.0
Max	42.5	31.0	95.4	113.8	123.6
Mean	32.3	17.9	39.9	46.6	67.2
Median	32.0	17.9	37.4	40.0	67.0
Skewness	−0.1	0.3	0.5	0.6	0.1
Kurtosis	−0.7	0.0	0.0	−0.6	−1.0
Standard deviation (SD)	5.2	5.2	22.1	28.0	27.8

the mean thickness of the colluvial deposits in zones defined by the signs of basic curvatures. Minimal mean thickness of deposits was observed in the zone of positive *kmin*. Maximal mean thickness of deposits was found in the zone of negative *kmax*. Hence, these curvatures describe the spatial distribution of colluvial deposits better than the other curvatures such as *kh* or *kv*. These results confirm the correlation between curvatures and thickness of colluvial layers (Table 5).

4.1. Correlations with morphometric variables

Correlation coefficients among thicknesses of colluvial layers are given in Table 4. The uppermost layer (MAp) had no significant correlations with other individual layers. The correlation between individual layers M1fA and M2 was weak. The strength of correlations between the MVs and thickness of colluvial layers generally increased from upper MAp to deeper M1fA (Table 5). For individual colluvial layers the strongest correlation was detected between the oldest layer M1fA and *H*.

The sum of layers reflects a longer period of sedimentation and has fewer random errors than individual layers. As a result, correlations between the sum of layers and the MVs were often stronger than between individual layers and the MVs (Table 5). The strongest correlation found was between M1fA + M2 and *kmin* ($r_s = -0.84$; $n = 71$). In general, correlations of MVs with M1fA + M2 were somewhat stronger than with M total.

There was no reason to consider correlations of colluvial deposits with altitude, *MCA*, and *MDA* separately. These MVs describe regional aspects of accumulation of material in the valley bottom. In small experimental plots these MVs usually have strong relationships with curvatures (mainly *kmin* and *kh*). Along the profile in coordinates of *MCA* (Fig. 3A), a monotonous increase of colluvium thickness was observed and confirmed by rank correlation with *MCA*. Many short-wave oscillations of thickness of colluvial layers along this profile (Fig. 3A) were related to other parameters and, probably, to noise in the data set.

kh is related to convergence and divergence of flows in plan, while *kv* is related to relative acceleration and deceleration of flows in profile. The processes of matter accumulation of these two types of events are known as the first and second accumulation mechanisms (e.g. Aandahl, 1948). Comparisons of r_s with *kv* and *kh* can indicate what types of accumulation mechanisms have stronger impact on the spatial distribution of colluvial deposits. The strength of r_s between *kh* and thickness of buried layers increased with depth. At the same time r_s with *kv* was relatively stable. The strongest r_s was found between the thickness of the upper layer (MAp) and *kv*; r_s with *kh* was not significant.

Thus the youngest colluvial layer is better linked with landform in profile, and older layers with landform in plan. The dynamic nature of the second accumulation mechanism, and the variation of correlations of *kh* and *kv* with colluvial layers of different ages, have probably shown that landforms in plan are more stable than in profile.

Characteristics of land surface dissection are the least studied MVs. Curvatures in this group are important for landform classification (Shary, 1995). These curvatures often improve regression models for predictive mapping of spatial distribution of landscape properties (e.g. Mitusov and Mitusova, 2005). Total ring curvature (*KR*) shows the curve of flow lines; a positive r_s value with colluvium thickness indicates a statistical tendency of increased thickness where flow lines are most curved. If a data set is restricted by valley borders, the flow lines are mainly convergent. In this condition, *KR* can be interpreted as an analogue of *kh*. For the middle layer (M2), *KR* was more sensitive than *kh*. Two slopes of a valley can be distinguished by rotor (*rot*) based on the direction of flow line rotation. Absence of r_s with *rot* indicates that the balance of colluvial mater is similar on two slopes of the valley. Apart from temperature regime, differences can arise, for example, if one slope is considerably longer or steeper than the other.

Horizontal and vertical excess curvatures (*khe* and *kve*) have negative relationships (Table 2). Positive r_s between *kve* and colluvium thickness (Table 5) showed the tendency of thickness increase in points where *kh* tends to *kmin* and *kv* to *kmax* at the same time. Positive r_s between *khe* and colluvium thickness (Table 5) indicated a thickness increase at points where *kh* tends to *kmax* and *kv* to *kmin*. The correlation coefficients showed different tendencies for spatial distribution of the upper layer (MAp) and deeper layers. This also coincided with a non-significant r_s ($p = 0.05$) between MAp and other layers (Table 4). Such results highlight the important role of the convergent–accelerative landform types for the deeper layer M1fA and divergent–decelerative landform types for the upper layer MAp. For the layer M2 a unique situation was observed: two excess curvatures simultaneously showed the same signs of r_s (Table 5).

4.3. Detection of memory effects

Memory effects are observed where descriptors of geometrical landforms store more information about past erosion–accumulation processes than about morphometric pre-requisites of surface runoff. Considering the distribution of sampling points in coordinates of *kh* and *kmin* is necessary in order to understand the mechanism of memory effect detection (Fig. 5). The sampling points were distributed in three clusters (Fig. 5A). Cluster IV is empty because in all situations $kh \geq kmin$ (Shary, 1995). Cluster III is most dense and contains points with $kmin < kh < 0$. Cluster II includes points with $kmin < 0 < kh$. Cluster I contains the smallest number of sampling points with $0 < kmin < kh$. The frequencies of sampling points in these clusters (Fig. 5B) were in accordance with the statistical hypothesis of Shary (1995). According to this hypothesis, $kmin < 0$ occurs in one-third more often than $kh < 0$.

The mean thickness of M total was 40.3 ± 18.4 cm (error range = *SD*) for Cluster I; 50.7 ± 20.7 cm for Cluster II; and 84.7 ± 20.6 cm for Cluster III. In at least one-half of the points of Cluster II, the thickness of colluvial deposits was higher than the mean for Cluster I. That is an absolute indicator of colluvium accumulation in the past. However, the shape of the modern land surface at all points in Cluster II had a positive *kh* value. From a geomorphometrical point of view, a positive value of *kh* cannot be considered as a predictor of colluvium accumulation (e.g. Aandahl, 1948; Shary, 1995). Therefore a disagreement between thickness of colluvium and the sign of *kh* occurred at the points in Cluster II. This disagreement reduced the correlation between *kh* and colluvium thickness for the whole data set. However, values of *kmin* for Cluster II were still negative. As a result, the correlation of colluvium thickness with *kmin* was stronger than that with *kh*. This is the basis for land surface memory detection.

5. Discussion

5.1. Correlations between thickness of colluvial layers and the MVs

The strength of correlations between the thicknesses of individual colluvial layers and the MVs mainly increased with depth. In general, correlations between the thickness of the upper colluvial layer (MAp) and the MVs were not so strong; the strongest correlation was with *kv* ($r_s = -0.41$). For the deepest colluvial layers, the other MVs such as

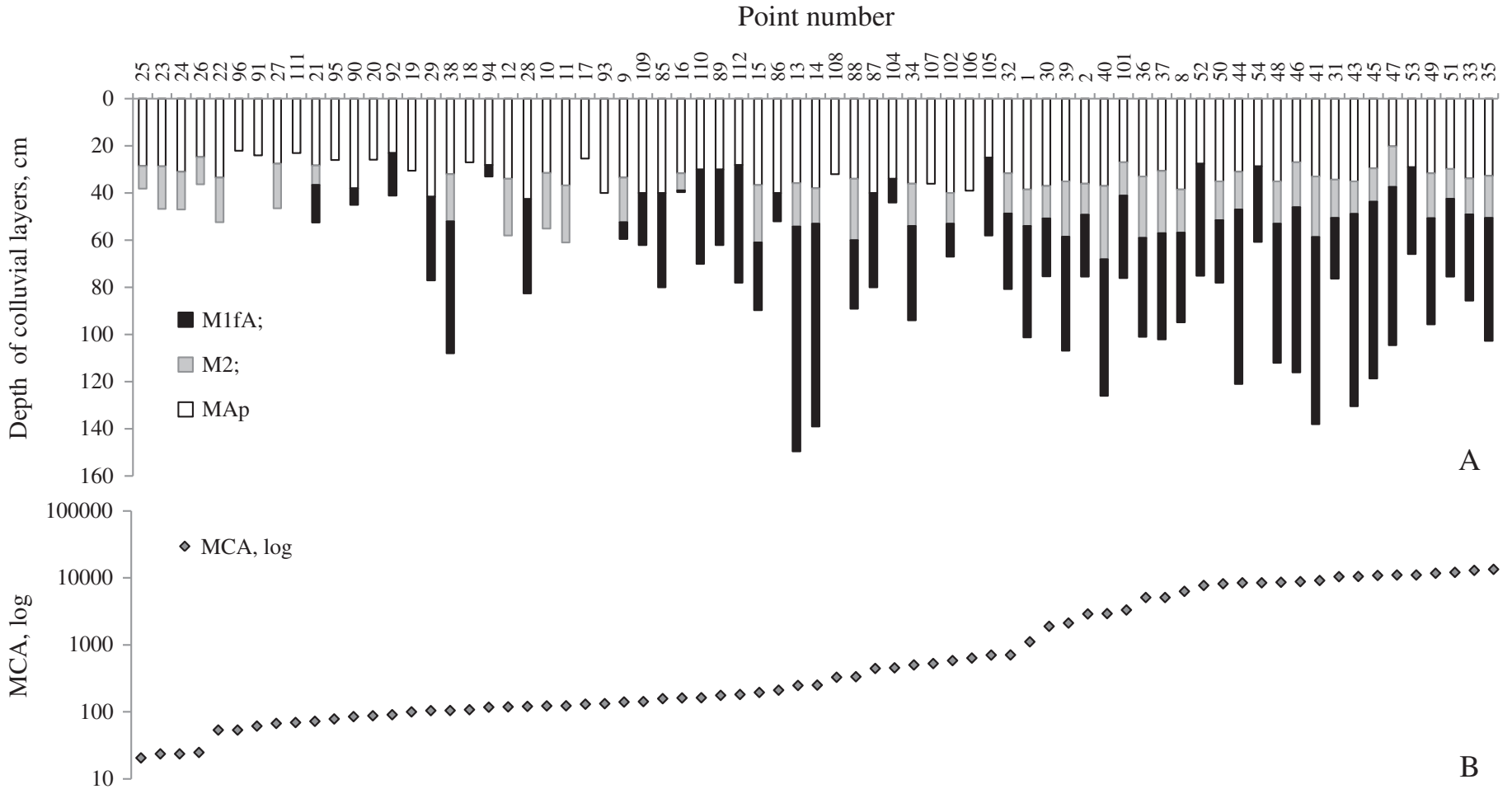

Fig. 3. General profile of sampling points in coordinates of maximal catchment area (*MCA*). A: Colluvial layer thicknesses. B: Values of *MCA*, on a logarithmic scale.

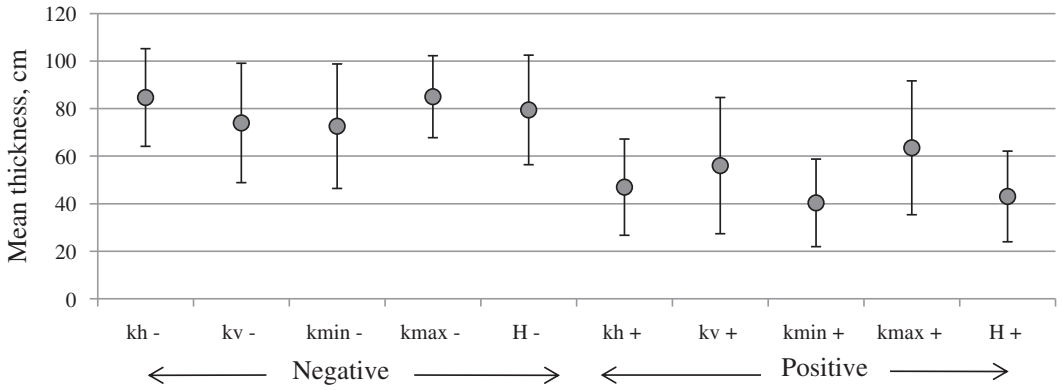

Fig. 4. Mean thickness of all colluvial deposits (layer M total) in positive and negative intervals of basic curvatures. Frames show two standard deviations.

characteristics of geometrical landforms came to the fore. The strongest correlation for individual layers was found between the oldest layer M1fA and H ($r_s = -0.78$). In general, the absolute value of r_s is larger after summing up the layers: hence the strongest correlation was found between M1fA + M2 and *kmin* ($r_s = -0.84$).

Clear internal relationships among curvatures facilitate interpretation of r_s between the MVs and the thickness of colluvial layers. Correlations with all groups of the MVs reflected different aspects of land surface impact on the spatial distribution of the colluvial deposits due to erosion–accumulation processes. Based on the results obtained and the ages of colluvial layers, it is possible to assume that the local landform is most unstable in profile (described by *kv*) over time. The local landform in plan (described by *kh*) is relatively more stable due to the permanent influence of surface flow. Geometrical landform types are the most resistant to land surface modification.

5.2. Memory effects

In general terms the distribution of mass on the land surface can be described as the product of erosion (a property that is not expressed) in the upper parts of a landscape and accumulation (a property that is expressed) in the lower parts. From this approximation it can be expected that the distribution of these properties is first of all correlated with morphometric pre-requisites of surface runoff. But occasionally the strongest correlation of such soil or deposit properties can be observed with another group of MVs. These MVs describe geometrical landforms and are not directly related to modern flows. This group of curvatures contains information about past shape of the land surface. These specific correlations between MVs and the thickness of deposits or soil properties reflect the memory effect. This explanation is possible only based on Shary's theory of curvatures and accompanying statistical hypothesis (Shary, 1995). For the exemplification of correlations of material properties with *kh* and *kmin*, the general mechanism of statistical detection of memory effects has here been described.

If the data set contains only two groups of points, with $kmin < kh < 0$ and $0 < kmin < kh$, the tendency is clear. Material is eroded at positive points and accumulated at negative points. Such points are restricted to Clusters I and III (Fig. 5A). Thus, the points in these clusters formed the main trend for the whole data set. According to both field observation and the statistical hypothesis, however, negative values of *kmin* occur more frequently than negative values of *kh*. Hence, if points are not deliberately selected, the situation with $kmin < 0 < kh$ will arise in any data set. These points are restricted to Cluster II (Fig. 5A). Conformity of *kmin* and *kh* distributions with the statistical hypothesis (Fig. 5B) suggests that the memory effect is independent of data set size.

On the one hand, when material property such as colluvium thickness, soil elements, or vegetation type of points in Cluster II is weakly expressed, the deviation from the main trend is low. Hence, the strength of the negative correlation between a material property and *kh* becomes stronger. On the other hand, when a material property of points in Cluster II is strongly expressed, the deviation from the main trend is high. As a result, the strength of correlation of a material property with *kh* is decreased and correlation with *kmin* can be stronger.

5.3. Phases of land surface evolution under the influence of colluvial sedimentation

Three phases of land surface evolution can be determined using various points in a dry valley. The period of gully growth can be taken as the initial phase when $kmin < kh < 0$. The second phase is the beginning of colluvial sedimentation. It is likely that the second phase will be characterised by a new proportion of the curvatures, $kmin < 0 < kh$. During the second phase, memory effects can be observed. The third phase of colluvial sedimentation will be characterised by another proportion of the curvatures such as $0 < kmin < kh$. In the third phase an inversion between the primary and new surfaces can be observed.

Table 4
Spearman correlations among colluvial layer thicknesses ($n = 71$).

	MAp	M2	M1fA	M total
M2	*			
M1fA	*	0.31		
M total	0.38	0.62	0.90	
M1fA + M2	*	0.63	0.92	0.98

* Correlation not significant at $p \leq 0.05$.

Table 5
Spearman correlations between thickness of colluvial layers and morphometric variables ($n = 71$).

	MAp	M2	M1fA	M1fA + M2	M total
Z	*	*	−0.62	−0.58	−0.56
GA	*	−0.63	−0.50	−0.65	−0.63
MCA	*	0.28	0.71	0.69	0.69
MDA	−0.24	−0.49	−0.76	−0.80	−0.80
kh	*	−0.30	−0.72	−0.71	−0.69
kv	−0.41	−0.36	−0.35	−0.41	−0.45
E	−0.27	*	*	*	*
KA	*	*	*	*	*
rot	*	*	*	*	*
KR	*	0.36	0.56	0.60	0.58
khe	0.30	0.29	*	*	*
kve	*	0.26	0.47	0.50	0.44
kmin	*	−0.57	−0.77	−0.84	−0.83
kmax	−0.30	*	−0.54	−0.47	−0.49
H	*	−0.49	−0.78	−0.82	−0.81
K	*	−0.41	−0.35	−0.41	−0.42
M	*	0.63	0.60	0.73	0.71

* Correlation not significant at $p \leq 0.05$.

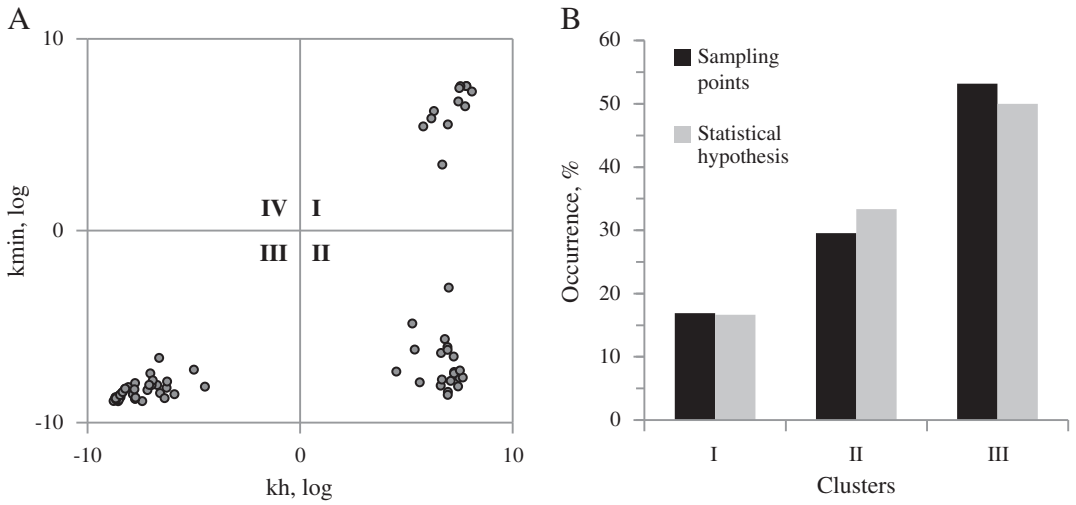

Fig. 5. Distribution of sampling points in coordinates of horizontal (*kh*) and minimal (*kmin*) curvatures. A: Clusters with different signs of the curvatures; logarithmic scale according to Shary et al. (2005). B: Frequency of occurrence of sampling points in the clusters according to the statistical hypothesis and experiment.

Most probably, this inversion can be detected by a negative correlation between the thicknesses of the oldest and the youngest colluvial layers.

Therefore, the proportion of curvatures can be used as an objective parameter for the identification of phases of land surface evolution under conditions of long-term sedimentation. Correlations between thickness of the colluvial layers and their r_s with the MVs quantitatively indicate the phase of land surface evolution.

Acknowledgements

This study was partly supported by the Graduate School "Human Development in Landscapes" of Christian-Albrechts-University of Kiel, Germany. We thank the group of archaeologists headed by Ingo Lütjens for successful cooperation in the field, Peter Shary for important consultations during the article preparation, and Jürgen Zahrer for helpful discussion. We are very grateful to Ian Evans, Takashi Oguchi, Daniel Contreras and an anonymous reviewer for valuable comments and corrections of the text.

References

Aandahl, A.R., 1948. The characterization of slope positions and their influence on the total nitrogen content of a few virgin soils of Western Iowa. Soil Science Society of America Proceedings 13, 449–454.

Ad-hoc-Arbeitsgruppe Boden (Ed.), 2005. Bodenkundliche Kartieranleitung, 5th edition. Schweizerbart'sche Verlagsbuchhandlung, Stuttgart (438 pp.).

Dotterweich, M., 2008. The history of soil erosion and fluvial deposits in small catchments of central Europe: deciphering the long-term interaction between humans and the environment — a review. Geomorphology 101, 192–208.

Dreibrodt, S., Bork, H.-R., 2005. Historical soil erosion and landscape development at Lake Belau (North Germany) — a comparison of colluvial deposits and lake sediments. Zeitschrift fur Geomorphologie Neue Folge, Supplement Band 139, 101–128.

Dreibrodt, S., Nelle, O., Lütjens, I., Mitusov, A., Clausen, I., Bork, H.-R., 2009. Investigations on buried soils and colluvial layers around Bronze Age burial mounds at Bornhöved (northern Germany). An approach to test the hypothesis of 'landscape openness' by the incidence of colluviation. The Holocene 19, 487–497.

Dreibrodt, S., Lubos, C., Terhorst, B., Damm, B., Bork, H.-R., 2010. Historical soil erosion by water in Germany: scales and archives, chronology, research perspectives. Quaternary International 222, 80–95.

Evans, I.S., 1972. General geomorphometry, derivations of altitude and descriptive statistics. In: Chorley, R.J. (Ed.), Spatial Analysis in Geomorphology, 2. Methuen & Co. Ltd., London, pp. 17–90.

Evans, I.S., 1980. An integrated system of terrain analysis and slope mapping. Zeitschrift fur Geomorphologie Neue Folge, Supplement Band 36, 274–295.

Evans, I.S., Cox, N.J., 1999. Relations between land surface properties: altitude, slope and curvature. In: Hergarten, S., Neugebauer, H.J. (Eds.), Process Modelling and Landform Evolution. Springer, Berlin, pp. 13–45.

FAO, 1998. World reference base for soil resources. FAO Report Nr. 84.

Follain, S., Minasny, B., McBratney, B.A., Walter, C., 2006. Simulation of soil thickness evolution in a complex agricultural landscape at fine spatial and temporal scales. Geoderma 133, 71–86.

Garbe-Schönberg, C.-D., Wiethold, J., Butenhof, D., Utech, C., Stoffers, P., 1998. Geochemical and palynological record in annually laminated sediments from Lake Belau (Schleswig–Holstein) reflecting paleoecology and human impact over 9000 a. Meyniania 50, 47–70.

Gauss, K.F., 1827. Disquisitiones generales circa area superficies curvas. Göttingische Gelehrte Anzeigen Stück 177, 1761–1768 (in Latin).

Hartz, S., 2004. Aktuelle Forschungen zur Chronologie und Siedlungsweise der Ertebølle- und frühesten Trichterbecherkultur in Schleswig-Holstein. Jahrbuch Bodendenkmalpflege in Mecklenburg-Vorpommern 52, 61–81.

Hengl, T., Reuter, H.I. (Eds.), 2009. Geomorphometry: concepts, software, applications. Developments in Soil Science, vol. 33. Elsevier, Amsterdam (765 pp.).

Hoika, J., 1993. Grenzfragen oder: James Watt und die Neolithisierung. Archäologische Informationen 16 (1), 6–19.

Hoika, J., 1994. Zur Gliederung der frühneolithischen Trichterbecherkultur in Holstein. In: Hoika, J., Meurers-Balke, J. (Eds.), Beiträge zur frühneolithischen Trichterbecherkultur im westlichen Ostseegebiet: Untersuchungen und Materialien zur Steinzeit in Schleswig-Holstein, 1, pp. 85–132.

Krcho, J., 1983. Teoreticka' concepcia a interdisciplinarne aplikacie komplexne'ho digitalneho modelu relie'fu primodelovanı¨ dvojdimenzionalnych poli. Geograficky Casopis 35, 265–291 (in Slovak).

Lin, H., 2011. Three principles of soil change and pedogenesis in time and space. Soil Science Society of America Journal 75, 2049–2070.

Lütjens, I., Wiethold, J., 1999. Vegetationsgeschichtliche und archäologische Untersuchungen zur Besiedlung des Bornhöveder Seengebietes und seines Umfeldes im Neolithikum. Archäologische Nachrichten aus Schleswig-Holstein 9 (10), 30–67.

McBratney, A.B., Odeh, I.O.A., Bishop, T.F.A., Dunbar, M.S., Shatar, T.M., 2000. An overview of pedometric techniques for use in soil survey. Geoderma 97, 293–327.

McBratney, A.B., Mendoça Santos, M.L., Minasny, B., 2003. On digital soil mapping. Geoderma 117, 3–52.

Mitusov, A.V., 2001. Influence of land surface on soil fertility of grey forest soils of European part of Russia. PhD thesis. Orel — SAU. 120 pp. (in Russian).

Mitusov, A.V., Mitusova, O.E., 2005. The evaluation of soil properties spatial variability by using the new extended system of morphometric variables in Analytical GIS Eco. The report for Department of Ecotechnology and Ecosistem Development, Ecology Centre, Christian Albrechts University of Kiel. Kiel, Germany. (21 pp.).

Mitusov, A.V., Mitusova, O.E., Pustovoytov, K., Lubos, C.C.-M., Dreibrodt, S., Bork, H.R., 2009. Palaeoclimatic indicators in soils buried under archaeological monuments in the Eurasian steppe — a review. The Holocene 19, 1153–1160.

Mitusova, O.E., 2010. Quantification of spatial distribution of colluvial matter: case study Perdoel (Schleswig-Holstein, Germany). Master thesis. University Kiel. 54 pp.

Moore, I.D., Gessler, P.E., Nielsen, G.A., Peterson, G.A., 1993. Soil attribute prediction using terrain analysis. Soil Science Society of America Journal 57, 443–452.

Munsell, 2000. Munsell soil color charts. Gretag MacBeth, NY.

Piotrowski, J., 1991. Quartär- und hydrogeologische Untersuchungen im Bereich der Bornhöveder Seenkette, Schleswig-Holstein. Ph.D. Thesis University Kiel. 194 pp.

Reiss, S., Bork, H.-R., Hoernes, U., Rinker, A., Mitusov, A., 2008. Die Verbreitung der Boeden auf den Ackerflaechen von Hof Ritzerau. In: Borkenhagen P., Irmler U., Roweck H. (Eds.) Faunistisch–Oekologische Mitteilungen, Suppl. 35. Wachholtz Druck, Kiel, pp. 59–74.

Ries, H., 2002. GIS-gestuetzte Rekonstruktion der Reliefentwicklung der Wolfsschlucht (Ostbrandenburg). Diplomarbeit zur Diplomprufung im Fach Geographie. Christian-Albrechts-Universitaet zu Kiel. Kiel. 152 pp.

Schleuss, U., 1991. Böden und Bodenschaften einer Norddeutschen Moränenlandschaft – Ökologische Eigenschaften, Vergesellschaftung und Funktionen der Böden im Bereich der Bornhöveder Seenkette. I – Textband. Ph.D. Thesis University Kiel. 186 p.

Scull, P., Franklin, J., Chadwick, O.A., McArthur, D., 2003. Predictive soil mapping: a review. Progress in Physical Geography 27, 171–197.

Sharaya, L.S., Shary, P.A., 2003. Use of morphometric statistics to describe internal geometry of gently sloping and mountainous territories. Izvestiya Samarskogo Nauchogo Centra RAS 5, 278–286 (in Russian).
Shary, P.A., 1991. Topographic method of second derivatives. In: Stepanov, I.N. (Ed.), The Geometry of Earth Surface Structures. Poushchino Scientific Center, Poushchino, pp. 28–58 (in Russian).
Shary, P.A., 1995. Land surface in gravity points classification by a complete system of curvatures. Mathematical Geology 27, 373–390.
Shary, P.A., 2005. Assessment of relationships relief-soil-vegetation with using of new approaches in geomorphometry (on the example of agrolandscape and forest ecosystem of South of Moscow region. PhD thesis. Pushino — IFHBPS RAN. 224 pp. (in Russian).
Shary, P.A., Sharaya, L.S., Mitusov, A.V., 2002. Fundamental quantitative methods of land surface analysis. Geoderma 107, 1–35.
Shary, P.A., Sharaya, L.S., Mitusov, A.V., 2005. The problem of scale-specific and scale-free approaches in geomorphometry. Geografia Fisica e Dinamica Quaternaria 28, 81–101.
Speight, J.G., 1968. Parametric description of land form. In: Stewart, G.A. (Ed.), Land Evaluation. MacMillan, London, pp. 239–250.
Speight, J.G., 1974. A parametric approach to landform regions. In: Brown, E.H., Waters, R.S. (Eds.), Progress in Geomorphology. Institute of British Geographers Special Publ. No.7. Alden Press, Oxford, pp. 213–230.
StatSoft, Inc., 2010. Electronic Statistics Textbook. StatSoft, Tulsa (WEB: http://www.statsoft.com/textbook/).
Targulian, V.O., 1999. Particularity of soil as the uppermost mantle of the biospheric planet. Ecology and Soils. Selected Lectures of the VIII-IX All-Russian schools (1998–1999). 131–145 (T3. - M: POLTEKS).
Targulian, V.O., Goryachkin, S.V. (Eds.), 2008. Soil Memory: Soil as a Memory of Biosphere–Geosphere–Anthroposphere Interactions. Institute of Geography, Russian Academy of Sciences, Moscow (692 pp.).
Targulian, V.O., Sokolova, T.A., 1996. Soil as a bio-abiotic natural system; a reactor, memory and regulator of biospheric interactions. Eurasian Soil Science 29, 34–47.
Zhou, Q., Lees, B., Tang, G. (Eds.), 2008. Advances in Digital Terrain Analysis. Lecture Notes in Geoinformation and Cartography. Springer, Berlin (462 pp.).

Appendix II

Mitusov, A.V., Mitusova, O.E., Wendt, J., Dreibrodt, S., Bork, H.-R., 2014. Correlation of colluvial deposits with the modern land surface and the problem of slope profile description. Geomorphology 220, 30–40.

Geomorphology 220 (2014) 30–40

Contents lists available at ScienceDirect

Geomorphology

journal homepage: www.elsevier.com/locate/geomorph

Correlation of colluvial deposits with the modern land surface and the problem of slope profile description

A.V. Mitusov *, O.E. Mitusova, J. Wendt, S. Dreibrodt, H.-R. Bork

Institute for Ecosystem Research, Christian-Albrechts-University Kiel, Olshausenstrasse 75, D-24118 Kiel, Germany

ARTICLE INFO

Article history:
Received 2 September 2013
Received in revised form 12 May 2014
Accepted 25 May 2014
Available online 4 June 2014

Keywords:
Colluvial deposits
Morphometric variables
Slope profile
Land surface
Geomorphometry

ABSTRACT

This article focuses on features of spatial distribution of colluvial (slope) deposits on a micro scale. These features were detected by the non-parametric rank correlation of Spearman (r_S) between thickness of colluvial layers and morphometric variables (MVs) of the modern land surface. The strongest correlation was found between total thickness of colluvial layers and maximal catchment area ($r_S = 0.85$). A negative correlation was observed between thicknesses of younger and older colluvial layers. Additionally, if young colluvial layers have a negative correlation with slope steepness (*GA*), relatively old buried colluvial layers have a positive correlation with *GA*. These facts indicate an inversion of the zones of actual matter accumulation due to transformation of the land surface in profile during long-term sedimentation.

Vertical curvature (*kv*) characterises acceleration and deceleration of surface flow caused by the shape of the slope profile along flow lines. Based on this, it was expected that *kv* would have a direct impact on the accumulation of colluvium. However, in this study, the correlations between the thickness of colluvial deposits and *kv* were low. Functional relationships between colluvial accumulation and the shape of profiles along flow lines were reflected by correlations with *GA*. Based on these observations, it is assumed that the regional nature of surface flow velocity affects the shift between existing accumulation zones reflected by colluvial deposits and potential accumulation zones reflected by MVs.

Signs of correlation coefficients between the thickness of colluvial deposits and curvatures reflect the tendency of increased colluvial depositions at three out of 12 local landforms of Shary's classification. These landforms are located in the valley bottom. The mean thickness of colluvial deposits at these three landforms was 167 ± 18.7 cm (error range = standard deviation); the other nine landforms show a mean thickness of 130.1 ± 34.1 cm.

1. Introduction

In small dry valleys, most of the eroded matter is distributed along downslopes and thalwegs as colluvial deposits (e.g. de Moor and Verstraeten, 2008; Houben, 2012). The investigation of past spatial distribution of colluvial deposits and related soil erosion is an important direction of geomorphology and geoarchaeology (e.g. Rommens et al., 2005; Houben, 2008; Vanwalleghem et al., 2010; Ciampalini et al., 2012). However, thorough literature reviews by Dotterweich (2008) and Dreibrodt et al. (2010) have pointed to one important fact: the low number of investigations based on spatial variability of colluvial deposits at micro scale and based on modern quantitative methods. One of the reasons for this is the insufficiency of information with detailed spatial and temporal resolution on the processes during the Holocene. In this situation, morphometric variables (MVs) are often the only source of additional information for predictive mapping of colluvium (e.g. Ries, 2002; Follain et al., 2006; Reiss et al., 2008; Mitusova, 2010; Schneider et al., 2011). It should be mentioned that land use and climate are important triggers, but the land surface play a predominant role in the distribution of colluvial sediments on a micro scale. The MVs describe different prerequisites of processes that take place on the land surface (Shary, 1995; Shary et al., 2002a, 2005). Hence, the MVs enable us to understand the spatial variability of colluvial deposits that is not visually detectable.

However, the statistical relationships between MVs and colluvial deposits are not well investigated. The specifics of correlations among them are caused mainly by:

1) properties of colluvial layers (type of matter, thickness, density etc.), specifics of deposition and spatial distribution, transformation of the deposits due to soil formation and land use, and;
2) type of MVs and statistical relationships for MVs due to mathematical reasons or strong modification of the land surface e.g. by surface flow and location of sampling points.

MVs can be considered as both prerequisites and indicators of the processes on the land surface. However, not all known processes linked with the land surface can be directly described by the existing MVs. In this case the indirect information from other known MVs can be used

* Corresponding author. Tel.: +49 431 880 4030; fax: +49 431 880 4083.
E-mail address: a_mitusov@mail.ru (A.V. Mitusov).

http://dx.doi.org/10.1016/j.geomorph.2014.05.020
0169-555X/

(e.g. Shary et al., 2002b). For example, variability of slope steepness along flow lines is the geomorphometrical prerequisite of relative deceleration and acceleration of surface flows. The local zones of relative deceleration and acceleration of surface flows can be defined by the sign of vertical curvature, whereas such an MV for the identification of these zones on a regional scale does not exist because the zones are related to site location in a catchment. This is one of the most important problems of geomorphometry (Shary et al., 2002a).

The impact of the relative velocity of flows on the actual matter accumulation can be logically detected from relationships among MVs, correlations between known MVs, and the thickness of colluvial layers as well as the distribution of sampling points.

In comparison with geological scales, the process of colluvial matter distribution and deposition during the Holocene is usually characterized by relatively small areas, short time of deposition, and low energy. Therefore, the detailed features of spatial and temporal distribution of colluvial deposits cannot be visually detected. Geomorphometrical and statistical techniques have played a major role as the main procedures for investigating spatial distribution of colluvial deposits. The goal of this article is, therefore, the detection of basic statistical properties of colluvial deposits, the calculation of correlations between the thicknesses of colluvial layers and MVs of the modern land surface, and the explanation of the obtained relationships.

2. Study area and methods

The study area (54° 6′ 31″ N; 10° 15′ 2.76″ E) is located in the dry subcatchment of Lake Belau near the farm "Perdöler Mühle" in Northern Germany, approximately 35 km south of Kiel (Fig. 1). The geomorphological elements surrounding Lake Belau were formed mainly during the Middle Weichselian and later modified during the Late Weichselian (e.g. Piotrowski, 1991; Svendsen et al., 2004). Between the Neolithic period and the Iron Age, soils which had developed during the early Holocene were eroded on agriculturally used upslopes and midslopes, and deposited downslopes in small valley bottoms. On slopes and in these colluvial deposits, Cambisols and Luvisols developed from the Iron Age until Medieval Times. During the Medieval Times and early Modern Times, the upper horizons of Cambisols and Luvisols were eroded again (e.g. Dreibrodt and Bork, 2005).

Four trenches and 18 auger cores (Fig. 1) were made in 2007 (Dreibrodt and Wiethold, submitted for publication). The area, covered by points of measurement, has been used as a permanent pasture for more than 50 years; surrounding areas have been ploughed. Locations and depths of the trenches were defined so that all sequences of colluvial layers could be investigated; individual colluvial layers in auger cores were not distinguished. Structure and characteristics of colluvial layers were described using conventional field methods (Ad-hoc-Arbeitsgruppe Boden, 2005). A digital elevation model (DEM) with 1 m grid spacing from the Land Survey Office of State Schleswig-Holstein was used (Landesvermessungsamt Schleswig-Holstein, 2012). The DEM was prepared from airborne Light Detection and Ranging (LiDAR) data.

The mean thickness of colluvial layers in the trenches was calculated for every grid cell of the DEM (1 m^2). For auger cores, this procedure was not necessary. As a result, the colluvial database consisted of 46 points from trenches and 18 points from auger cores. The points from trenches mainly described the valley bottom. The points from auger cores characterised the slopes.

In contrast to the location of soils, colluvial deposits are restricted in space. Moreover, data obtained from thick deposits is more reliable than those from thin ones, because of their resistance to possible disturbances. Consequently, dense point observations with thick deposits in valleys lead to an optimal ratio between information quality and workload.

Well known statistical methods were used for data analysis (StatSoft Inc., 2013). An overview was made using basic descriptive statistics. For the determination of normality, two different tests (Shapiro-Wilk and Anderson-Darling) were used. Quantitative comparisons were made with the help of the non-parametric rank correlation coefficient of Spearman (r_S). Correlation coefficients with a significance level (p) of more than 0.05 were not considered.

Because colluvial layers have fragmentary spatial distribution, the database was modified for r_S computation. At points where a layer was not found, the thickness was marked as zero. Zero impacts on statistical results but many landscape parameters have fragmentary distribution. Hence, during investigations, this feature must be taken into account. At binary consideration zero means logic variable "NO", whereas other values mean "YES".

The land surface was described by the system of 17 MVs that are divided into four groups (Table 1). Additionally, based on different calculation methods, local and regional MVs can be distinguished (e.g. Shary, 1995). Regional MVs are maximal catchment area (*MCA*) and maximal dispersal area (*MDA*). For calculation of regional MVs, extended terrain portions have to be taken into account (e.g. Tarboton, 1997). Local MVs are curvatures and slope steepness (*GA*). For calculation of local MVs, only a small number of grid cells around the investigated point have

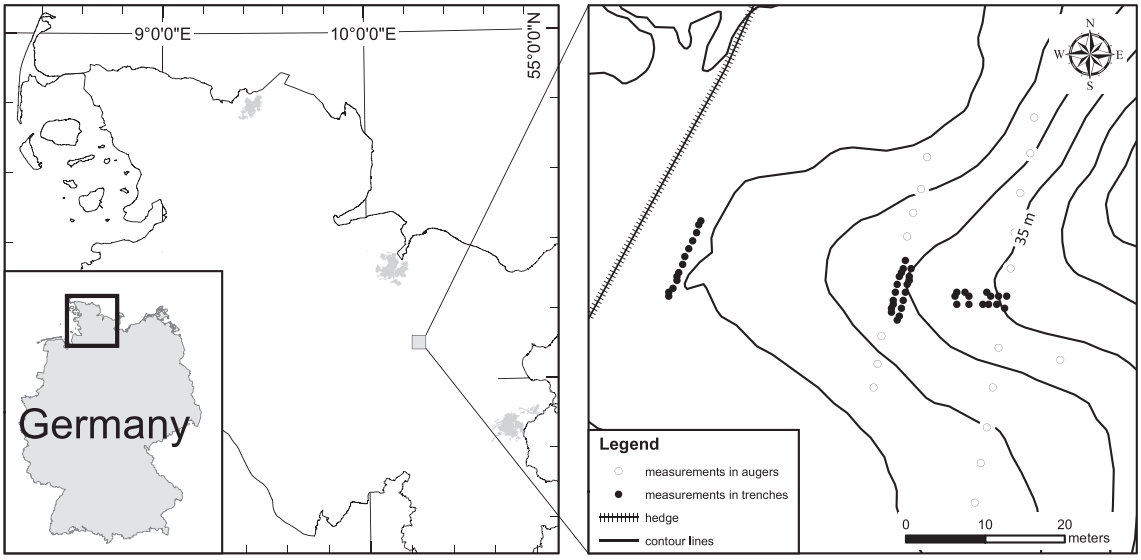

Fig. 1. Location of the study area and points of measurements in trenches and cores. Contour lines have 1 m vertical interval.

Table 1
System of morphometric variables.

Variable name, Unit	Description	Reference
Vertical zonation		
Altitude (*Z*), m	Vertical changes in climate conditions	e.g. Shary et al. (2002a)
Morphometric pre-requisites of surface runoff and soil throughflow generation		
Slope steepness (*GA*), degrees	Flow velocity	e.g. Shary et al. (2002a)
Maximal catchment area (*MCA*), m^2	Maximum area from which material moving downslope may be collected	Speight (1968)
Maximal dispersal area (*MDA*), m^2	Maximal area at which materials moving downslope may be diffused	Speight (1974)
Horizontal (tangential) curvature (*kh*), m^{-1}	Flow convergence/divergence	Krcho (1983)
Vertical (profile) curvature (*kv*), m^{-1}	Relative flow deceleration/acceleration	Evans (1972)
Difference curvature (*E*), m^{-1}	Compares *kh* (in plan) and *kv* (in profile)	Shary (1995)
Total accumulation curvature (*KA*), m^{-2}	Reveals relative accumulation zones	Shary (1995)
Characteristics of land surface dissection		
Rotor (*rot*), m^{-1}	Flow line rotation direction	Shary (1995)
Total ring curvature (*KR*), m^{-2}	Flow line twisting	Shary (1995)
Vertical excess curvature (*kve*), m^{-1}	Describes to what extent *kv* is larger than minimal curvature (*kmin*) at the same point	Shary (1995)
Horizontal excess curvature (*khe*), m^{-1}	Describes to what extent *kh* is larger than minimal curvature (*kmin*) at the same point	Shary (1995)
Characteristics of geometrical landforms		
Maximal curvature (*kmax*), m^{-1}	Geometrical ridge forms	e.g. Gauss (1828)
Minimal curvature (*kmin*), m^{-1}	Geometrical valley forms	e.g. Gauss (1828)
Total Gaussian curvature (*K*), m^{-2}	Separated elliptic and saddle landforms	Gauss (1828)
Mean curvature (*H*), m^{-1}	Connected to "equilibrium" surface condition	e.g. Gauss (1828)
Unsphericity (*M*), m^{-1}	Surface deviation from spherical form	Shary (1995)

to be considered (Shary et al., 2002a). Gridded maps of *GA*, vertical and horizontal curvatures are given in Fig. 2.

The correct equations for local MVs that are used in this article were given by Shary (2012). The mathematical theory explains statistical relationships among MVs and links every MV with physical processes on the land surface (Shary et al., 2002a). The used MVs are free from specific coefficients and subjective manipulations. As a result, these MVs can be comparably applied to sufficiently different landscapes. This gives for the selected MVs an advantage over other MVs. For calculation of all MVs, Analytical GIS Eco developed by P. Shary was used (Wood, 2009).

3. Properties of layers of colluvial deposits

3.1. Source of colluvial deposits

Based on the DEM with 1 m grid spacing, the map of maximal catchment area (*MCA*) was calculated (Fig. 3). This map reflects the location of surface flows and depressions. The hedges around arable lands are well visible on this map. The water catchment of the investigated area is 16.07 ha. The area of water catchment was divided into three segments (Fig. 3).

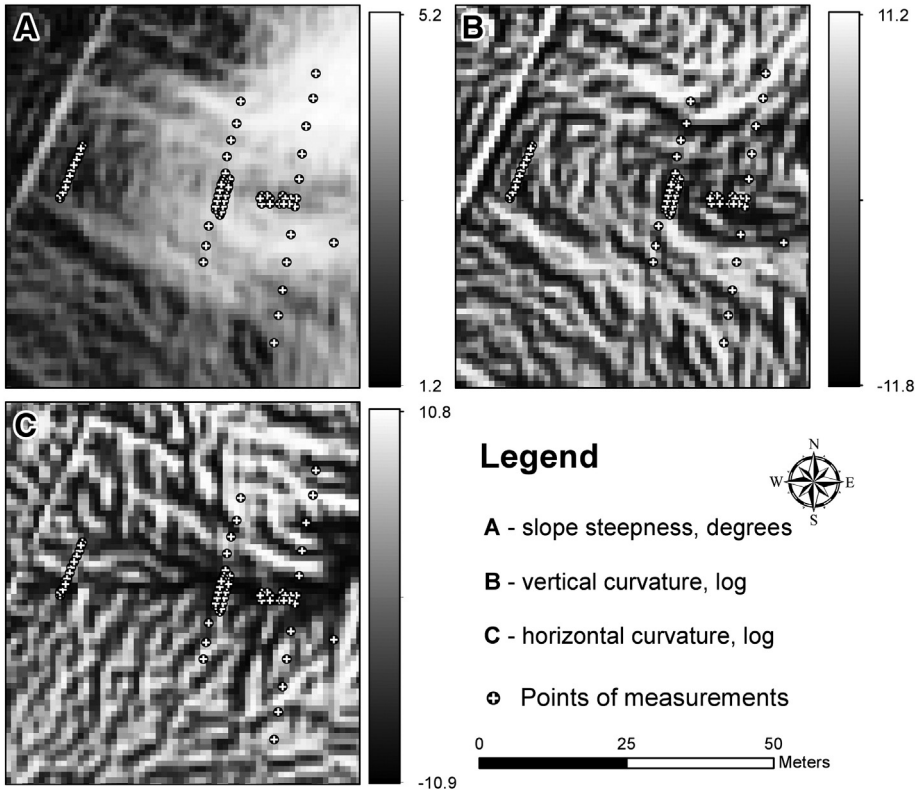

Fig. 2. Gridded maps of basic morphometric variables (slope, vertical curvature and horizontal curvature) with points of measurements of colluvial deposits.

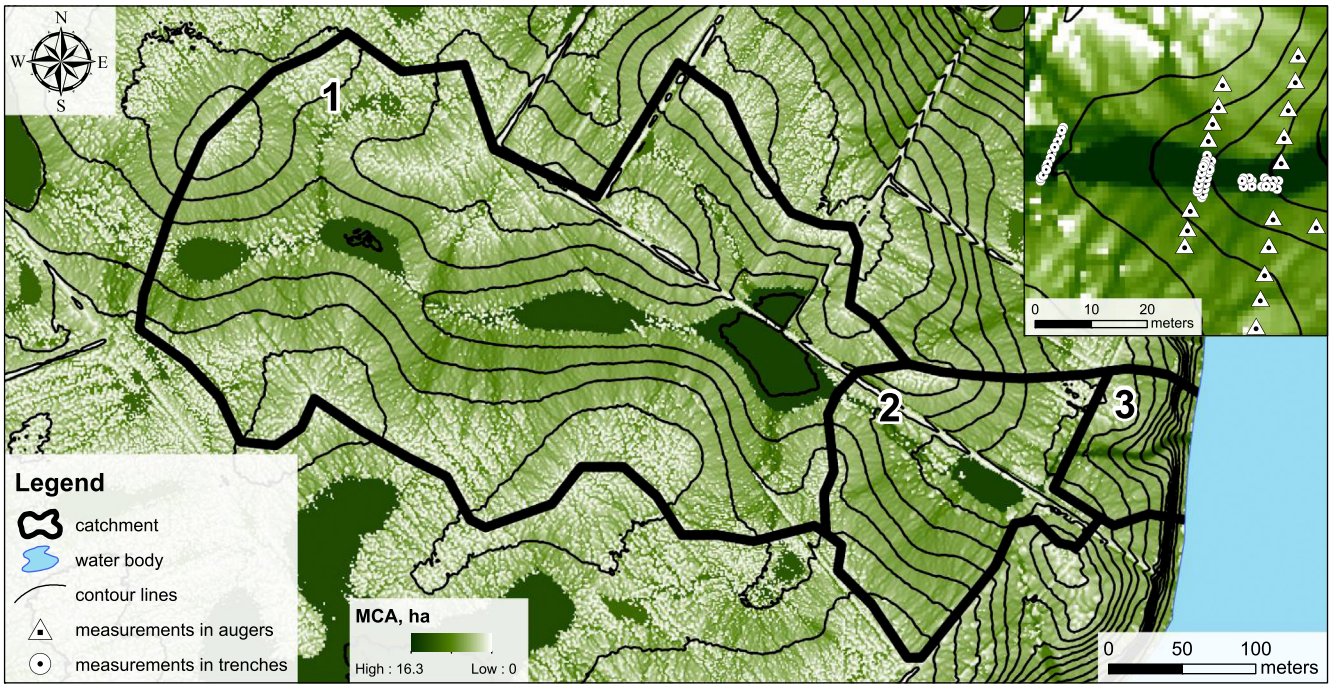

Fig. 3. Gridded map of maximal catchment area (*MCA*) reflects water catchment. Dark spots indicate closed depressions. Contour lines have 1 m vertical interval. The catchment divides into three segments according to possibilities for colluvial matter collection: 1- segment with accumulation of the colluvial matter in natural closed depressions, but not in the area of the points of measurements; 2- segment with potential source of matter for colluvium before hedges erection; 3- segment with potential source of matter for colluvium before and after hedges erection.

Segment 1 contains four depressions with mean depths ranging from 10 to 36 cm (Fig. 3). Accumulation of solid matter mostly takes place in the above-mentioned depressions. The last depression in segment 1 has a catchment area of 12.86 ha. Hence, this size has to be excluded from consideration as a potential source of colluvial matter that is deposited in the points of measurements. The depression in the centre of segment 2 (Fig. 3) is artificial. It was formed after erection of the hedges approximately 200 years ago. Until the construction of the hedges, the area of potential source for the formation of colluvial deposits in the points of measurements was 3.21 ha. After erection of the hedges, this area was reduced to less than 0.5 ha (segment 3 on Fig. 3) because the hedges play the role of artificial dams in the path of surface flows. The area of segments 2 and 3 can be considered a potential source for colluvial deposits in the points of measurements.

3.2. Sequences and history of colluvial layers

Five colluvial layers were identified and labelled from M1 to M5 in a stratigraphic sequence (Fig. 4). In the uppermost (M5) and deepest (M1) colluvial layers, humus horizons were formed *in situ*. It is the result of relatively long exposure of M5 at present and M1 in the past. The humus horizons in these layers were labelled as AhM5 and M1fAh respectively. The sum of all layers and horizons was labelled as M total-46 or M total-64: M total-46 consists of points from trenches; whereas M total-64 consists of points from trenches and auger cores. Based on the specific history of the region, some individual colluvial layers were combined. M5-total is the sum of M5 and AhM5. M1-total is the sum of M1 and M1fAh. M-middle is the sum of M2, M3 and M4 (Fig. 4). Hereafter, for general identification of such layers, the term "combined layers" is used.

In the surroundings of the investigation area, humans started to clear small areas of woodland for agricultural land use during the Neolithic (Garbe-Schönberg et al., 1998; Dreibrodt and Bork, 2005). On the agriculturally used fields, topsoil horizons were eroded by runoff and deposited at accumulative zones of slopes and valleys as colluvial layer M1-total approximately 4200–3700 BC. Then, for a relatively long period, no new colluvial material was deposited. As a result, the humus horizon M1fAh was formed.

Between the Late Neolithic time approximately since 2800 BC and the Migration Period approximately 400–700 AD several phases of human colonization of surrounding landscapes took place. Agricultural land use and deforestation characterised these phases (e.g. Dreibrodt

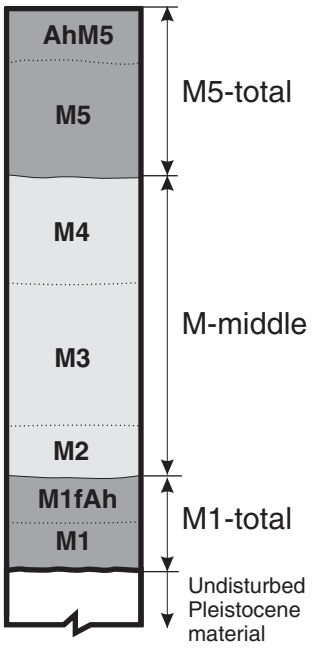

Fig. 4. General sequence of colluvial layers.

and Bork, 2005). Probably, M2, M3, and M4 were deposited during these phases. M2 was formed from humus material of the upper soil horizons, M3 consists of material of deeper soil horizons, and M4 consists of material of B soil horizon. The sequence of these layers shows that the agricultural potential of the area was very low at the end of this period.

Upper colluvial layer M5-total was formed between the Medieval and Modern Times. The material of this layer is more humic. This indicates a relative increase of soil fertility due to natural factors, although effects of systematic fertilization by manure during the last centuries cannot be excluded. Since the erection of the hedges around the arable fields, the colluvial input to the observation points was sharply decreased. This fact leads to the assumption that the humus horizon AhM5 was formed during the last 200 years without strong inputs of solid material.

3.3. Statistical properties of the thickness of colluvial layers

Basic descriptive statistics of the thickness of colluvial layers are shown in Table 2. The positive skewness shows that a peak of a bar chart has a shift in the left direction and *vice versa*. The highest positive skewness was found for the upper humus horizon AhM5. The lowest negative skewness was found for M total-46. Kurtosis assesses the shape of a bar chart relative to the normal law. Positive kurtosis indicates that a peak is sharper than for the normal law and *vice versa*. M3 has the highest negative kurtosis.

The Shapiro-Wilks test is used for the identification of normality. The resulting p-values accept ($p > 0.05$) or reject ($p \leq 0.05$) the hypothesis of normality (H0). A rejection of H0 at $p \leq 0.05$ implies with a 95% degree of confidence that the data do not fit the normal distribution. Passing the normality test points to no significant deviation from normality. Additionally, the Anderson-Darling test for normality was used to corroborate the results of the Shapiro-Wilks test. The results of the tests (Table 2) indicate distributions close to normal for M5, M4, M2, M-middle, M1fAh, M1, M1-total and M total-18. The results for the other layers do not indicate the normal distribution (H0 rejected).

The bar chart (Fig. 5C) with more than one peak and the theoretical quartile (Q–Q) plots (Fig. 5D) with outliers at larger quartiles indicate a tendency for bimodal distribution of M total-64. Since the bar chart of M total-46 (data from trenches) has only one major peak (Fig. 5A), bimodal distribution of M total-64 can be the result of data combination from the slopes (cores) and the bottom (trenches). The abnormal distribution of M total-46 is illustrated by a right shift of the bar chart (Fig. 5A). This shift is caused mainly by five points with thickness of M total-46 less than 100 cm. In the Q–Q plot, all these points were located lower than the linear trend (Fig. 5B). Geographically, these points were located at the maximal thalweg distance.

3.4. Spatial generalisation of colluvial layers in coordinates of MCA

The physical meaning of *MCA* allows the combination of data from all trenches into one profile (Fig. 6). The bar chart in Fig. 6A shows the depth of the individual colluvial layers for all trenches. The data are ranked according to the values of *MCA* from minimum to maximum. The ranked values of *MCA* are presented in Fig. 6B.

Based on Fig. 6A the general consideration of the stratigraphy in the whole data is possible. M1 appears at intermediate values of *MCA*. M2 appears at relatively high values of *MCA*. Also, long and short wave variations of colluvial layers can be recognised. Long wave trends are realised as a monotonous increase of the thickness of colluvial layers in coordinates of *MCA*. In the ranked values of *MCA*, short wave oscillations cannot be seen (Fig. 6B). Hence, it is possible to assume that short wave oscillations of colluvial layer thickness, is connected with other random and systematic factors such as local landforms described by curvatures.

3.5. Correlation among the thickness of colluvial layers

The negative correlations between individual colluvial layers as well as between M-middle and M5-total (Table 3) indicated an inversion of statistical extremes of the thickness of young colluvial layers relative to older layers. Based on the landscape position of the sampling points, it is possible to assume that the inversion was caused by long-term sedimentation of slope deposits at the valley bottom.

The negative r_S value was also observed between M1fAh and M1. This inversion can be explained by the specifics of humus horizon formation in the body of sediments: the thicker the upper humus horizon, the thinner the body of the untransformed sediment. Low M1fAh thickness at certain points with relatively high values of *MCA* (Fig. 6) can be associated with secondary erosion during the formation of M2.

Relatively strong positive correlations of M1 and M2 with other layers illustrate zero impaction. More than half of these points are zero. In this case, not micro oscillations but facts of existence of M1 or M2 are considered. For example, M2 is present only in places with high values of *MCA* which also coincides with the thickest part of other layers.

4. Correlations of the thickness of colluvial layers with MVs

4.1. Strongest correlations in groups of MVs and colluvial layers

Significant r_S values for all groups of MVs and colluvial layers were established (Table 4). The strongest correlation for the whole dataset was found between *MCA* and M total-64. Among the groups, the

Table 2
Basic descriptive statistics of the thickness of colluvial layers.

Colluvial layer	n	Min, cm	Max, cm	Mean, cm	Standard deviation, cm	Skewness	Kurtosis	Test for normality: Shapiro–Wilk (p)	Test for normality: Anderson–Darling (p)
AhM5	46	9.0	36.0	16.6	6.5	0.9	0.2	0.0014	0.0012
M5	46	8.0	60.0	34.2	11.4	0.1	−0.2	0.8956	0.6639
M5-total	46	22.0	83.0	50.8	15.6	0.4	−0.9	0.0564	0.0201
M4	46	14.0	58.0	32.7	8.9	0.1	0.2	0.4814	0.4221
M3	41	14.0	80.0	43.6	19.0	0.1	−1.2	0.0434	0.0375
M2	15	7.5	23.3	15.3	4.9	0.0	−0.9	0.6726	0.6992
M-middle	46	16.0	125.5	76.5	26.4	−0.6	−0.1	0.0805	0.0534
M1fAh	39	0.5	29.0	13.8	7.1	0.3	−0.1	0.2386	0.2451
M1	20	7.0	24.0	14.6	4.5	0.2	0.0	0.7899	0.7283
M1-total	42	4.0	35.5	19.7	7.1	0.1	−0.5	0.7758	0.3901
M total-46[a]	46	50.0	199.0	145.4	33.9	−1.1	0.8	0.0014	0.0005
M total-18[b]	18	6.0	84.0	50.3	24.9	−0.4	−1.1	0.2042	0.2463
M total-64[c]	64	6.0	199.0	118.6	53.3	−0.5	−1.0	0.0003	0.00002

[a] Data from trenches
[b] Data from augers.
[c] Data from trenches and augers.

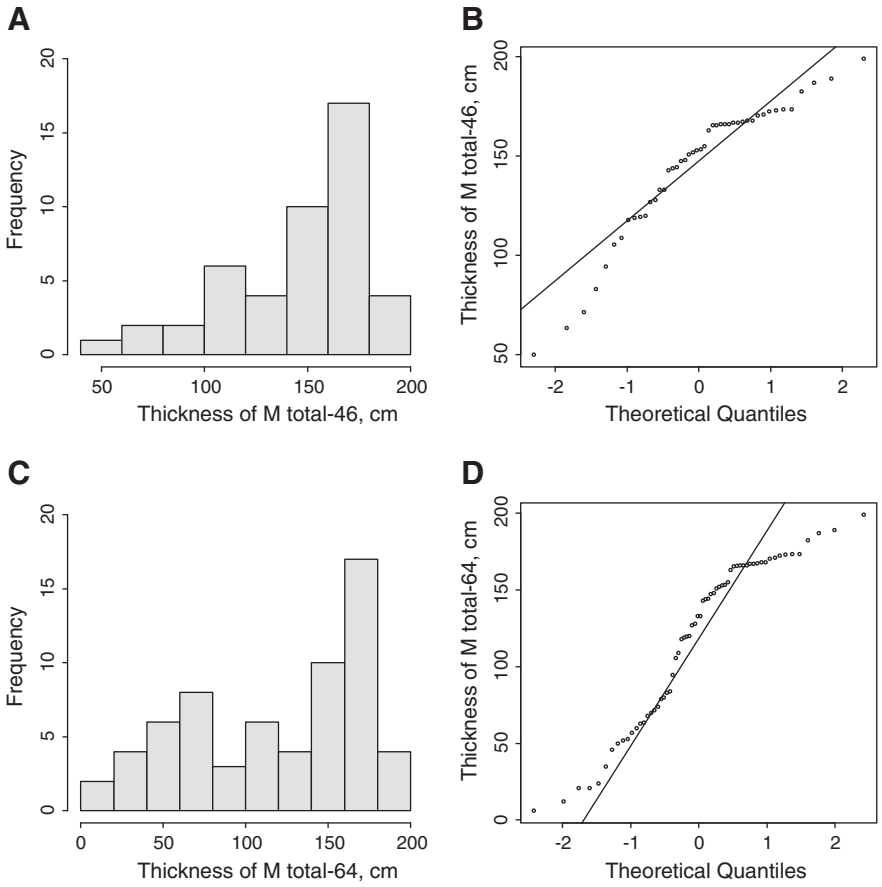

Fig. 5. Statistical distribution of sum of thicknesses of all colluvial layers. A and B: M total-46 (data from the trenches). C and D: M total-64 (data from the trenches and cores).

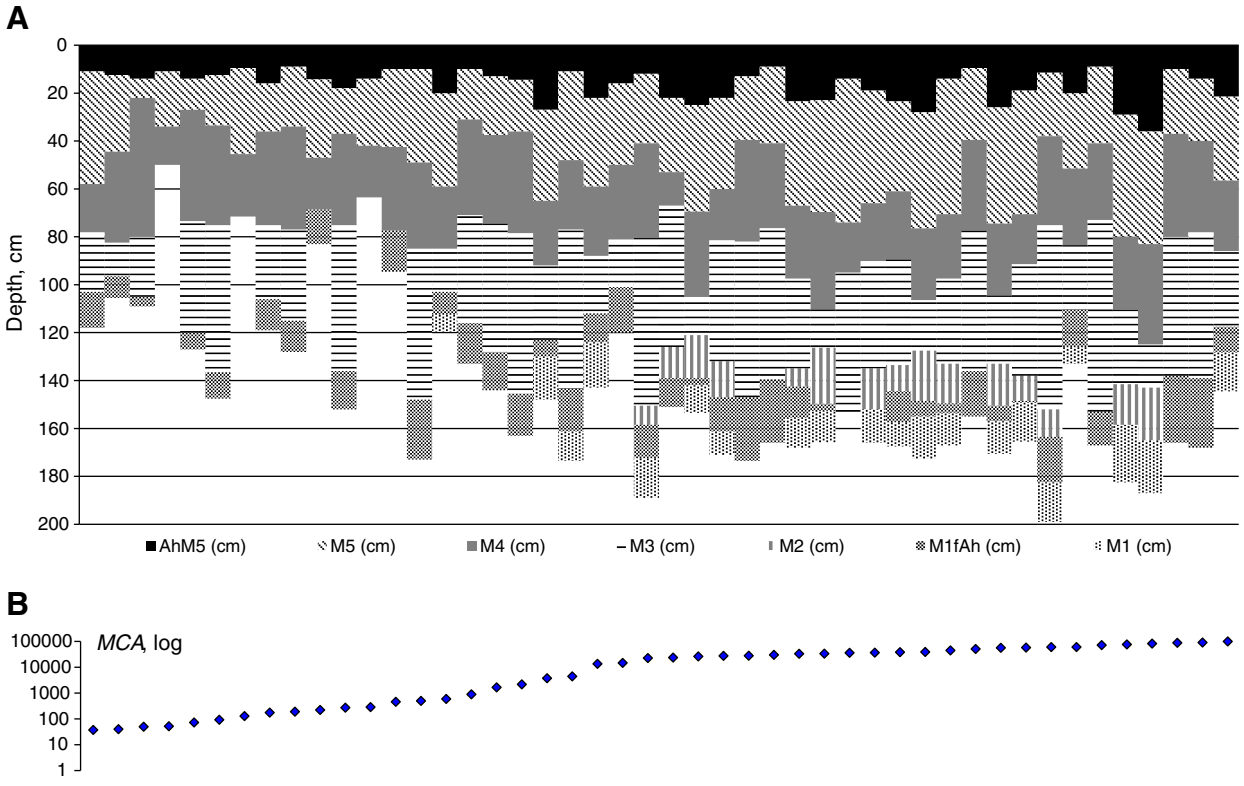

Fig. 6. General profile of the 46 points from trenches in coordinates of maximal catchment area (*MCA*). A: The thickness of colluvial layers. B: Values of *MCA* on a logarithmic scale.

Table 3
Spearman correlation between the thickness of colluvial layers (points from trenches, $n = 46$).

	AhM5	M5	M5-total	M4	M3	M2	M-middle	M1fAh	M1	M1-total
M5	0.46									
M5-total	0.67	0.95								
M4	*	−0.57	−0.55							
M3	−0.32	−0.27	−0.31	*						
M2	0.61	0.58	0.67	*	*					
M-middle	*	−0.34	−0.36	0.54	0.91	*				
M1fAh	−0.45	−0.43	−0.47	0.36	0.55	−0.43	0.49			
M1	0.65	0.61	0.70	*	*	0.69	*	−0.39		
M1-total	*	*	*	*	0.38	*	0.34	0.52	0.52	
M total-46	*	0.35	0.37	*	0.60	0.58	0.65	*	0.53	0.68

* The correlation is not significant at $p \leq 0.05$.

combined layers had the strongest correlation with MVs. As compared with the groups of upper and deeper layers, the group of intermediate layers shows the strongest correlation with MVs. The thickness of humus horizons (AhM5 and M1fAh) that were formed in the body of colluvial layers has the weakest correlation with MVs. It is similar to the previously reported results for soils (e.g. Mitusov, 2001). It can be explained by the dominant role of biota during formation of humus horizons in the considered scales of time and space.

4.2. Functional and non-functional correlations with MCA and altitude

Altitude is often used in landscape investigations, but physically, it describes vertical zonality in mountains. In low-lands, correlation with altitude can be considered as a function of depth to ground water level (e.g. Husson et al., 2000). For relatively small key sites of plain landscapes, correlation with altitude shows that altitude is a surrogate of other MVs (e.g. Shary et al., 2002b).

The relationship between altitude and M-total (Fig. 7A) only reflects distribution of data clouds depending on location of the trenches. The relationship between *MCA* and M-total (Fig. 7B) is closer to a monotonous trend and is more logical. This relationship confirms proportion between catchment area and volume of material input. A positive r_S value shows that the input of colluvial matter is higher than output. A comparison of M total-46 and M total-64 shows that an increase in diversity of the thickness of colluvial layers both decreases the power of correlation with altitude and increases the power of correlation with *MCA*.

4.3. Signs of correlation coefficients with curvatures

Traditionally, signs of correlations between curvatures and parameters related with surface flows are explained by erosion in convex landforms and accumulation in concave landforms (e.g. Florinsky and Kuryakova, 1996, 2000; Mitusov, 2001; Florinsky et al., 2002, 2004; Shary, 2005). In current investigations, colluvial deposits of upper (relatively young) layers have shown significant r_S only with one curvature (Table 4), which is not enough for the identification of clear tendencies. The thickness of intermediate and deeper layers as well as the thickness of combined layers shows better sets of r_S with curvatures (Table 4).

At local zones of flow convergence (local valleys), negative correlations with *kh* show statistical tendency for an increase in colluvial thickness. Positive correlations with *E* show that these local landforms are more twisted in plan than in profile. Although the proportion between r_S for *kh* and *kmin* shows that the geometrical shape of local valleys in plan has been modified by surface flows, there are no markers of transformation of signs of *kh* and *kmin* relative to the former land surface.

A traditional descriptor of local landforms in profile such as *kv* has only two significant r_S with colluvial layers. More r_S were found for *kve* that describe twisting of local landforms in profile relative to geometrical landforms described by *kmin*. A sign of r_S with *kve* is the tendency to increase colluvial deposits on landforms of slope profile where differences between *kv* and *kmin* are at a maximum. It explains that this difference is as a result of the land surface transformation due to the long-term deposition of colluvium.

Generally, signs of r_S with curvatures indicate the tendency of former colluvial deposits to increase on saddles ($kmin < kh < 0 < kv < kmax$) and

Table 4
Spearman correlation between the thickness of colluvial layers and morphometric variables (MVs).

Layers	*Z*	MVs that describe surface runoff					MVs that describe geometrical landforms						MVs that describe land surface dissection				
		GA	*MCA*	*MDA*	*kh*	*kv*	*E*	*KA*	*kmin*	*kmax*	*H*	*K*	*M*	*khe*	*kve*	*KR*	*rot*
Upper layers																	
AhM5	−0.32	*	0.33	*	*	*	*	0.34	*	*	*	*	*	*	*	*	*
M5	−0.41	−0.36	0.42	*	*	*	*	*	*	*	*	*	*	*	*	*	*
M5-total	−0.45	−0.39	**0.49**	−0.31	*	*	*	*	*	*	*	*	*	*	*	*	*
Intermediate layers																	
M4	*	0.57	*	*	*	*	*	*	−0.29	*	*	*	0.45	*	0.30	0.43	*
M3	−0.41	0.64	*	*	*	0.33	0.48	*	*	*	*	−0.37	0.43	*	0.53	*	*
M2	−0.71	*	0.48	*	−0.34	*	*	*	*	*	*	*	*	*	*	*	*
M-middle	−0.47	**0.75**	0.30	*	*	0.30	0.49	*	−0.35	0.29	*	−0.35	0.55	*	0.59	*	*
Deeper layers																	
M1fAh	*	0.36	*	*	*	*	0.38	*	*	*	*	*	*	*	0.32	*	*
M1	−0.35	*	0.53	−0.44	−0.35	*	*	*	*	*	*	*	*	*	*	*	*
M1-total	*	*	0.58	**−0.67**	−0.61	*	0.62	*	−0.47	*	−0.39	*	0.40	−0.29	0.59	*	*
All layers together																	
M total-46	**−0.73**	0.39	0.68	−0.48	−0.62	*	0.64	*	−0.56	*	−0.41	*	0.57	*	0.71	*	*
M total-64	−0.49	−0.25	**0.85**	−0.75	−0.53	*	0.55	*	−0.51	*	−0.36	*	0.50	*	0.62	*	*

* The correlation is not significant at $p \leq 0.05$. A bold number shows the highest correlation for each layer group.

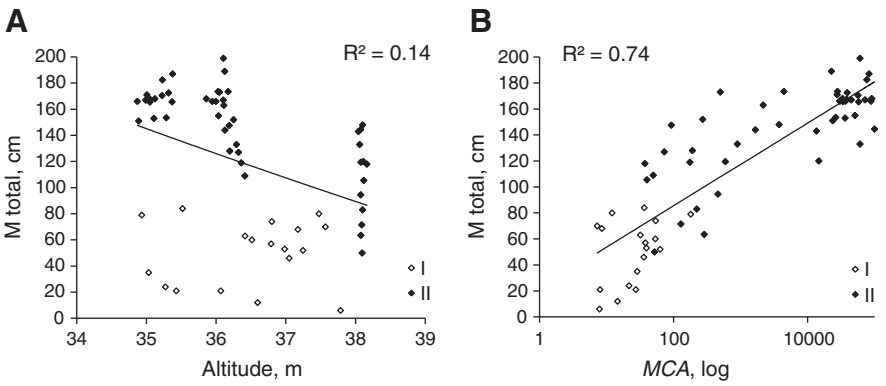

Fig. 7. Non-functional relationship of M total with altitude (A) and functional relationship with *MCA* (B). I – points from the cores, II – points from the trenches. Logarithmic trends drawn for the whole data set (M total-64) on both figures.

depressions ($kmin < kmax < 0 < E$). M total-46, which describes total thickness of colluvial deposits in the valley bottom, has the strongest r_S with curvatures. Hence, tendencies indicated by signs of r_S for M total-46 can be considered in details.

Signs of r_S indicate the tendency of thickness of M total-46 to increase at points with the following geomorphometrical criteria: *kmin, kh*, $H < 0$; $E > 0$; $M > M(mean)$; $kve > kve(mean)$, where "*mean*" is the mean value of *M* or *kve*. Because *M* and *kve* are obligatory > 0, the mean value of these curvatures is used as a hypothetical border between values that are related to accumulation and erosion of solid material. Nineteen points of measurements have geomorphometric criteria as described above. The mean value of M total-46 at these points is 167 ± 18.7 cm (error range = standard deviation) which is more than mean (130.1 ± 34.1 cm) for other points of M total-46. Thus, the mean confirms tendency reflected by signs of r_S.

5. Problem of geomorphometrical description of a slope profile

The youngest colluvial layers (M5 and M5-total) have negative correlations with *GA* (Table 4). In contrast to this, buried older layers (M4, M3 and M1fAh) have positive correlations with *GA*. In addition, different signatures of r_S with *GA* were found for M total-46 and M total-64 (Table 4).

The negative correlations with *GA* can be related to water erosion. However, no acceptable explanation for the positive correlations between the thickness of colluvial layers and *GA* was found in known publications. Besides the peculiarities mentioned above, one of the strongest positive correlation was found between M-middle and *GA* (Table 4).

For a better understanding of the obtained results, the physical meaning of *GA* should be determined. Oscillations of *GA* on slope along flow lines are caused by local zones of relative acceleration (potential erosion) and deceleration (potential accumulation) of flows on the land surface. These zones are described by positive and negative values of *kv* (e.g. Shary, 1995). Hence, *GA* characterises potential velocity of surface flows while *kv* describes potential acceleration/deceleration of surface flows.

Both *GA* and *kv* are characteristics of a mechanism of colluvial distribution along flow lines on slope profile. The correlation between *GA* and *kv* in sampling points was not significant. This indicates the independence of these MVs. Also in coordinates of *MCA,* the fluctuations of trends for *GA* and *kv* did not coincide (Fig. 8). Contrary to this, the extremes in trends for *GA* and M-middle coincide (Fig. 8), supported by strong positive r_S between *GA* and M-middle (Table 4).

Negative correlations between M5-total and other buried colluvial layers (Table 3) indicate inversion between zones of actual accumulation and deflection at the same point of observation. Such an inversion is improbable without the transformation of a former land surface. The variability of correlation signs between *GA* and colluvial layers of different ages shows that inversion caused by relative deceleration of migrants along flow lines occurred for zones of actual accumulation.

The result reflects the problem of geomorphometric description of a slope profile. Nowadays, zones of relative (potential) acceleration and deceleration of flows are described as local convex and concave terraces by signs of *kv*. Indeed, flow velocity is a dynamic event. As a result, a spatial shift can be observed between actual zones of colluvial accumulation, which are caused by relative deceleration of migrants and concave terraces defined by *kv*. Such a shift may decrease the strength of correlation between the thickness of deposits and *kv*.

The relationships between the velocity of surface flows and the shape of a land surface was used for constructing one of the first numerical models of spatial distribution of colluvial deposits (Mitas and Mitasova, 1998). However, this model is not taking into account the spatial shift between functionally related zones of colluvial accumulation and concave terraces defined by *kv*. If the data collection is made from only one slope, the relationships of actual accumulation zones with slope profile may be detected by a cubic trend of altitude (Tomer and Anderson, 1995; Shary et al., 2002b). However, due to difficult organisation of slope profiles, this approach needs special examinations in each and every case. Moreover, application of cubic trend of altitude does not solve the problem of considering extended terrain portions.

The topographical index (Beven and Kirkby, 1979) and similar combinations between *MCA* and *GA* were developed for a slope profile description with extended terrain portions considerations. The essential disadvantage of the topographic index is that it inadequately describes various kinds of terraces (Fig. 9). Furthermore, at small *GA* values, the topographic index takes unrealistically large values, which is forcing researchers to use empirical methods for correction of this variable (McKenzie and Ryan, 1999). Almost no correct MV for this purpose has been introduced until now. The only exception as far as the authors know is the "hydrodynamic area" described by Shary et al. (2002a). The hydrodynamic area is based on the idea of taking valleys and terraces into account at the same time (including saturation zones), and has no unrealistically large values. The main idea of this attribute is the immediate consideration of dynamic depressions. These depressions represent dynamic storages of migrants, which are moved downslope by gravity. The algorithm for its calculation has not been developed yet.

6. Conclusions

Colluvial deposits are distributed under the control of buried land surfaces. However, the significant correlations of colluvial deposits thickness were established with characteristics of the modern land surface. This indicates that the modern land surface contains information on former surfaces. The structures that contain this information are not visually detectable at detailed scales. Hence, sensitive techniques

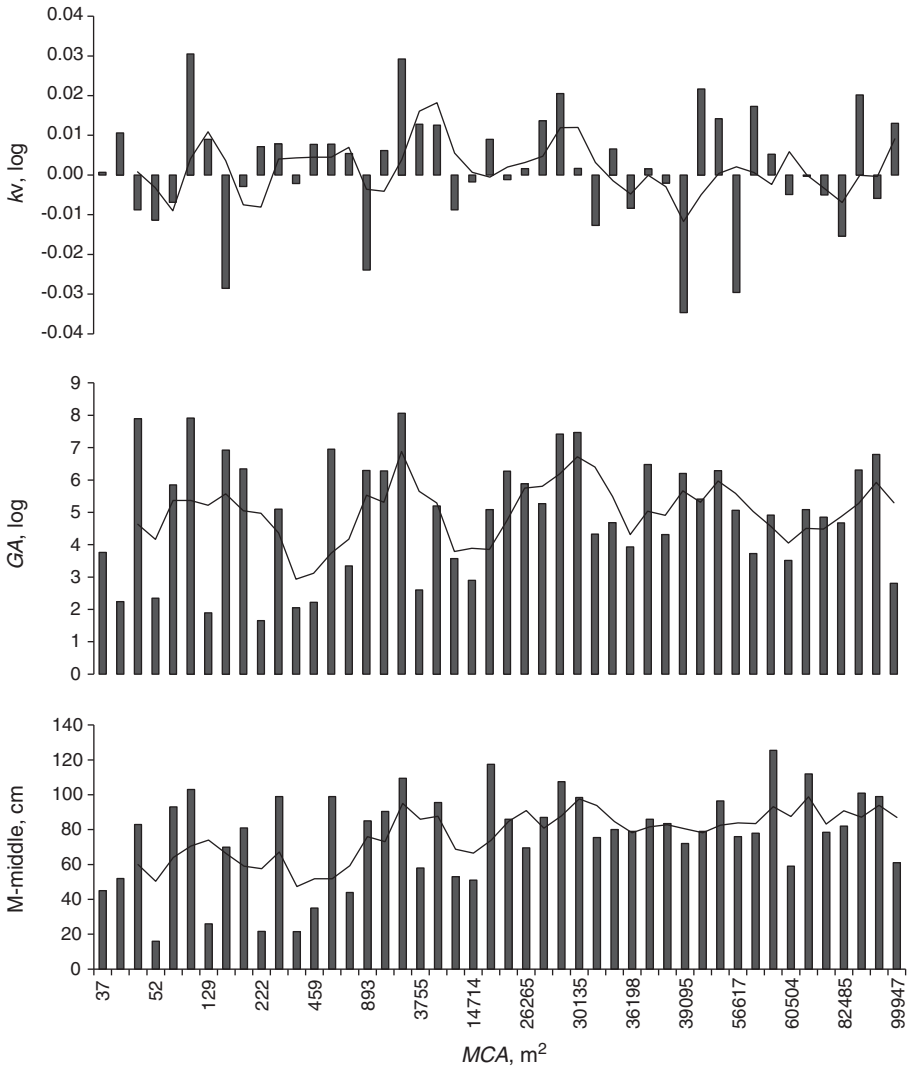

Fig. 8. Distribution of slope steepness (*GA*), vertical curvature (*kv*) and thickness of M-middle in coordinates of maximal catchment area (*MCA*). The trends are based on three windows linear filtration.

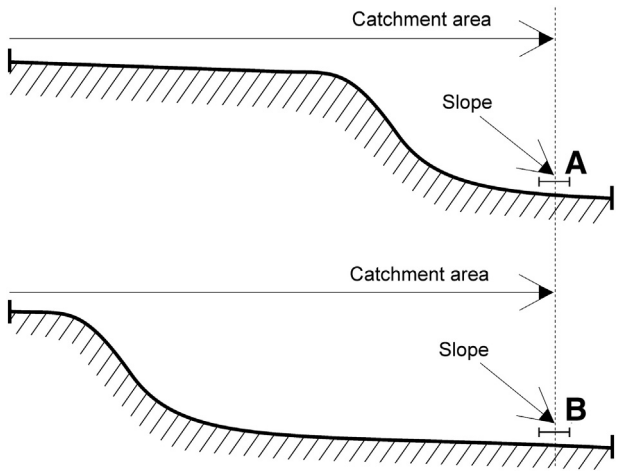

Fig. 9. Two sufficiently different land surface portions. In segments A and B they cannot be distinguished by existing morphometric variables. The slope, catchment area and the topographic index in these segments are the same. It is expected that potential velocity of surface flows at segment A should be higher than at segment B.

of geomorphometry for the description of hidden structures of the modern land surface should be used. The comparison of MVs of the modern land surface with sediment properties such as the thickness of colluvium may enable a detailed reconstruction of land surface transformation. Analysis of correlations between MVs of the modern land surface and the thickness of colluvial deposits yielded the following results:

- MVs have stronger correlations with combined layers. The strongest r_S was found between M total-64 and *MCA* (Table 4). On the one hand it is because combined layers reflect a longer period of sedimentation and more resistance to both random errors of measurements and natural disturbances. On the other hand, *MCA* is one of the best prerequisites of surface flows, which play an important role in spatial distribution of colluvial deposits. Moreover, *MCA* as a regional MV better describes long wave spatial variations of landscape properties as compared with local MVs such as curvatures.
- Significant correlations with the thickness of colluvial deposits were found for both *Z* and *MCA*. However, the key site was too small for the assumption that altitude is the trigger of any physical process of spatial variability of colluvial deposits in the valley. Hence, the correlation with altitude was significant, but non-functional. *MCA* shows the physical process of mass transport on small key sites. The correlation with *MCA* reflects the accumulation of colluvial deposits at the valley bottom. Hence, the correlation with *MCA* was significant and

functional. These results illustrate the importance of logical interpretation of correlation coefficients. It should be based on the correct meaning of MVs according to the theory of geomorphometry.

- The signs of correlation coefficients reflect the tendency of an increase of colluvial deposits in three main local landforms of classification according to Shary (1995). These landforms are located in the valley bottom and are described as: *kmin*, *kmax*, *H*, *kv*, *kh* < 0 < *E*; *kmin*, *H*, *kh*, *kv* < 0 < *kmax*, *E*; and *kmin*, *H*, *kh* < 0 < *kv*, *E*, *kmax*. The mean values of M total-46 at these three local landforms were higher than at the other nine main local landforms. This result shows that several curvatures were not enough for a detailed description of the land surface. The description of the land surface with the help of the system of 12 curvatures detects local landforms that were most sensitive to accumulation of colluvium.
- The negative correlation was observed between the thickness of relatively young and old colluvial layers. In relation to long-term sedimentation this indicates an inversion of the land surface shape from concave to convex. However, such terms as "concave" and "convex" cannot be accepted in geomorphometry without considering the direction in which such a shape was measured. The variability of signs of correlation coefficients between thickness of colluvial layers and slope steepness reflects transformation of the land surface shape along flow lines. Such a transformation was caused by different velocities of surface flows in time for a constant point in space.
- It was expected that the distribution of colluvium along flow lines should be reflected by correlations of these sediments with both slope steepness and vertical curvature. However, under the given conditions, only slope steepness was a good geomorphometrical descriptor of actual colluvium accumulation zones caused by deceleration of migrants along flow lines. The problem refers to the regional nature of real flow velocity and the absence of a corresponding regional MV that considers the impact of extended terrain portions. This indicates one of the main problems of geomorphometry: the necessity to introduce a new regional MV for a complete assessment of geomorphometric prerequisites of surface flow dynamics along flow lines.

Acknowledgements

The research was partly supported by the Graduate School "Human Development in Landscapes" of Christian-Albrechts University Kiel, Germany. We thank Peter Shary, Stéphane Follain, an anonymous reviewer and Takashi Oguchi for their very helpful comments; Igor Florinsky for providing useful information; Ashie Okai for English language editing; owners of the farm "Perdöler Mühle" family Overath for allowing excavations; and students of the master program "Environmental management" in Kiel University and Mathias Bahns for the excavation and assistance during the field campaign.

References

Boden, Ad-hoc-Arbeitsgruppe (Ed.), 2005. Bodenkundliche Kartieranleitung, 5th edition. Bundesanstalt für Geowissenschaften und Rohstoffe in Zusammenarbeit mit den Staatlichen Geologischen Diensten, Hannover (438 pp.).

Beven, K.J., Kirkby, M.J., 1979. A physically based, variable contributing area model of basin hydrology. Hydrol. Sci. Bull. 24, 43–69.

Ciampalini, R., Billi, P., Ferrari, G., Borselli, L., Follain, S., 2012. Soil erosion induced by land use changes as determined by plough marks and field evidence in the Aksum area (Ethiopia). Agric. Ecosyst. Environ. 146, 197–208.

de Moor, J.J.W., Verstraeten, G., 2008. Alluvial and colluvial sediment storage in the Geul River catchment (The Netherlands) – Combining field and modelling data to construct a Late Holocene sediment budget. Geomorphology 95, 487–503.

Dotterweich, M., 2008. The history of soil erosion and fluvial deposits in small catchments of central Europe, Deciphering the long-term interaction between humans and the environment – A review. Geomorphology 101, 192–208.

Dreibrodt, S., Bork, H.-R., 2005. Historical soil erosion and landscape development at Lake Belau (North Germany) – a comparison of colluvial deposits and lake sediments. Z. Geomorph. N.F. 139 (Suppl.-Bd), 101–128.

Dreibrodt, S., Wiethold, J., 2014. Lake Belau and its catchment (northern Germany) – a northern central Europe key site of human impact on the landscape since the onset of agriculture. The Holocene, (submitted for publication).

Dreibrodt, S., Lubos, C., Terhorst, B., Damm, B., Bork, H.-R., 2010. Historical soil erosion by water in Germany, scales and archives, chronology, research perspectives. Quat. Int. 222, 80–95.

Evans, I.S., 1972. General geomorphometry, derivations of altitude and descriptive statistics. Spatial analysis in geomorphologyMethuen and Co. Ltd, London, pp. 7–90.

Florinsky, I.V., Kuryakova, G.A., 1996. Influence of topography on some vegetation cover properties. Catena 27, 123–141.

Florinsky, I.V., Kuryakova, G.A., 2000. Determination of grid size for digital terrain modelling in landscape investigations – Exemplified by soil moisture distribution at a micro-scale. Int. J. Geogr. Inf. Sci. 14, 815–832.

Florinsky, I.V., Eilers, R.G., Manning, G., Fuller, L.G., 2002. Prediction of soil properties by digital terrain modelling. Environ. Model. Softw. 17, 295–311.

Florinsky, I.V., McMahon, S., Burton, D.L., 2004. Topographic control of soil microbial activity, a case study of denitrifiers. Geoderma 119, 33–53.

Follain, S., Minasny, B., McBratney, B.A., Walter, C., 2006. Simulation of soil thickness evolution in a complex agricultural landscape at fine spatial and temporal scales. Geoderma 133, 71–86.

Garbe-Schönberg, C.-D., Wiethold, J., Butenhoff, D., Utech, C., Stoffers, P., 1998. Geochemical and palynological record in annually laminated sediments from Lake Belau (Schleswig-Holstein) reflecting paleoecology and human impact over 9000 a. Meyniania 50, 47–70.

Gauss, C.F., 1828. Disquisitiones generales circa superficies curvas. Comm. Soc. Reg. Sci. Gott. Rec. 6, 99–146 (in Latin).

Houben, P., 2008. Scale linkage and contingency effects of field-scale and hillslope scale controls of long-term soil erosion: Anthropogeomorphic sediment flux in agricultural loess watersheds of Southern Germany. Geomorphology 101, 172–191.

Houben, P., 2012. Sediment budget for five millennia of tillage in the Rockenberg catchment (Wetterau loess basin, Germany). Quat. Sci. Rev. 52, 12–23.

Husson, O., Verburg, P.H., Mai, Thanh Phung, Van Mensvoort, M.E.F., 2000. Spatial variability of acid sulphate soils in the Plain of Reeds, Mekong delta, Vietnam. Geoderma 97, 1–19.

Krcho, J., 1983. Teoretická concepcia a interdisciplinarne aplikacie komplexného digitalneho modelu reliéfu pri modelovaní dvojdimenzionalnych poli. Geogr. Cas. 35 (3), 265–291 (In Slovak).

Landesvermessungsamt Schleswig-Holstein, 2012. http://www.schleswig-holstein.de/LVERMGEOSH/DE/LVERMGEOSH_node.html.

McKenzie, N.J., Ryan, P.J., 1999. Spatial prediction of soil properties using environmental correlation. Geoderma 89, 67–94.

Mitas, L., Mitasova, H., 1998. Distributed erosion modeling for effective erosion prevention. Water Resour. Res. 3, 505–516.

Mitusov, A.V., 2001. Influence of land surface on soil fertility of grey forest soils of European part of Russia. PhD thesis , (Orel – SAU. 120 pp. (in Russian)).

Mitusova, O.E., 2010. Quantification of spatial distribution of colluvial matter, case study Perdoel (Schleswig-Holstein, Germany). Master thesis University Kiel, (54 pp.).

Piotrowski, J., 1991. Quartär- und hydrogeologische Untersuchungen im Bereich der Bornhöveder Seenkette, Schleswig-Holstein. Ph.D. Thesis University Kiel, (194 pp.).

Reiss, S., Bork, H.R., Hoernes, U., Rinker, A., Mitusov, A., 2008. In: Borkenhagen, P., Irmler, U., Roweck, H. (Eds.), Die Verbreitung der Boeden auf den Ackerflaechen von Hof Ritzerau. In Faunistisch – Oekologische Mitteilungen. Kiel, Wachholtz Druck, pp. 59–74 (Suppl. 35).

Ries, H., 2002. GIS-gestuetzte Rekonstruktion der Reliefentwicklung der Wolfsschlucht (Ostbrandenburg). Diplomarbeit zur diplomprufung im fach geographieChristian-Albrechts-Universitaet zu Kiel. Kiel, (152 pp.).

Rommens, T., Verstraeten, G., Lang, A., Poesen, J., Govers, G., Van Rompaey, A., Peeters, I., 2005. Soil erosion and sediment deposition in the Belgian loess belt during the Holocene: establishing a sediment budget for a small agricultural catchment. The Holocene 15, 1032–1043.

Schneider, A., Gerke, H.H., Maurer, T., 2011. 3D initial sediment distribution and quantification of mass balances of an artificially-created hydrological catchment based on DEMs from aerial photographs using GOCAD. Phys. Chem. Earth 36, 87–100.

Shary, P.A., 1995. Land surface in gravity points classification by a complete system of curvatures. Math. Geol. 27, 373–390.

Shary, P.A., 2005. Assessment of relationships relief-soil-vegetation with using of new approaches in geomorphometry (on the example of agrolandscape and forest ecosystem of South of Moscow region. PhD thesis Pushino – IFHBPS RAN, (224 pp. (in Russian)).

Shary, P.A., 2012. The mathematical basis of local morphometric variables. In: Florinsky, I. V. (Ed.), Digital terrain analysis in soil science and geology. Appendix a. Elsevier, Amsterdam, Boston, Heidelberg, London, New York, Oxford, Paris, San Diego, San Francisco, Singapore, Sydney, Tokyo, pp. 289–313.

Shary, P.A., Sharaya, L.S., Mitusov, A.V., 2002a. Fundamental quantitative methods of land surface analysis. Geoderma 107, 1–35.

Shary, P.A., Rukhovich, O.V., Sharaya, I.S., Mitusov, A.V., 2002b. Soils and topography, accumulation zones and non-local approaches. 17-th World Congress of Soil Science, (Bangkok, Thailand, August, 2002). Abstract 1493. Paper 2310 (11 pp.).

Shary, P.A., Sharaya, L.S., Mitusov, A.V., 2005. The problem of scale-specific and scale-free approaches in geomorphometry. Geogr. Fis. Din. 28, 81–101.

Speight, J.G., 1968. Parametric description of land form. In: Stewart, G.A. (Ed.), Land evaluation. MacMillan, London, pp. 239–250.

Speight, J.G., 1974. A parametric approach to landform regions. Progress in geomorphology. Institute of British Geographers special publ. No.7. Alden and Mowbray Ltd. at the Alden Press, Oxford, pp. 213–230.

StatSoft Inc., 2013. Electronic statistics textbook. StatSoft, Tulsa, OK, (WEB: http://www.statsoft.com/textbook/).

Svendsen, J.I., Alexanderson, H., Astakhov, V.I., Demidov, I., Dowdeswell, J.A., Funder, S., Gataullin, V., Henriksen, M., Hjort, C., Houmark-Nielsen, M., Hubberten, H.W., Ingólfsson, Ó., Jakobsson, M., Kjær, K.H., Larsen, E., Lokrantz, H., Lunkka, J.P., Lyså, A., Mangerud, J., Matiouchkov, A., Murray, A., Möller, P., Niessen, F., Nikolskaya, O., Polyak, L., Saarnisto, M., Siegert, C., Siegert, M.J., Spielhagen, R.F., Stein, R., 2004. Late Quaternary ice sheet history of northern Eurasia. Quat. Sci. Rev. 23, 1229–1271.

Tarboton, D.G., 1997. A new method for the determination of flow directions and upslope areas in grid digital elevation models. Water Resour. Res. 30, 9–17.

Tomer, M.D., Anderson, J.L., 1995. Variation of soil water storage across a sand plain hillslope. Soil Sci. Soc. Am. J. 59, 1091–1100.

Vanwalleghem, T., Laguna, A., Giráldez, J.V., Jiménez-Hornero, F.J., 2010. Applying a simple methodology to assess historical soil erosion in olive orchards. Geomorphology 114, 294–302.

Wood, J., 2009. Overview of software packages used in geomorphometry. In: Hengl, T., Reuter, H.I. (Eds.), Geomorphometry: Concepts, software, applications. Developments in Soil Science, Vol. 33. Elsevier, Chapter 10, Amsterdam, Boston, Hiedelberg, London, New York, Oxford, Paris, San Diego, San Francisco, Singapore, Sydney, Tokyo, pp. 257–267.

Appendix III

Dreibrodt, S., Nelle, O., Lütjens, I., Mitusov, A., Clausen, I., Bork, H.-R., 2009. Investigations on buried soils and colluvial layers around Bronze Age burial mounds at Bornhöved (northern Germany): an approach to test the hypothesis of ‘landscape openness’ by the incidence of colluviation. The Holocene 19, 487–497.

Investigations on buried soils and colluvial layers around Bronze Age burial mounds at Bornhöved (northern Germany): an approach to test the hypothesis of `landscape openness' by the incidence of colluviation

S. Dreibrodt, O. Nelle, I. Lütjens, A. Mitusov, I. Clausen and H.-R. Bork

The Holocene 2009 19: 487
DOI: 10.1177/0959683608101397

The Holocene 19,3 (2009) pp. 487–497

Investigations on buried soils and colluvial layers around Bronze Age burial mounds at Bornhöved (northern Germany): an approach to test the hypothesis of 'landscape openness' by the incidence of colluviation

S. Dreibrodt,[1]* O. Nelle,[1] I. Lütjens,[2] A. Mitusov,[1] I. Clausen[2] and H.-R. Bork[1]

([1]Ecology Centre, University of Kiel, Germany; [2]State Office of Archaeology Schleswig-Holstein, Germany)

Received 8 February 2008; revised manuscript accepted 12 September 2008

Abstract: The idea of open landscapes around prehistoric burial mounds is founded on their topographical position and findings of plaggen clots within the hills at some sites. We have investigated the surroundings of four Bronze Age burial mounds at Bornhöved (northern Germany) to test whether this assumed landscape openness enabled soil erosion and colluviation or not. The soils and colluvia within a watershed below the burial mounds were investigated in six large exposures and additional auger cores. The chronology is based on 21 AMS-radiocarbon dates, complemented by charcoal analysis and the content of selected heavy metals in the sediments. Colluvia were deposited in the Late Neolithic (~2500–2200 cal. BC), Roman Emperor Times (~ 250–400 cal. AD), Mediaeval Times (~ AD 600–1400) and Modern Times (~ AD 1800–2000). Our findings indicate that the soil surfaces were protected against soil erosion during the phase of Bronze Age funeral use (~ cal. 1800–600 BC). Either the prehistoric gravediggers practised a well suited form of pasturing to keep the scenery open or the surroundings of the burial mounds were forested at the time of funeral use. The results of charcoal analysis reflect the known succession of woody taxa in the region and underline the great potential of anthracology on colluvial layers for palaeoenvironmental reconstructions apart from traditional archives such as lakes or mires. Bulk radiocarbon dating of organic matter overestimated the time of burial of a buried soil as well as the time of deposition of colluvial layers considerably.

Key words: Bronze Age burial mounds, historical soil erosion, charcoal analysis, landscape history, landscape openness, Holocene palaeoecology, northern Germany.

Introduction

Burial mounds were erected in northern Europe since the Early Neolithic (~ 3700 cal. BC) until Early Mediaeval Times (~ AD 1000) (eg, Hingst, 1976, 1979; Struwe, 1979; Laux, 1996; Ethelberg, 2000; Jørgensen, 2000; Eisenschmidt, 2004). Besides these specific funeral practises, burials in ordinary shallow graves were common throughout these times (Hingst, 1974; Zich, 1992). Burial mounds from the Neolithic until the Late Bronze Age exposed diameters of around 10 to 20 m (Laux, 1996: 174). Data about the former height of the mounds are rare, since the structures were often destroyed through intentional removal, soil erosion and plough action. Struwe (1979: 32) gives reconstructions of about 1 to 3 m for the majority of prehistorical burial mounds (a measure which may fit the mounds at the investigation site), whereas some mounds may have reached 10 m. Usually, the development of a burial mound started with a single grave and a first mound body. Later, additional graves were dug; some of them even have new mound layers. Therefore, many burial mounds in northern Germany are polygenetic in their history (Struwe, 1979: 32ff; Ethelberg, 2000: 149). Many burial mounds of the Early

*Author for correspondence (e-mail: s3brodt@ecology.uni-kiel.de)

10.1177/0959683608101397

Bronze Age were erected at special topographical positions: on top of hills within the landscape (Ethelberg, 2000: 149) as is the case at the investigation site at Bornhöved. Since these topographical positions are dominant, archaeologists have assumed that the landscape around the burial mounds was open, in order to make them visible from the surrounding scenery. A significant opening of the surrounding landscape is also indicated at selected sites from palaeobotanical results (eg, Odgaard, 1988; Schmidt, 1993; Hannon *et al*., 2007; Karg, 2008). It is not clear in every case if the reconstructed landscape openness is related to the settlement and sites used for agriculture, or to the burial mounds. Willroth (1999: 56ff, figure 13) assumes at least open woodland surrounding the Early Bronze Age burial mounds. At other sites, traces of agricultural field use (plough horizons) were associated with Early Bronze Age burial mounds. For instance, Zich (2005) found plough layers below and beside burial mounds at Flintbek, testifying agricultural field use during the growing phases of the mound structures.

Soil erosion is a process supposed to be enabled or amplified by forest clearings and agricultural land use worldwide. Recent studies estimate global sediment flux associated with soil erosion under cropland to be ~ 22 Pg/yr but also ~ 11 Pg/yr under pasture- and rangelands from recent observations (van Oost *et al*., 2007). Therefore any clearing of a pristine forest cover should result in soil erosion and deposition of the sediment. The history of soil erosion resulting from human impact on central European landscapes has been reconstructed at numerous sites, where most of the sediment volume was found to be deposited in proximity to its sources (eg, Bork *et al*., 1998; Bork and Lang, 2003; Dotterweich 2008).

Since the results of archaeological research testified to the construction of burial mounds on top of hills within a scenery of a considerable relief at the Bornhöved site, we tested whether or not the assumed landscape openness enabled soil erosion and colluviation. Another focus of the present study was to test whether or not it is possible to gain insights into vegetation history additionally to pollen analysis from charcoal analysis on colluvial sediments.

Material and methods

Study area

The Bronze Age burial field 'Mang de Bargen' (translation: 'in between the hills') is located in northern Germany, approximately 40 km south of the city of Kiel (Figure 1). The main morphological elements of the landscape, as well as the substrate (outwash sands at the studied site) are the result of the Weichselian glaciation (Piotrowski, 1991). After some alteration of the relief during the Lateglacial, natural soil formation proceeded until the Neolithic settlers cleared the forests ~ 4300 cal. BC (Hoika, 1993, 1994; Hartz, 2004). Today, Cambisols and Luvisols (Food and Agriculture Organization (FAO), 1998) are the dominant soils in the region (Schleuss, 1991). At many sites, these soils developed in the remnants of capped pristine soils on upper slopes, or in the associated colluvia on lower hills. The land use and the settlement history of the region are well known from archaeological (eg, Schwerin von Krosigk, 1976; Lütjens and Wiethold, 1999) and historical (eg, Kock, 1972; Dege, 1988) investigations. On a profundal sediment core from Lake Belau, which is situated 3 km north of the research site, Wiethold (1998) and Garbe-Schönberg *et al*. (1998) established a high resolution palynological and geochemical record. Additional results about historical land use, soil formation and soil erosion history within the catchment area of Lake Belau was presented by Dreibrodt (2005) and Dreibrodt and Bork (2005).

The Bronze Age burial mounds at Bornhöved were first investigated by Schwerin von Krosig (1976). The results of the ongoing archaeological investigations will be published in a separate paper

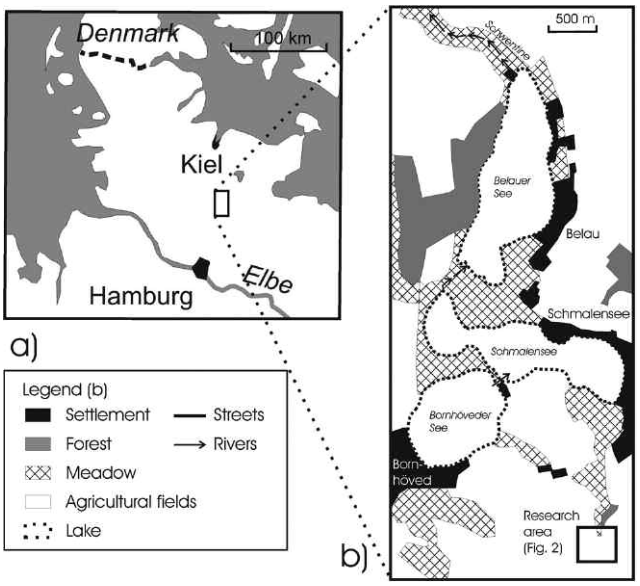

Figure 1 Bornhöved: site and location showing the actual mean land-use classes around the research area and its proximity to the Belauer See

(I. Lütjens and I. Clausen, unpublished data, 2008). Therefore, only the most important findings are outlined in the following. The oldest finding was a remnant of a shallow grave from the early Funnelbeaker Culture (Early/Middle Neolithic, ~ 3600–3400 cal. BC). The oldest burial mound was constructed during the late Middle Neolithic to late Neolithic (~ 2700–1800 cal. BC). The following main phase of burial activity dates into the early to late Bronze Age (~ 1800–1200 cal. BC). Four burial mounds of diameters of 10 m or more and heights of about 1–3 m were constructed. At the bases of two of these Bronze Age burial mounds traces of plough layers were identified. Continued burial use of the area during the late Bronze Age (~ 1100–600 cal. BC) is documented in fields of shallow graves adjacent to the older mounds. One of the fields was used until the early Pre-Roman Iron Age (~ 400 cal. BC).

In the vicinity (~ 500 m to the north) traces of a Roman Emperor Age settlement site (per convention AD 1 to 400) were detected during a survey.

Field methods

The selected study site lies within a watershed below five Bronze Age burial mounds (Figure 2). At the site six exposures up to 3 m deep and up to 200 m long were dug with an excavator (Figure 2). After carefully cleaning the sidewalls, colluvial layers and soil horizons in the sequences were identified and described using the following field methods:

(a) Colours were determined using the Munsell-System (Munsell, 2000).
(b) All soil types and horizons were denoted according to the instructions of FAO (1998). Colluvial layers were denoted with the abbreviation M for 'migrare' (lat.) according to AG Boden (2005).
(c) Archaeological relics, such as artefacts, traces of fire or settlement pits, were documented in detail and interpreted together with specialists.
(d) All exposures were documented by scaled drawings and photographs.
(e) Additional information about the spatial distribution of soils and sediments was acquired from dense augering (35 cores, up to 2 m in length) in the watershed area.
(f) A relative chronology of the deposited sediments and soils was established through the stratigraphic order.

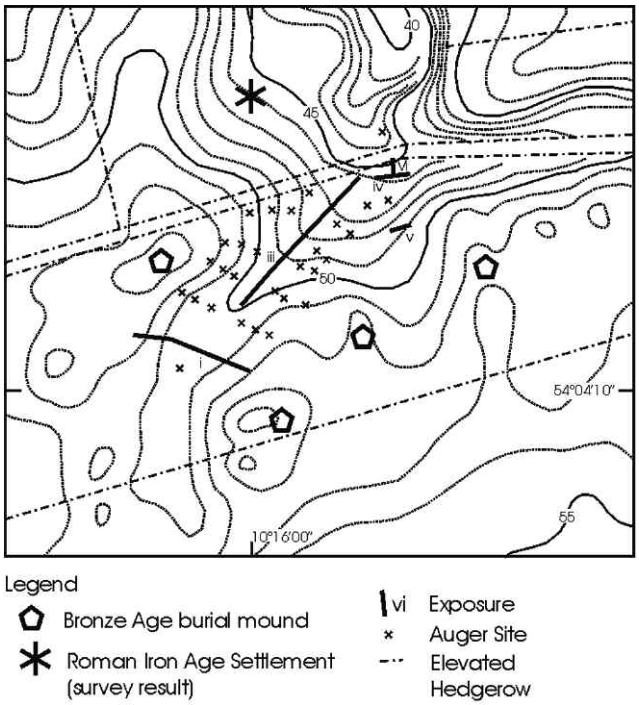

Figure 2 Bornhöved: relief and location of the exposures and the archaeological findings

Laboratory methods

For selected samples additional laboratory analyses were applied:

(a) Texture analysis using the sieve and pipette method (Schlichting *et al*., 1995).

(b) Soil organic matter content was determined via the content of Carbon and Nitrogen using an elemental analyser with dry combustion. The total organic carbon content of the samples was multiplied by 1.72 (according to AG Boden, 2005) to get the soil organic matter content.

(c) For measurements of the content of selected heavy metals continuous series of samples were taken in steps of increasing depth (increments of 10 cm in exposure (i) and 20 cm in exposure (vi), the locations of sample profiles are given in Figures 3 and 4). The content in Pb, Cr, Cu, Cd and Zn of the dried and grinded samples was measured at an ICP-OES after digestion in aqua regia according to the instructions of DIN 38414 (1983). The limits of detection were 5 ppm for Pb, 1 ppm for Cr, 0.2 ppm for Cd, 1 ppm for Zn and 0.5 ppm for Cu.

(d) Dating. Radiocarbon dating of charcoal fragments and soil matrix was carried out in order to convert the relative stratigraphy of colluvial layers into chronometric information. To identify charcoals that were reworked repeatedly, at least two were dated per layer. Since no indication for bioturbation was observed in the field, the youngest object in a layer was used to derive a maximum age of the deposition of the layer. Radiocarbon ages from charcoals found in fire places or pits were used to derive minimum ages for the underlying sediment layers and maximum ages for sediments layers that cover the *in situ* findings. When possible the taxa of the charred wood were determined before radiocarbon dating. Samples of soil matrix for radiocarbon dating were taken from the lowest parts of a humic horizon (exposure (i); SM1) and two colluvial layers (exposure (vi); SM2, SM3). The fraction < 500 µm was selected after carefully removing any charcoal particles or other organic remains under the microscope. The organic matter was extracted first with 1% HCl, then with 1% NaOH (60°C), finally precipitated with 1% HCl and dried. The residue and the extracted humic acid were dated. All age data are given as calibrated radiocarbon ages AD/BC on the 2σ range (calibrated after Reimer *et al*., 2004).

(e) Charcoal analysis. Samples for charcoal analysis were taken from all colluvial layers of exposure (vi) at three profile columns (Figure 3). Each sample with a volume of 10 l substrate was wet-sieved (mesh with 1 mm), air-dried and weighed before microscopical analysis. The determination of wood taxa follows Schweingruber (1990a, b) using a stereoscope with magnification up to 112× (Nikon SMZ 1500) and an incident-light microscope with magnification up to 500× (Nikon ME 600) as well as a reference collection. The small fragments were cut manually under the stereoscope at a magnification of 7.5–10×, in order to attain fractured surfaces of transversal, tangential and radial orientation. The determined fragments were again weighed to calculate percentages as numbers as well as weight. A wood diameter measurement, which is possible when analysing larger charcoal fragments because of the visible growth ring curvatures and angle of wood rays (Nelle, 2002, 2003; Ludemann *et al*., 2004), was not applied here because fragments were too small.

Results

Distribution of colluvia, eroded and buried soils in the exposures and auger cores

Figure 2 gives an overview of the locations of the exposures and auger coring sites. An overall stratigraphy of the Holocene colluvial sediments was worked out by a combination of results from all exposures and additional auger cores. Four distinct colluvial layers (M1 to M4) were found to be deposited within the investigated watershed. For illustrating the stratigraphy and the results we selected the exposures (i) (Figure 3) and (vi) (Figure 4). In general, the colluvial sediments are thicker in exposure (vi) than in exposure (i) reflecting the topographical positions of the profiles and the relief gradient between them.

In exposure (i) a section through a depression in between two hills topped with burial mounds was exposed (Figure 3).

At the base brown sand rich in large stones (up to 15 cm in diameter) was exposed. Frequently, thin (~ 1 cm) dark brown clay bands have penetrated the sand. Above lies a sediment body without large stones, with a slightly more silty texture. The lower part of this sand (thickness ~ 15 cm) has a brown colour. The upper part (thickness ~ 15 cm) is paler in colour. No artefacts or charcoal particles were found within the material. A buried Ah-horizon in the uppermost part indicates the former surface. This horizon has a thickness of up to 20 cm. Because it exceeds the usual thickness of Ah-horizons on sandy substrates it may already contain humus rich colluvia (M1) in its upper part to some extent. Approaching the hills the soil horizons described are eroded and gradually disappear. At the upper hillslopes only remnants of the Bw/BBt-horizon are preserved. At both slopes, patches of a loamy material (exposed as two sections of about 2 m in length, more than 1 m in depth, Figure 3), probably representing remnants of former glacial tills, were exposed.

The soil described above was buried by a sequence of colluvial layers in the centre of the investigated valley. As these sediments, which reach their maximum thickness within the centre of the valley, originate from the soil the horizons of the Lammellic Luvisol (FAO, 1998) disappear stepwise to the adjacent slopes. Layer M2 is of brown colour and contains charcoal fragments. The distribution of the layer is limited to the centre of the investigated valley, where it reaches a maximum thickness of up to 50 cm. Towards

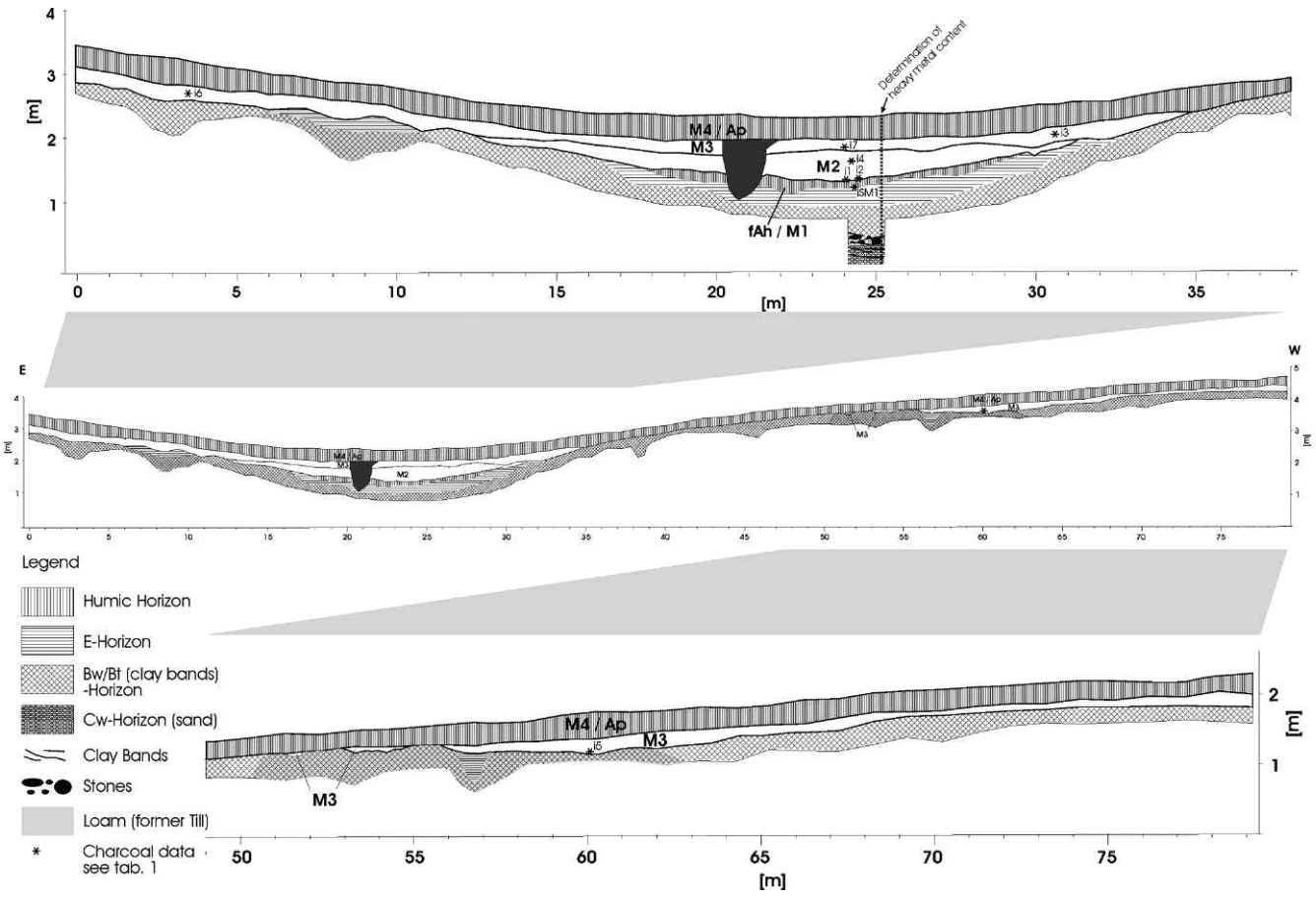

Figure 3 Exposure (i): superelevation two-fold

the hillslopes its thickness decreases gradually. Above M2 the sediment M3 with slightly higher humus content and a little darker in colour was deposited. M3 is exposed within the deepest part of the exposure continuing to the eastern hillslope. It reaches a maximum thickness of about 15 cm. At the western hillslope M3 is present within a small pocket-like depression at the upper hill with a thickness of about 25 cm. The layer M4 forms the top of the sequence. It contains the recent plough horizon and is therefore rich in humus and of dark grey colour. The M4 (Ap) layer reaches a maximum thickness of ~ 40 cm and thins gradually to the hillslopes. At the western middle slope position it is present in a minimum thickness of about 20 cm. At the length of 20 m within the exposure a modern disturbance was existent, buried below the plough horizon.

Exposure (vi) cuts through an elevated hedgerow (Figure 4). These linear landscape structures are typical for the region. Founded at around 200 years ago these structures delineate borders of historical estates and create enclosures for cattle etc. In exposure (vi) the sequence of colluvial layers reaches a cumulative thickness of about 2 m. At the base a sand of brown colour, probably indicating a former Bw-horizon was exposed. No clay bands were found within the layer. Large stones (up to 20 cm in diameter) were present in the sand layer. Above the sand a colluvial layer M1 rich in humus and of dark grey colour was exposed. It reaches a maximum thickness of about 50 cm below the hedgerow and contained abundant charcoal fragments and large stones. Towards the hillslope the thickness of M1 decreases to approximately 20 cm and most probably merges there into the remnants of a buried Ah horizon. Above M1 the brown colluvial layer M2 was deposited. It contains abundant charcoals and reaches a maximum thickness of about 70 cm in exposure (vi). A shallow pit of pale grey colour containing a few charcoal pieces was dug into the layer M2. The pit was buried by another colluvial layer M3. It has a darker and more greyish colour than M2 and contains fewer charcoals. The colluvial layer M4 forms the top of the sequence. The present plough horizon is developed in M4 and it is rich in humus and has a dark grey colour. M4Ap covers the lower section of the hedgerow body: the linear structure raised in former times exposes the character of a terrace today because of the deposition of M4Ap.

Laboratory data

Texture and soil organic matter content

The texture and soil organic matter values of the colluvial sediments and soils are given in Figure 5. According to the instructions of AG Boden (2005) the substrate at the base is pure sand and the colluvial sediments are loamy sands. The stone content (> 2 mm) in the parent material is respectively high. But even a high stone content was measured for the oldest colluvial layer (M1) in exposure (vi). The sediment sequence of exposure (vi) shows a slight trend to finer sediment (silt + clay) from the lower to the upper layers. This trend is not visible in exposure (i). The buried soil in exposure (i) has developed in layers with a different texture. The sand content of the upper horizons (fAh, fE) is clearly smaller than that of the underlying fBw/fBbt horizon. Also, the fE horizon of the buried soil shows a slight increase in silt and a slight decrease in clay, compared with the overlaying fAh/M1 horizon. This difference is explained by the accumulation of clay bands and the slight increase within the clay content in the fBbt horizon at the base of the soil profile.

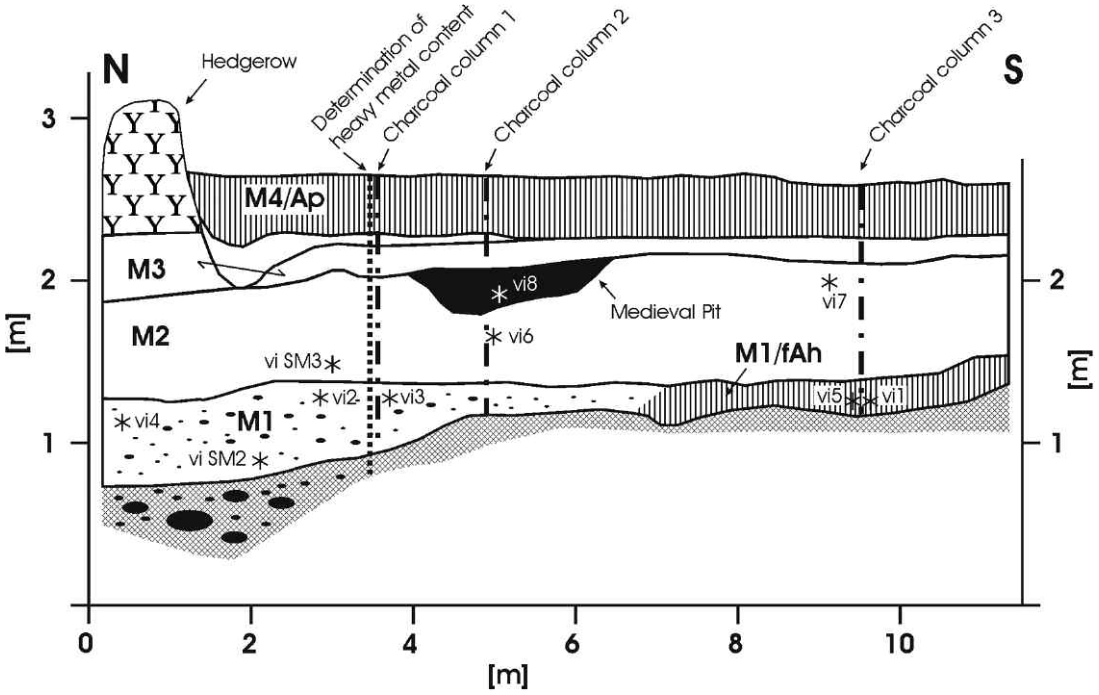

Figure 4 Exposure (vi): superelevation two-fold

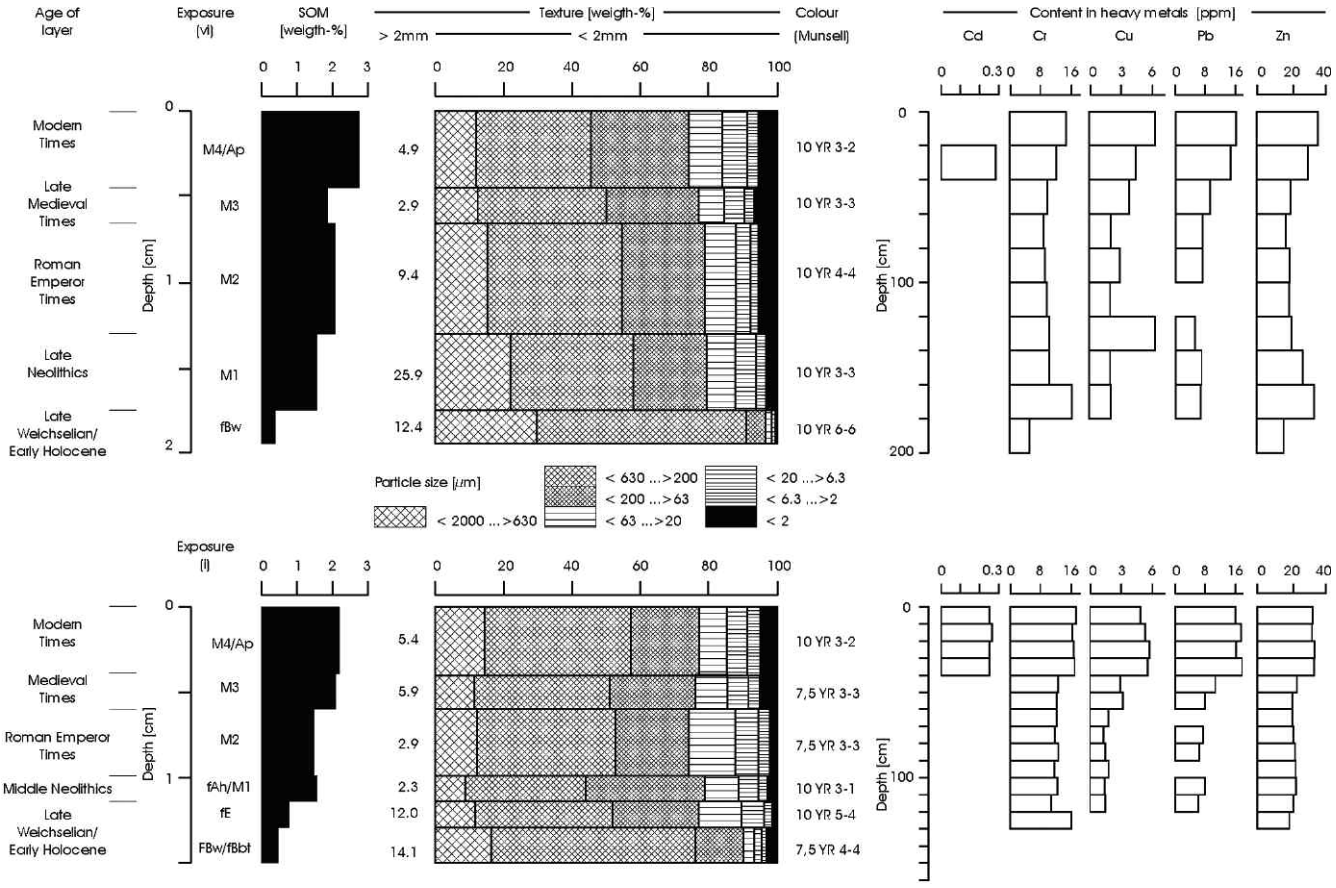

Figure 5 Results of laboratory analysis. Heavy metals contents below the detection limit (see text) where no bar is plotted

The organic carbon and soil organic matter content decreases from the top of the sequence to the deeper layers. The buried humic horizon in exposure (i) (a certain amount of colluvial material should be assumed, see above) is visible with slightly higher organic matter content, compared with the overlying colluvial layer.

The finer texture and higher organic matter content of M4 in exposure (vi) compared with exposure (i) indicates that a supply

Table 1 AMS-radiocarbon data of charcoals and soil matrix samples

Exposure	Sample no.	Layer/horizon/pit (taxa)	Sample type	Radiocarbon age (BP)	Calibrated age (2σ range)	$\Delta^{13}C$ (‰)	Lab. no.
i	1	fAh/M1	C	4556 ± 35	cal. 3486–3474, 3370–3305, 3304–3264, 3239–3167, 3164–3101 BC	−23.75 ± 0.08	KIA 29082
i	2	fAh/M1	C	4494 ± 28	cal. 3346–3092 BC	−23.74 ± 0.16	KIA 29927
i	3	M3	C	3387 ± 24	cal.1744–1615 BC	−26.25 ± 0.09	KIA 28729
i	4	M2	C	2273 ± 22	cal. 396–354, 293–232, 217–212 BC	−25.80 ± 0.22	KIA 29928
i	5	M3	C	1314 ± 24	cal. AD 660–723, 742–771	−26.92 ± 0.18	KIA 28730
i	6	M3	C	1126 ± 24	cal. AD 879–986	−25.10 ± 0.17	KIA 29926
i	7	M3	C	589 ± 23	cal. AD 1303–1368, 1383–1408	−26.86 ± 0.13	KIA 29929
i	SM 1	fAh/M1	SM, H	5390 ± 25	cal. 4333–4220, 4196–4161, 4149–4143, 4120–4110, 4086–4080, 4063–4052 BC	−26.22 ± 0.11	KIA 29442
			SM, HA	5040 ± 25		−26.09 ± 0.20	
vi	1	fAh/M1 (pinus)	C	9543 ± 43	cal. 9142–8985, 8983–8970, 8961–8740 BC	−25.85 ± 0.13	KIA 32318
vi	2	M1	C	4375 ± 27	cal. 3087–3060, 3035–2913 BC	−25.29 ± 0.16	KIA 29568
vi	3	M1	C	3884 ± 24	cal. 2460–2293 BC	−22.63 ± 0.10	KIA 29565
vi	4	M1	C	3877 ± 26	cal. 2462–2286, 2247–2235 BC	−25.69 ± 0.06	KIA 29567
vi	5	fAh/M1 (betula)	C	3550 ± 35	cal. 2010–2001, 1976–1769 BC	−28.05 ± 0.52	KIA 32317
vi	6	M2 (carpinus)	C	1712 ± 25	cal. AD 256–304, 316–408	−24.20 ± 0.17	KIA 32016
vi	7	M2	C	1678 ± 23	cal. AD 262–278, 324–335, 335–423	−27.72 ± 0.09	KIA 29566
vi	8	pit (carpinus)	C	918 ± 24	cal. AD 1032–1164, 1168–1187	−20.25 ± 0.30	KIA 32017
vi	SM 2	M1	SM, H	4446 ± 46	cal. 3336–3210, 3192–3152, 3138–3005, 3004–2923 BC	−28.38 ± 0.13	KIA 29930
vi	SM 3	M2	SM, HA	4085 ± 25	–	−25.18 ± 0.21	KIA 32316
			SM, H	–	–	–	
			SM, HA	2740 ± 33	cal. 971–958, 937–817 BC	−26.97 ± 0.10	
iii	1	pit (at the base of the colluvial sequence)	C	5589 ± 31	cal. 4489–4478, 4461–4352 BC	−23.36 ± 0.06	KIA 28731
iv	1	M3	C	1154 ± 28	cal. AD 781–792, 804–904, 910–976	−28.44 ± 0.32	KIA 31588
v	1	M2	C	1836 ± 24	cal. AD 90–99, 126–242	−27.61 ± 0.22	KIA 31587

Calibration with 'CALIB rev 4.3' data set of Stuiver *et al*. (1998), abbreviations of sample type: C, charcoal; SM, soil matrix; H, humin; HA, humic acid.

of finer textured upper soil particles was transferred to the lower positions of the watershed during the formation of layer M4.

Content of selected heavy metals

The content of heavy metals in the sediments and soils shows a comparable pattern in the exposures (i) and (vi) (Figure 5). The content of all measured heavy metals is clearly the highest in the top 40 cm of the profiles (except for some values that may reflect variation in natural background concentrations). The lower colluvial layers, the buried soil and the sand in exposure (i) have a moderate to low heavy metal content. Cr, Cu and Zn (exposure (vi)) values are increased at the base of the exposures too, indicating a source within the parent material.

Analysing soils of 393 sites with different textures, Wiegmann (1999) has calculated the natural heavy metal contents of soils in northern Germany. He gives the medians for sandy soils ($n = 106$) as follows: Cd, 0.07 ppm; Cr, 5.6 ppm; Cu, 3.2 ppm; Pb, 6.3 ppm; Zn, 20.3 ppm. Therefore the measured contents for the upper 40 cm of the colluvial layers are not only enriched in heavy metal content with respect to the deeper layers but also have higher values than can be assumed from the natural background.

Radiocarbon dating

On several samples of charcoal pieces and soil matrix 21 AMS radiocarbon ages were determined (Table 1).

The oldest object was a *Pinus* charcoal from the very early Holocene (9.1–8.7 ka cal. BC). First traces of anthropogenic activity were detected in a late Mesolithic pit buried by 1.5 m of colluvial sediment at the base of exposure (iv) (4.5–4.3 ka cal. BC, exposure not shown here). First charcoal pieces that date into the Neolithic Times appear at ~ 3.5–3.0 ka cal. BC and relate to the Middle Neolithic Times (Funnelbeaker culture). Only one charcoal dates to Bronze Age (1744–1615 cal. BC) but was found embedded in colluvial layer M3 associated with younger charcoals. M2 contains charcoals of Iron Age. Two of them date into Roman Emperor Times (~ AD 0.25–0.4 cal.) and one into Pre-Roman Iron Age (396–212 cal. BC). A charcoal from the pit dug into the colluvial layer M2 in exposure (vi) was dated to High Mediaeval Times (AD 1032–1187 cal.). The variation of radiocarbon data (~ AD 700–1400 cal.) within the Mediaeval Period from layer M3 indicates that the watershed was under agricultural land use since early Mediaeval Times (Slavonic Period).

The ages of soil and sediment matrix samples deliver some additional clues. When possible, the two fractions of humines and humic acid were dated separately to minimize age errors accompanied with the addition of younger organic matter (via Dissolved Organic Carbon) from the respective surface. The resulting age differences between the humine and the humid acid of the samples SM1 and SM2 (~ 400 years) indicate that the addition of fresh organic matter (dissolved organic carbon) from the respective

Table 2 Result of charcoal analysis from soil and colluvial sediments, exposure Bor (vi) (Börnhoved)

	M1			M2 a			M2 b	Pit	M3			M4Ap			Sum / means
	Late Neolithics			Roman Emperor Times				1100 AD	Late Mediaeval Times			Modern Times			
	I	II	III.1b	I	II	III	I		I	II	III	I	II	III	
Pinus	.	.	1	.	.	.	.	.	.	.	.	.	.	.	1
Betula	.	.	6	.	.	.	.	.	.	.	.	.	.	.	6
cf. *Betula*	.	.	.	.	.	.	.	.	.	.	.	.	.	1	1
Quercus	31	22	6	7	6	8	3	10	2	1	.	1	1	2	100
Corylus	.	.	.	3	2	3	1	1	.	.	.	.	.	2	12
cf. *Corylus*	.	.	.	.	.	1	.	.	.	.	.	.	.	.	1
Carpinus	.	.	1	2	6	1	9	7	3	1	1	.	2	2	35
Corylus/Carpinus	.	.	.	2	.	.	1	.	.	.	.	2	.	.	5
Fagus	.	.	.	1	2	7	5	5	2	.	2	10	1	4	39
Ulmus	.	.	.	.	.	5	.	.	.	.	.	.	.	.	5
Fraxinus	.	.	.	1	.	.	.	.	.	.	.	.	.	.	1
cf. *Prunus*	.	.	.	1	1	.	.	.	.	.	.	.	.	.	2
Populus/Salix	.	.	.	.	.	.	1	.	.	.	.	.	.	.	1
cf. *Populus/Salix*	.	.	.	.	3	.	.	.	.	.	.	.	.	.	3
Alnus	.	.	.	.	.	.	.	.	1	.	.	.	.	.	1
cf. *Sambucus*	.	.	.	.	.	.	.	.	.	.	.	.	1	.	1
cf. *Euonymus*	.	.	.	.	.	.	.	.	.	.	.	.	1	.	1
indet.	4	1	6	3	4	6	1	5	1	.	.	5	4	5	45
N det.	31	22	14	17	20	25	20	23	8	2	3	13	6	11	215
sample volume (l)	10	10	10	10	10	10	10	10	10	10	10	20	10	10	150
W_{HK} (mg)	185	81	25	51	38	40	22	32	12	2	4	15	11	21	539
W_{HK}/V (mg l.1)	19	8	3	5	4	4	2	3	1	<1	<1	<1	1	2	3.5
W det.+ id. HK (mg)	65	47	23	29	22	33	19	24	12	2	4	12	8	20	320
W/N (mg)	1.9	2.0	1.2	1.5	0.9	1.1	0.9	0.9	1.4	1.0	1.4	0.7	0.8	1.3	1.1

Numbers of analysed charcoal, column I–III (see Figure 6), sample volumes (V), weights (W) of all served charcoal fragments >1 mm, concentration of charcoal per volume (W_{HK}/V), weight of microscopic charcoal (det + indet.) and mean weight per fragment.

surface soil formation was comparatively low. For the sample SM3 not enough material was extracted from the humine fraction for a separate dating.

The bulk radiocarbon age of the buried humus horizon in exposure (i) falls into the late Mesolithic Age (Table 1). This age is almost 1.0 kyr greater than the charcoals found within M1 in (i). Within the colluvial layers M1 and M2 in exposure (vi) similar offsets of around 1.0 kyr between the age of the youngest embedded charcoals and the bulk radiocarbon ages of the soil organic matter appears. Assuming that the offset between humine and humic acid is at a comparable level (~ 400 years), an age of about 1501–1311 cal. BC for the bulk soil organic matter of M2 would result.

Charcoal analysis

The samples contained between 1 and 19 mg charred wood per litre. The charcoal concentration was especially high in layer M1 of exposure (vi). From 15 samples of three columns, 215 fragments in all could be determined. Forty-five remained undetermined (indet.), partly because it is likely that they are either derived from the bark of a wooden plant or because they were too small for identification. Thus, the high number of indeterminata reflects the small size of the fragments, which makes species determination sometimes vague ('cf.'), and often impossible. The analysed fragments weigh between 0.5 and 2 mg. However, because of their three-dimensional form it is mostly possible to determine the species.

The charcoal spectrum includes 11–12 (the differentiation between *Populus* and *Salix* was not possible, thus a *Populus*/*Salix*-type) determined taxa and three further taxa, which were not determined unequivocally (Table 2). Most fragments were oak (*Quercus*), which is either *Quercus robur* or *Quercus petraea*. *Fagus* (*Fagus sylvatica*) and *Carpinus* (*Carpinus betulus*) occurred significantly in samples of layer M2 to M4. All three profile columns show comparable results: high values of oak in layer M1 and increasing values of hornbeam and beech beginning in layer M2 up to layer M4. Thus, data of the individual columns were summarized according to their layer origin for graphical presentation (Figure 6).

Discussion

Landscape development and historical soil erosion

The main landscape features at the studied site were shaped during the last glaciation and the following transition to the Holocene. During the Weichselian Glaciation tills and outwash sands were deposited by the large inland ice sheets that covered the site. Lateglacial fluvial activity cut valleys into these deposits and gave rise to the accumulation of large stones at the bases of the depressions. Later, aeolean activity led to the addition of some silty material, visible within the texture. Within these sandy substrates, exposed at the base of the investigated exposures, soil development started as the closing forest cover led to slope stability at the beginning of the Holocene at around 9650 cal. BC (Nelle and Dörfler, 2008). We found remnants of an early-Holocene humic horizon in exposure (vi) indicated by embedded charcoal pieces of *Pinus* dating to 9142–8740 cal. BC. The accumulation of organic matter was followed by the oxidation of iron bearing minerals in the underlying substrate resulting in the development of cambisols

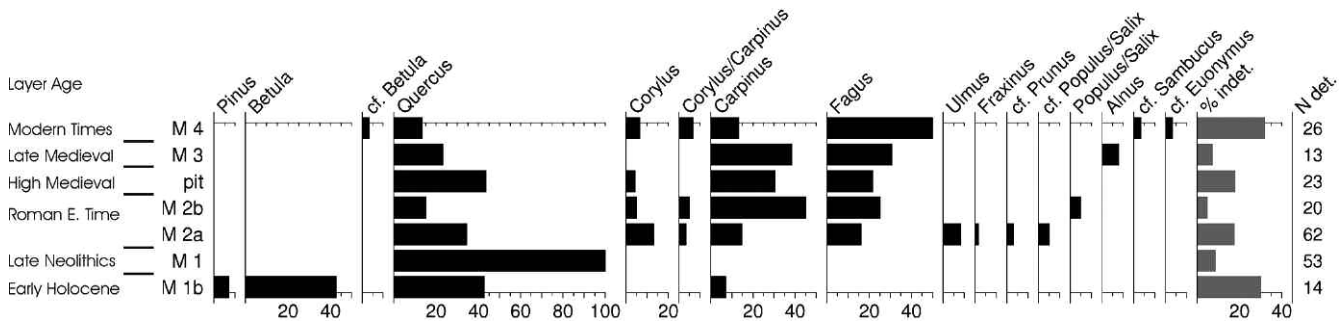

Figure 6 Charcoal spectra from soils and colluvial sediments, exposure Bor (vi) (Bornhöved). Percentages of taxa in the sampled layers and one pit (see Figure 4). Percentages of indeterminate – '% indet.' – based on the sum of the determined and indetermined charcoal fragments

(FAO, 1998). As the archaeological findings at one hillside (see above), signals in the pollen record (Wiethold, 1998), lake sediments (Garbe-Schönberg *et al.*, 1998) and deposition of colluvial sediments (Dreibrodt, 2005; Dreibrodt and Bork, 2005) within the lake catchment of Belauer See indicate, the region was first cleared for agriculture during the middle Neolithic, around 3600 cal. BC. We found charcoals dated to the Funnelbeaker Culture in the upper part of the buried fAh/M1 in exposure (i). Shallow burying of the soil by a thin humic colluvial layer is probable at ~ 3400 cal. BC in exposure (i). The first unequivocal evidence for agricultural land use is given with the deposition of the colluvial sediment M1 during the late Neolithic Times at around 2200 to 2400 cal. BC found in exposure (vi). The enrichment of large stones in M1 usually may be interpreted as a result of high intensity runoff. But as the layer contains a high amount of humic matter and almost no subsoil matter, the incision of gullies in the course of this soil erosion phase can be excluded. Therefore the increased stone content may rather be explained by an enrichment layer of large clasts originating from the Lateglacial–Holocene transition at a shallow depth below the soil surface here. Also the distribution of the late Neolithic colluvial layer is very limited to the lowest position of the investigated watershed. Therefore the soil erosion intensity may have been on a rather moderate level. As remnants of settlement, land use (plough horizon) and funeral activities from late Middle Neolithic to late Neolithic were detected during the archaeological campaign on the surrounding hills, the detected soil erosion signal may have been triggered by this phase of land use. During the Bronze Age (1800–600 cal. BC) the four surrounding hills (Figure 2) were used for funeral purposes (Schwerin von Krosigk, 1976; I. Lütjens and I. Clausen, unpublished data, 2008). Investigating six large exposures (see Figure 2) and 35 additional auger cores, we found no colluvial layer to be deposited during the Bronze Age. Furthermore, only one of 18 charcoals was dated to the Bronze Age and found embedded in a colluvial layer together with younger charcoals. Thus, clearing of wood seems to have been restricted to small areas, probably to the top of the hills to enable the construction of the burial mounds. The pocket-like depression found at the upper hill slope position in exposure (i) might be a relict of digging for burial construction material. It probably delineates therefore the area temporary used for burial mound construction at that hill. But the soil surface within large parts of the investigated watershed apparently remained protected against soil detachment during Bronze Age. After a time of slope stability probably associated with a soil formation phase spanning more than 2000 years another phase of soil erosion occurred. The colluvial layer M2 was deposited during Roman Emperor Times between AD 250 to 400 cal. The deposition of M2 buried the lammelic luvisol in exposure (i), therefore more or less infinitively stopping the development of this soil. As no E- or Bt-horizon nor clay bands have been found beyond the M1 layer in (vi), the formation of these horizons in (i) is likely to have occurred after Neolithic Times and is therefore probably of Holocene age, in contrast with other results of clay eluviation during glacial times (eg, Van Vliet-Lanoe, 1990) but in accordance with results from the lake catchment of Belauer See (Dreibrodt, 2005; Dreibrodt and Bork, 2005, 2006). Geomorphodynamic activity during the Roman Iron Age was not found within the catchment area of Belauer See, where a decrease in settlement activity and land-use intensity is indicated in the pollen diagram (Wiethold, 1998) and the soil profiles (Dreibrodt, 2005; Dreibrodt and Bork, 2005). But its occurrence at the site Bornhöved reflects the spatial variation of settlement and land-use activities during the past. A settlement site from the Roman Iron Age is indicated via surface findings in the vicinity of the research site (500 m to the north, Figure 2). Also, Schmidtchen (2003) found colluvial sediments from the Roman Iron Age at a site nearby the city of Kiel. Since the sediment M2 is present in all exposures, has a greater thickness than M1 and shows a larger content in subsoil matter the intensity of soil erosion during the Roman Emperor Time was higher than during the late Neolithic. This could be explained by larger fields contributing to a larger active watershed area, different agricultural techniques, a greater population density and/or more heavy rainfall events. During the Migration Period (~ AD 450–700, Nelle and Dörfler, 2008) the area was sparsely populated or even completely abandoned, as indicated by pollen analysis (Wiethold, 1998) and soil formation (Dreibrodt and Bork, 2005) from Belauer See. No colluvial layer was found to be deposited at the Bornhöved site. After this time of slope stability a renewed soil erosion phase started again during early Mediaeval Times at the Bornhöved site. As indicated by the pollen record from lake Belauer See (Wiethold, 1998) slavonic tribes immigrated from the east, cut down parts of the forests and began agricultural field use. At the study site this is reflected by the beginning of deposition of a colluvial layer M3. This phase of agricultural field use continued through High and late Mediaeval Times (until ~ AD 1100 to 1400), when Saxonian tribes captured the Slavonic area, expanded their territory eastwards and intensified agricultural field use in the region (Lammers, 1981; Wiethold, 1998; Dreibrodt and Bork, 2005).

Three different indicators testifying ongoing soil erosion throughout Modern Times: the extreme thinning of the M4Ap layer in exposure (i) towards the hills, the covering of the lower parts of the hedgerow – constructed at around AD 1800 in the region – in exposure (vi) and the increased content of heavy metals of M4 in both exposures.

Lead is a metal with a well known history of ecotoxicology and may therefore serve as a time-sensitive indicator. As Nriagu (1998) has reviewed, its principal output (85%) in history occurred after AD 1800, unless lead was introduced early into mining processes and released locally to regionally in ancient

times. Detailed studies on several peat bogs and lake sediments across Europe reflected increased emissions since the Industrial Revolution (eg, Shotyk *et al.*, 1998; Dunlap *et al.*, 1999; Kober *et al.*, 1999). This increase was also detected for the region investigated by Garbe-Schönberg *et al*. (1998) in the sediments of Belauer See (3 km north of the studied site). These investigators found increased amounts in Pb, Zn, Cu, Cd and Cr in the modern part of their sequence. As the sediment of the upper 40 cm of the investigated profiles at the Bornhöved site shows increased heavy metal contents (except for some outlayers in the deeper part of (vi), which could reflect natural variation within the substrate or early local human activity) we conclude that its relocation took place during the past 200 years, when atmospheric emission of heavy metals increased through industrialization.

Aspects of vegetation history reflected in the charcoal spectra

The origin of the charcoals remains unknown. They might be derived from local natural fires or – more likely – from human activities, such as campfires or burning down woodland to open up the landscape for agriculture or pasturing. The findings of the archaeological excavations yielded indication of sparse settlement and agricultural field use activity during the late Neolithic. During the Bronze Age and Iron Age exclusively, an indication of burial activities was found at the investigated hills. Although the settlement site of Roman Emperor Times lies downhill, influence of settlement activities on the sediment-delivering hills cannot be excluded. Therefore, a selection of species associated with settlement activities is more probable during the Neolithics and Iron Age than during Bronze Age. Since Mediaeval Times this is rather improbable as no relicts of a deserted Mediaeval town were found or are known from written sources.

Charcoal spectra show the Holocene succession from oak-dominated woodlands during the Atlantic to beech-dominated stands with an admixture of hornbeam and oak since the migration period (Wiethold, 1998). This is in agreement with the obtained radiocarbon dates. With the absence of *Fagus* in the older colluvia, we can support the hypothesis that the very low percentages of beech in the pollen diagram of Belauer See are due to long distance transport from southern low mountain ranges during the Neolithic (Wiethold, 1998). With more charcoal samples being analysed in the future, we will be able to check this further, and have the opportunity of dating the first local occurrence of *Fagus* in the area. *Tilia* is lacking in our Neolithic samples, pointing to the low proportions of lime trees on poor sandy soils (Wiethold, 1998). *Fagus* spreads slowly during the Bronze Age, with low proportions in the pollen diagrams. It is not until the Migration period that beech becomes the dominant tree on the groundwater-distant sites.

Hornbeam was promoted by the establishment of coppiced woodlands in Mediaeval Times, or maybe even earlier. Compared with the pollen record (Wiethold, 1998) hornbeam has higher values in the charcoal record. With our, as yet only three, profiles of one exposure, this might be due to very local effects, or it might point to a problem yet not seen in palynology: the under-representation of *Carpinus* in the pollen record.

Overall, we found no sign of woodland degradation in the charcoal spectra, eg, the increase of pioneer species such as birch, poplar or willow. This might indicate that the phases of reforestation, which interrupted the phases of slope instability and colluviation, were long enough to allow the development of advanced succession stages. Also hazel was only rarely found in the upper layers, whereas it was more common in older layers. The relative decrease of *Corylus*, though interpreted cautiously to be due to the small data base, confirms also the decrease of *Corylus* in the pollen diagrams, probably connected with the spread of *Fagus*.

Since there is in general a good accordance of the observed charcoal record with the pollen data of Wiethold (1998) we hypothesize that charcoal analysis is a promising additional tool for reconstructions of vegetation history on a local scale. Whether the observed variations in species spectra reflect a higher spatial distribution of the record or are affected by local human activities has to be tested via further analyses.

Radiocarbon age of the soil organic matter

We found the bulk radiocarbon ages of soil organic matter in the buried fAh/M1 (i) and the colluvial sediments M1 and M2 (vi) to be older than the youngest charcoal found within the layer (Table 1).

The difference between the bulk radiocarbon age of the soil organic matter of the buried humus horizon in exposure (i) and the youngest charcoal found in its upper part (assumed to be of colluvial origin- fAh/M1) is 566–1232 years (according to the two δ standard deviation interval of the radiocarbon ages). The differences of the bulk radiocarbon ages of the colluvial layers and the youngest charcoals embedded within the layers of exposure (vi) are 493–1043 years for M1 and 1079–1394 years for M2. Since the radiocarbon data of the bulk soil organic matter of M2 is based on the humic acid fraction, this age might be an underestimation (see results).

From the site conditions (sandy texture, no indication of waterlogging), it seems reasonable to assume that mainly an inactive pool of soil organic matter, probably of recalcitrant structure, has resisted decomposition. The observed time offsets between depositional time and radiocarbon age of the bulk organic matter are in accordance with modelling considerations for buried soils of Wang *et al*. (1996) or calculated turnover times of the passive fraction of organic carbon in surface soils (Parton *et al*., 1987, 1989, 1993; Schimel *et al*., 1994).

Therefore, the different radiocarbon ages of soil organic matter and charcoals indicate an input of fresh organic matter into the surface soils and deliver further indication of soil formation phases between the individual phases of soil erosion and burial via sedimentation. The preservation of these patterns within the buried soils and colluvial layers indicates a potential for soil organic matter decomposition research. Furthermore, our results demonstrate that bulk radiocarbon data of soil organic matter overestimate not only the burial time of soils but also the depositional time of colluvial layers.

Conclusions

As we found colluvial layers deposited during the late Neolithic, the Roman Emperor Times, Mediaeval Times and Modern Times the incidence of colluviation at the site is a suitable indicator for landscape openness resulting from agricultural land use. As no colluvial layer was found to be deposited during the Bronze Age, the soil surface within the surroundings of the investigated burial mounds was protected against soil erosion during that time. After the clearing of the sites to construct the burial mounds a rapid stabilization of the soil surface seems to have occurred at the site. Either a very well suited system of pasture (that maintained a sheltering vegetation cover) was used to realize the assumed landscape openness or the watershed area was forested. Soil erosion occurs under pastures and rangelands as well (eg, van Oost *et al*., 2007) and the duration of burial practices is considerably long (> 1000 years) at the studied site. Therefore, it is more probable that the soils on the hills topped with the burial mounds were protected against soil erosion by a forest cover. We conclude that the assumption of open landscapes surrounding burial mounds on hilltops is rather improbable at the Bornhöved site. Investigations of colluvial layers and buried soils at other sites have to prove

whether this result is of site specific or of regional significance. The potential of colluvial sediments to detect slope instability at a local scale (adjacent slope) might then enable reconstructions of landscape openness at a high spatial resolution.

The history of soil erosion in the studied watershed is similar to that within the lake catchment of Belauer See that is located only 4 km to the north but shows some variations. Intensive soil erosion occurred at both sites during Mediaeval and Modern Times. Whereas slope instability was found at the lake during the Middle Neolithic and Pre-Roman Iron Age it occurred at late Neolithic and Roman Emperor Times at the Bornhöved site. These differences documented temporal and spatial variability of settlement patterns and land use in the Holocene draws attention to the question: how can we get representative reconstructions of Holocene development of our landscapes?

The analysis of charcoal fragments embedded within colluvial layers reflected well the results of woody taxa within the pollen spectra from Belauer See (Wiethold, 1998). Since this pollen diagram is thought to represent the development of the region (Behre, 2000), the analysis of charcoals from colluvial layers may help to differentiate the local dynamics of woodland composition and human impact. Furthermore, it helps to cross-check the radiocarbon datings and provides therefore another method to recognize the repeated reworking of sediments observed by Lang and Hönscheid (1999). This was the first time for northern Germany that charcoal species identification analysis was done within the presented context. It shows the potential of a fine-scale, site-related reconstruction of Holocene vegetation change, and has to be checked and developed further through the analysis of more profiles in the region and elsewhere.

Our results confirm the modelling considerations of Wang *et al.* (1996), which conclude that radiocarbon data of soil organic matter overestimate the burial time of buried soils. That this is true in a similar manner for the age of colluvial layers is a new result. Therefore, results of former investigations on colluvial layers based on such data must be checked for correctness. Furthermore our results illustrate the promising potential of colluvial layers and buried soils to contribute to estimations of historical organic carbon fluxes in landscapes and soil organic matter decomposition research.

Acknowledgement

We are grateful to the landowner, who allowed extensive field studies, P.M. Grootes (Leibniz Laboratory for Radiometric Dating and Stable Isotope Research, Christian-Albrechts-University of Kiel) for the radiocarbon analyses, Doris Jansen for flotation of charcoal samples and Carolin C.M. Lubos for improving the English of this text and two unknown reviewers for their valuable comments.

References

AG Boden 2005: *Bodenkundliche Kartieranleitung*. 5th edition.

Behre, K.-E. 2000: Pollen, Samen, Früchte. Geschichte der Pflanzenwelt und Ernährung. In v. Freeden, U. and v. Schnurbein, S., editors, *Spuren der Jahrtausende. Archäologie und Geschichte in Deutschland*. Wissenschaftliche Buchgesellschaft Darmstadt, 448–63.

Bork, H.-R. and **Lang, A.** 2003: Quantification of past soil erosion and land use/land cover changes in Germany. In Lang, A., Hennrich, K. and Dikau, R., editors, *Long term hillslope and fluvial system modelling. Concepts and case studies from the Rhine river catchment*. Springer. Lecture Notes in Earth Sciences 101, 231–39.

Bork, H.-R., Bork, H., Dalchow, C., Faust, B., Piorr, H.-P. and **Schatz, T.** 1998: *Landschaftsentwicklung in Mitteleuropa*. Klett-Perthes.

Dege, E. 1988: *Die Gutswirtschaft Ostholsteins im Wandel*. Jahrbuch Lauenburgische Akademie Wissenschaften und Kultur, 151–66.

Dotterweich, M. 2008: The history of soil erosion and fluvial deposits in small catchments of central Europe: deciphering the long-term interaction between humans and the environment – a review. *Geomorphology* http://dx.doi.org/10.1016/j.geomorph.2008.05.023.

Dreibrodt, S. 2005: Detecting heavy rainfall events during the Holocene from soils, gully fills, colluvia and lake sediments – examples from the Belauer See catchment (northern Germany). *Zeitschrift der deutschen Gesellschaft fur Geowissenschaften* 165, 573–88.

Dreibrodt, S. and **Bork, H.-R.** 2005: Historical soil erosion and landscape development at Lake Belau (North Germany) – a comparison of colluvial deposits and lake sediments. *Zeitschrift für Geomorphologie Neues Funde Supplementenband* 139, 101–28.

—— 2006: Integrative analyse von Böden und Sedimenten zur Rekonstruktion der holozänen Landschaftsgeschichte – das Beispiel Belauer See (Schleswig-Holstein). *Nova Acta Leopoldina* 94, 213–40.

Dunlap, C.E., Steinnes, E. and **Fegal, A.R.** 1999: A synthesis of lead isotopes in two millennia of European air. *Earth and Planetary Science Letters* 167, 81–88.

Eisenschmidt, S. 2004: *Grabfunde des 8. bis 11. Jahrhunderts zwischen Kongeå und Eider. Zur Bestattungssitte der Wikingerzeit im südlichen Altdänemark. Band 2*. Studien zur Siedlungsgeschichte und Archäologie der Ostseegebiete 5, 2.

Ethelberg, P. 2000: Bronzealderen. In Ethelberg, P., Jørgensen, E., Meier, D. and Robinson, D., editors, *Det Sønderjyske Landbrugs Historie*. Sten- og Bronzealder, 135–280.

Food and Agriculture Organization 1998: *World reference base for soil resources*. FAO Report 84.

Garbe-Schönberg, C.-D., Wiethold, J., Butenhoff, D., Utech, C. and **Stoffers, P.** 1998: Geochemical and palynological record in annually laminated sediments from Lake Belau (Schleswig-Holstein) reflecting palaeoecology and human impact over 9000 a. *Meyniania* 50, 47–70.

Hannon, G.E., Bradshaw, R.H.W., Nord, J. and **Gustavsson, M.** 2007: The Bronze Age landscape of the Bjäre peninsula, southern Sweden, and its relationship to burial mounds. *Journal of Archaeological Science* 35, 623–32.

Hartz, S. 2004: Aktuelle Forschungen zur Chronologie und Siedlungsweise der Ertebølle- und frühesten Trichterbecherkultur in Schleswig-Holstein. *Jahrbuch Bodendenkmalpflege in Mecklenburg-Vorpommern* 52, 61–81.

Hingst, H. 1974: Flachgräber der Stein- und Bronzezeit aus Schleswig-Holstein. *Offa* 31, 19–67.

—— 1976: Grabhügelfelder der jüngeren Bronze- und frühen Eisenzeit aus Schleswig-Holstein. *Offa* 33, 66–122.

—— 1979: Die vorrömische Eisenzeit. In Klose, O., editor, *Geschichte Schleswig-Holsteins. Band 2. Von der Bronzezeit bis zur Völkerwanderungszeit*. Neumünster, 147–247.

Hoika, J. 1993: Grenzfragen oder: James Watt und die Neolithisierung. *Archäologische Informationen* 16, 6–19.

—— 1994: Zur Gliederung der frühneolithischen Trichterbecherkultur in Holstein. In Hoika, J. and Meurers-Balke, J., editors, *Beiträge zur frühneolithischen Trichterbecherkultur im westlichen Ostseegebiet*. Untersuchungen und Materialien zur Steinzeit in Schleswig-Holstein 1, 85–132.

Jørgensen, E. 2000: Yngre stenalder. In Ethelberg, P., Jørgensen, E., Meier, D. and Robinson, D., editors, *Det Sønderjyske Landbrugs Historie*. Sten- og Bronzealder, 63–133.

Karg, S. 2008: Direct evidence of heathland management in the early Bronze Age (14th century B.C.) from the grave-mound Skelhøj in western Denmark. *Vegetation History and Archaeobotany* 17, 41–49.

Kober, B., Wessels, M., Bollhöfer, A. and **Mangini, A.** 1999: Pb isotopes in sediments of Lake Constance, Central Europe constrain the heavy metal pathways and the pollution history of the catchment, the lake and the regional atmosphere. *Geochimica et Cosmochimica Acta* 63, 1293–303.

Kock, O. 1972: *Bilder aus dem Amt Wankendorf*. Wankendorf.

Lammers, W. 1981: *Das Hochmittelalter bis zur Schlacht von Bornhöved*. Gesch. Schleswig-Holstein 4,1.

Lang, A. and **Hönscheidt, S.** 1999: Age and source of colluvial sediments at Vaihingen-Enz. Germany. *Catena* 38, 89–107.
Laux, F. 1996: Tod und Bestattung. In Wegner, G., editor, *Leben-Glauben-Sterben vor 3000 Jahren. Eine niedersächsische Ausstellung zur Bronzezeit-Kampagne des Europarates*. Begleithefte zu Ausstellungen der Abteilung Urgeschichte des Niedersächsischen Landesmuseums Hannover. Heft 7, 173–94.
Ludemann, T., Michiels, H.-G. and **Nölken, W.** 2004: Spatial patterns of past wood exploitation, natural wood supply and growth conditions: indications of natural tree species distribution by anthracological studies of charcoal-burning remains. *European Journal of Forest Research* 123, 283–92.
Lütjens, I. and **Wiethold, J.** 1999: Vegetationsgeschichtliche und archäologische Untersuchungen zur Besiedlung des Bornhöveder Seengebietes und seines Umfeldes im Neolithikum. *Archäologische Nachrichten aus Schleswig-Holstein* 9/10, 30–67.
Munsell 2000: *Munsell soil color charts*. Gretag MacBeth.
Nelle, O. 2002: Charcoal burning remains and forest stand structure – examples from the Black Forest (south-west Germany) and the Bavarian Forest (south-east Germany). In Thiébault, S., editor, *Charcoal analysis. Methodological approaches, palaeoecological results and wood uses*. Proceedings 2nd International Meeting of Anthracology, Paris, September 2000, BAR International Series 1063, 201–207.
—— 2003: Woodland history of the last 500 years revealed by anthracological studies of charcoal kiln sites in the Bavarian Forest, Germany. *Phytocoenologia* 33, 667–82.
Nelle, O. and **Dörfler, W.** 2008: A summary of the late- and postglacial vegetation history of Schleswig-Holstein. In Dengler, J., Dolnik, C. and Trepel, M., editors, *Flora, vegetation, and nature conservation from Schleswig-Holstein to South America*. Mitteilung Arbeitsgem. Geobot. Schleswig-Holstein Hamb. 65, 45–68.
Nriagu, J.O. 1998: Palaeoenvironmental research: tales told in lead. *Science* 281, 1622–23.
Odgaard, B. 1988: Heathland history in Western Jutland, Denmark. In Birks, H.H., Birks, H.J.B., Kaland, P.E. and Moe, D., editors, *The cultural landscape. Past, present and future*. Cambridge University Press, 311–19.
Parton, W.J., Schimel, D.S., Cole, C.V. and **Ojima, D.S.** 1987: Analysis of factors controlling soil organic matter levels in Great Plain Grasslands. *Soil Science Society of America Journal* 51, 1173–79.
Parton, W.J., Cole, C.V., Steward, J.W.B., Ojima, D.S. and **Schimel, D.S.** 1989: Simulating regional patterns of soil, C, N, and P dynamics in the U.S. central grassland region. In Clarholm, M. and Bergström, J., editors, *Ecology of arable land*. Kluwer Academic Publishers, 99–108.
Parton, W.J., Scurlock, M.O., Ojima, D.S., Gilmanow, T.G., Scholes, R.V., Schimel, D.S., Kirchner, T., Menault, J.-C., Seastedt, T., Garcia Moya, E., Kamnalrut, A. and **Kinyamario, J.I.** 1993: Observations and modeling of biomass and soil organic matter dynamics for the grassland biome worldwide. *Global Biogeochemical Cycles* 7, 785–809.
Piotrowski, J. 1991: Quartär- und hydrogeologische Untersuchungen im Bereich der Bornhöveder Seenkette, Schleswig-Holstein. Ph.D. Thesis University Kiel.
Reimer, P.J., Baillie, M.G.L., Bard, E., Bayliss, A., Beck, J.W., Bertrand, C., Blackwell, P.G., Buck, C.E., Burr, G., Cutler, K.B., Damon, P.E., Edwards, R.L., Fairbanks, R.G., Friedrich, M., Guilderson, T.P., Hughen, K.A., Kromer, B., McCormac, F.G., Manning, S., Bronk Ramsey, C., Reimer, R.W., Remmele, S., Southon, J.R., Stuiver, M., Talamo, S., Taylor, F.W., van der Plicht, J. and **Weyhenmeyer, C.E.** 2004: IntCal04 terrestrial radiocarbon age calibration 0–26 cal kyr BP. *Radiocarbon* 46, 1029–58.
Schimel, D.S., Braswell, B.H., Holland, E.A., McKeown, R., Ojima, D.S., Painter, T.H., Parton, W.J. and **Townsend, A.R.** 1994: Climatic, edaphic, and biotic controls over storage and turnover of carbon in soils. *Global Biogeochemical Cycles* 8, 279–93.
Schleuss, U. 1991: Böden und Bodenschaften einer Norddeutschen Moränenlandschaft – Ökologische Eigenschaften, Vergesellschaftung und Funktionen der Böden im Bereich der Bornhöveder Seenkette. Ph.D. Thesis University Kiel.
Schlichting, E., Blume, H.-P. and **Stahr, K.** 1995: *Bodenkundliches Praktikum*. Blackwell.
Schmidt, J.-P. 1993: *Studien zur jüngeren Bronzezeit in Schleswig-Holstein und dem nordelbischen Hamburg*. Habelt.
Schmidtchen, G. 2003: Hang- und Moorentwicklung in der Knicklandschaft Ostholsteins – das Profil Kiel-Schlüsbek. In Bork, H.-R., Schmidtchen, G. and Dotterweich, M., editors, *Bodenbildung, Bodenerosion und Reliefentwicklung im Mittel- und Jungholozän Deutschlands*. Forschungen zur Deutschen Landeskunde. Band 253, 251–67.
Schweingruber, F.H. 1990a: *Anatomie europäischer Hölzer*. Haupt, 800 pp.
—— 1990b: *Mikroskopische Holzanatomie. Formenspektren mitteleuropäischer Stamm- und Zweighölzer zur Bestimmung von rezentem und subfossilem Material*. Eidg. Anstalt für das forstl. Versuchswesen, 226 pp.
Schwerin von Krosigk, H. 1976: *Untersuchungen zum vor- und frühgeschichtlichen Siedlungsablauf am Fundbild der Gemarkungen Bornhöved – Gönnebeck – Groß Kummerfeld – Schmalensee*. Krs. Seegeberg/Holstein. Offa-Erg.- R.1.
Shotyk, W., Weiss, D., Appleby, P.G., Cheburkin, A.K., Frei, R., Gloor, M., Kramers, J.D., Reese, S. and **van der Knaap, W.O.** 1998: History of atmospheric lead deposition since 12,370 14C yr BP from a peat bog, Jura Mountains, Switzerland. *Science* 281, 1635–40.
Struwe, K.W. 1979: Die Bronzezeit. In Klose, O., editor, *Geschichte Schleswig-Holsteins*. Band 2. Von der Bronzezeit bis zur Völkerwanderungszeit, 3–145.
Van Oost, K., Quine, T.A., Govers, G., De Gryze, S., Six, J., Harden, J.W., Ritchie, J.C., McCarty, G.W., Heckrath, G., Kosmas, C., Giraldez, J.V., Marques da Silva, J.R. and **Merckx, R.** 2007: The impact of agricultural soil erosion on the global carbon cycle. *Science* 318, 626–29.
Van Vliet-Lanoe, B. 1990: The genesis and age of the argillic horizon in Weichselian Loess of Northwestern Europe. *Quaternary International* 5, 49–56.
Wang, Y., Amundson, R. and **Trumbore, S.** 1996: Radiocarbon dating of soil organic matter. *Quaternary Research* 45, 282–88.
Wiegmann, S. 1999: *Natürliche Schwermetallgehalte als planungs- und umweltrechts-relevante Bewertungsgrundlage der Belastung norddeutscher Ackerböden*. Cuvillier Verlag.
Wiethold, J. 1998: *Studien zur jüngeren postglazialen Vegetations- und Siedlungsgeschichte im östlichen Schleswig-Holstein*. Habelt.
Willroth, K.-H. 1999: Krieger, Häuptlinge oder 'nur' freie Bauern. Zum Wandel in der Bronzezeitforschung. In Budesheim, W. and Keiling, H., editors, *Zur Bronzezeit in Norddeutschland*. Freie Lauenburgische Akademie für Wissenschaft und Kultur. Beiträge für Wissenschaft und Kultur. Band 3, 39–66.
Zich, B. 1992: *Ausgrabungen auf dem stein- und bronzezeitlichen Grabhügelfeld von Flintbek, Kreis Rendsburg-Eckernförde. Ein Vorbericht*. Archäologische Nachrichten aus Schleswig-Holstein, Heft 3, 6–21.
—— 2005: Flintbek. In Aner, E., Kersten, K. and Willroth, K.-H., editors, *Die Funde der älteren Bronzezeit des nordischen Kreises in Dänemark, Schleswig-Holstein und Niedersachsen*. Band XIX. Kreis Rendsburg-Eckernförde (südlich des Nord-Ostsee-Kanals) und die kreisfreien Städte Kiel und Neumünster, 31–84.

Appendix IV

Mitusov, A.V. Assessment of potential erosion/accumulation based on local landforms related with colluvial deposits. Geomorphology (*submitted*).

Ms. Ref. No.: GEOMOR-5204

Assessment of potential erosion/accumulation based on local landforms related with colluvial deposits

Andrey V. Mitusov*

Institute for Ecosystem Research, Christian-Albrechts-University Kiel, Olshausenstrasse 40, D-24098 Kiel, Germany

*Author for correspondence
E-mail: a_mitusov@mail.ru
Tel.:+49 (0)431-880-4030
Fax: +49 (0)431-880-4083

Highlights

Twelve local landforms are determined by signs of curvatures

Role of these landforms for distribution of colluvial deposits are established

60% of terrain covered by local landforms related with potential soil erosion

Occurrence frequency of landforms is criteria for description of erosion status

Maps of these landforms reflect location of potential zones for erosion/accumulation

Abstract

The local landforms were divided into twelve types by the signs of curvatures. A role of these local landforms in the distribution of colluvial deposits on a fine spatial resolution was determined on the example of two small dry valleys "Perdoel" and "Bornhoeved" located in Northern Germany. Two landform groups relating with erosion and accumulation were experimentally identified. The distribution of these groups approximately coincides with the pattern of the catchment area map. The proportion of occurrence frequency between two groups of local landforms indicates potential domination of the erosion or accumulation processes in the region. The intensity of these processes was assessed by comparing the occurrence frequency of these local landforms on a natural land and a random surfaces. Based on this approach the potential erosion/accumulation status in sampling points and the surrounding terrain was assessed. In sampling points of the key area Perdoel the land surface is potentially suitable for intensive accumulation. In sampling points of the key area Bornhoeved the land surface is potentially suitable for accumulation with a medium intensity. For the surrounding terrains erosion with a low intensity was assessed. The results coincided with the existing information obtained by traditional methods. Therefore, this approach can be used as an additional method for the assessment of the potential erosion/accumulation status of terrains from a geomorphometric point of view.

Key words: Local landforms; Curvatures; Erosion; Accumulation; Colluvium; Geomorphometry.

1. Introduction

Colluvial (slope) deposits are among the main indicators of human-triggered soil erosion during the Holocene (*e.g.* Lang, 2003; Dotterweich, 2008; Brown, 2009; Dreibrodt et al., 2010). Investigations of spatial distribution of colluvial deposits are based on a well-known concept. Runoff accumulates over remote areas and transports colluvial matter over local distances during heavy rain events (*e.g.* Lang et al., 1999). This is linked to the low output of colluvial matter from slopes into river-valley systems (*e.g.* de Moor and Verstraeten, 2008; Houben et al., 2012).

Traditionally it is assumed that distribution of colluvial deposits is linked with the landscape position and especially catchment area (*e.g.* Bork, 1983; Walling 1983). Such regional relationships were reflected in the form of several erosion/deposition models (*e.g.* Dietrich et al., 1995; Follain et al., 2006). In contrast to the regional level the shape of a landform on the local level is considered without taking into account their location in a landscape or catchment. Local landforms are described by the signs of curvatures (*e.g.* Troeh, 1964; Gauss, 1827). Local landforms impact on accumulation of different migrants on the land surface (*e.g.* Sinai et al., 1981; Florinsky et al., 2002) as well as on the spatial distribution of colluvial deposits (Mitusov et al., 2013; 2014).

The importance of local and regional orography is generally understood. For example, one of the first numerical models for simulation of erosion/deposition processes combine both local and regional attributes of the land surface (Mitasova et al., 1997). However, it can be pointed out that in comparison with regional orography the local landforms are often hidden from non instrumental landscape observations. In result, relationships between local landforms described by the signs of curvatures and spatial distribution of colluvial deposits are not well investigated. Hence, objectives of the article are:

- detection of local landforms characterized by colluvial deposits with the largest thickness;
- assessment of the spatial distribution of these local landforms;
- application of local landforms for the assessment of erosion/accumulation status of terrains from a geomorphometric point of view.

2. Study area and methods

2.1. Key areas and digital elevation models

The data on colluvial deposits were obtained from two key areas located in Northern Germany approximately 35 – 40 km south of Kiel (Fig. 1). The key area “Perdoel” is located in the lower part of a dry subcatchment of Lake Belau near the farm Perdoeler Muehle. The key area “Bornhoeved” is located in the upper part of a dry subcatchment of Lake Bornhoeved. The dataset of colluvial deposits consists of 64 points at the key area Perdoel (Fig. 1B) and 71 points at the key area Bornhoeved (Fig. 1C).

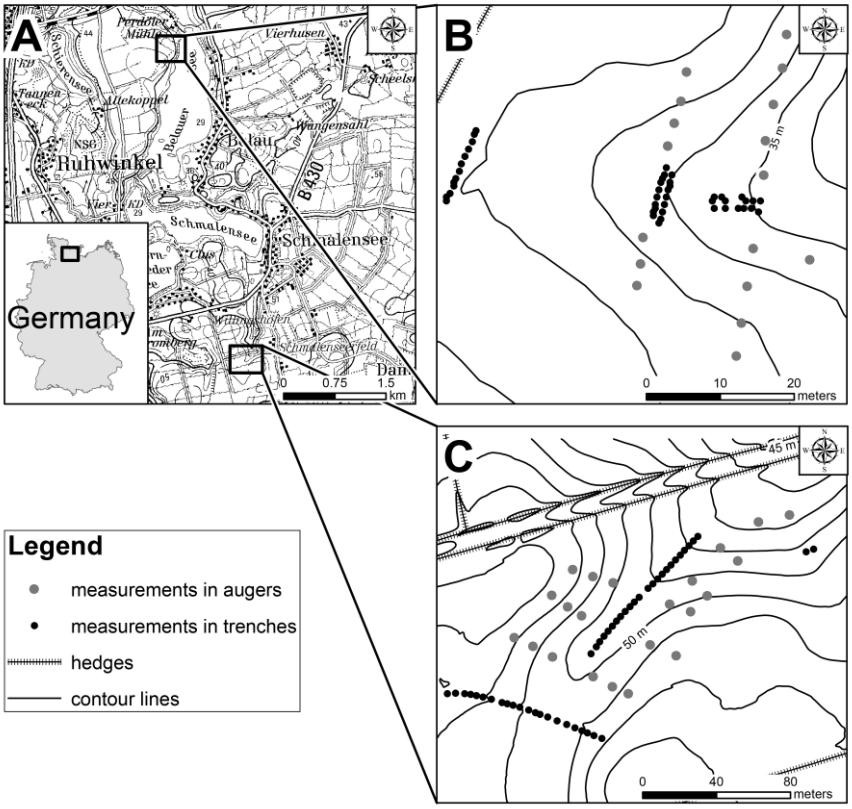

Fig. 1. Locations of the key areas and sampling points. A: Area overview. B: Key area Perdoel. C: Key area Bornhoeved. Contour lines have 1 m vertical interval.

A digital elevation model (DEM) with one meter resolution from the Land Survey Office of State Schleswig-Holstein (Landesvermessungsamt Schleswig-Holstein, 2012) was used during investigations at the key area Perdoel (Mitusov et al., 2013) and surrounding terrain. For the investigations at the key area Bornhoeved a DEM with a resolution of 5 m was prepared based on field measurements by a differential GPS (Mitusov et al., 2014). A terrain around the key area Bornhoved was analysed based on the DEM from Land Survey Office of State Schleswig-Holstein (Landesvermessungsamt Schleswig-Holstein, 2012) that was generalised up to 5 m resolution.

2.2. Morphometric variables

The land surface was described by a set of curvatures and maximal catchment area (*MCA*) considered by Shary et al., (2002). These morphometric variables (MVs) are divided into two groups according to their physical meaning (Table 1). Additionally, based on different calculation methods, curvatures are characterized as local MVs and *MCA* is characterized as a regional MV (*e.g.* Shary, 1995). For the calculation of regional MVs, extended terrain portions have to be taken into account (*e.g.* Tarboton, 1997). For the calculation of curvatures, only a small number of grid cells around a sampling point have to be considered (*e.g.* Shary et al., 2002).

Table 1. Set of morphometric variables (based on Shary et al., 2002).

Variable name, Unit	Description
Morphometric pre-requisites of surface runoff and soil throughflow generation	
Maximal catchment area (*MCA*), m^2	Maximum area from which material moving downslope may be collected
Horizontal (tangential) curvature (*kh*), m^{-1}	Flow convergence/divergence
Vertical (profile) curvature (*kv*), m^{-1}	Relative flow deceleration/acceleration
Difference curvature (*E*), m^{-1}	Compares *kh* (in plan) and *kv* (in profile)
Characteristics of geometrical landforms	
Maximal curvature (*kmax*), m^{-1}	Geometrical ridge forms
Minimal curvature (*kmin*), m^{-1}	Geometrical valley forms
Total Gaussian curvature (*K*), m^{-2}	Separated elliptic and saddle landforms
Mean curvature (*H*), m^{-1}	Connected to "equilibrium" surface condition

The mathematical theory explains statistical relationships among curvatures and links every curvature with physical processes on the land surface (Shary et al., 2002). For the calculation of all MVs, analytical GIS Eco developed by P. Shary was used (Wood, 2009). The maps of basic MVs for the key areas are shown in previous publications (Mitusov et al., 2013; 2014).

2.3. Landforms described by signs of curvatures

The land surface has four main directions (Shary et al., 2002). Two main directions of a surface itself are determined by normal sections with minimal (*kmin*) and maximal (*kmax*) curvatures. The other two main directions are formed by gravity field. The shape of the land surface in section along flow line as well as in perpendicular section is defined by vertical (*kv*) and horizontal (*kh*) curvatures. Other curvatures mainly describe different relationships between these four curvatures. Shary, (1995) developed a theory for the identification of twelve types of main local landforms (MLLFs) by signs of curvatures (Fig. 2). The set of these MLLFs is given in Table 2.

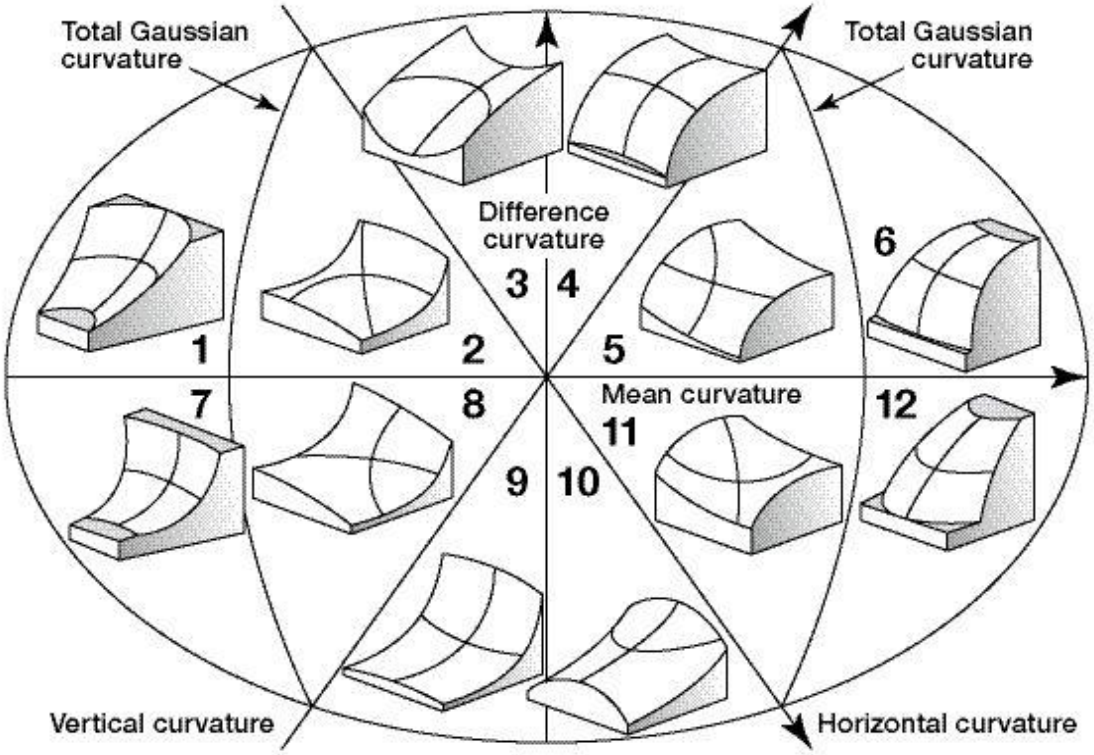

Fig. 2. Distribution of twelve types of main local landforms in coordinates of five curvatures (Shary et al., 2005).

Table 2. Signs of curvatures for identification of twelve types of main local landforms (based on Shary et al., 2005).

N	Title of landform types	*K*	*H*	*kh*	*kv*	*E*	*kmin*	*kmax*
1	C-depressions with positive difference curvature	+	–	–	–	+	–	–
2	C-saddles mean-concave, convergent-decelerating, with positive difference curvature	–	–	–	–	+	–	+
3	C-saddles mean-concave, convergent-accelerating, with positive difference curvature	–	–	–	+	+	–	+
4	C-saddles mean-convex, convergent-accelerating, with positive difference curvature	–	+	–	+	+	–	+
5	C-saddles mean-convex, divergent-accelerating, with positive difference curvature	–	+	+	+	+	–	+
6	C-hills with positive difference curvature	+	+	+	+	+	+	+
7	C-depressions with negative difference curvature	+	–	–	–	–	–	–
8	C-saddles mean-concave, convergent-decelerating, with negative difference curvature	–	–	–	–	–	–	+
9	C-saddles mean-concave, divergent-decelerating, with negative difference curvature	–	–	+	–	–	–	+
10	C-saddles mean-convex, divergent-decelerating, with negative difference curvature	–	+	+	–	–	–	+
11	C-saddles mean-convex, divergent-accelerating, with negative difference curvature	–	+	+	+	–	–	+
12	C-hills with negative difference curvature	+	+	+	+	–	+	+

According to the statistical hypothesis the occurrence of each of the MLLFs has equal probability (≈ 1/12) for a random surface (Shary, 1995). In nature a deviation from this probability depends on the type of terrain. The accumulative MLLFs occur more often within mountainous terrains and less often on flatlands. This can be explained by the development of the land surface under impaction of tectonics in mountains and denudation of local concavities on flatlands. Other properties of the MLLFs are considered by Shary et al., (2005).

The classification of Shary, (1995) can be considered as an extension of the classifications of Troeh, (1964) and Gauss, (1827). The classification of Troeh divides four local landforms based on signatures of *kh* and *kv*; the classification of Gauss divides four local landforms based on signatures of *kmin* and *kmax*. A curvature = 0 is very rare for the land surface. Landforms that include at least one curvature = 0 are entitled as rare local landforms (Shary, 1995). Such rare landforms were not observed in the DEMs used for the investigations.

2.4. Determination of colluvial deposits and statistics

The thickness of colluvial deposits (M) was measured in trenches and auger cores. Locations and depths of trenches were defined so that all sequences of colluvial layers could be investigated at the bottoms of both valleys. Auger cores were distributed on slopes. Sequences and characteristics of individual colluvial layers were described using conventional field methods (Ad-hoc-Arbeitsgruppe Boden, 2005) and considered in previous publications (Dreibrodt et al., 2009; Dreibrodt and Wiethold, *submitted*). The total duration of colluvial deposition at the key area Bornhoved can be assumed as approximately 2800 years and at the key area Perdoel as approximately 3000 years. For the goals of the present article the total thickness of colluvial deposits was analysed.

Statistical properties of the dataset are described in latest publications (Mitusov et al., 2013, 2014.). Quantitative comparisons were determined with the help of the non-parametric rank correlation coefficient of Spearman (r_S) (Spearman, 1904). Correlation coefficients with a significance level (p) of $p > 0.05$ were not considered. The link between MLLFs and the distribution of colluvial deposits was determined based on comparisons of the first, second (median) and third quartiles.

2.5. Determination of the potential function of the main local landforms for processes of erosion or accumulation

The role of MLLFs for processes of soil erosion or colluvial accumulation was determined according to the variability of the thickness of colluvial deposits. For every type of MLLFs the median thickness of colluvium (M_{group}) was calculated. Afterwards, values of M_{group} were compared with the median thickness of colluvium for a whole key area (M_{key}). If M_{group} was equal to or higher than M_{key} such type of MLLFs was accepted as potentially related with the accumulation. These types of MLLFs were denoted by the abbreviation $MLLFs^M$, where "^{M}" stands for colluvial deposits. If M_{group} was smaller than M_{key}, such types of MLLFs were accepted as potentially related with the erosion.

A determination of the role of MLLFs based on material content enables the assessment of geomorphometric prerequisites of these processes on large terrains. For example, outside of the sampling points, $MLLFs^M$ may not contain colluvial deposits at all. However, in case of the activation of erosion and accumulation processes, colluviation will take place at $MLLFs^M$ in the first order.

3. Results

3.1. Statistical properties of the thickness of colluvial deposits

The statistical distribution of the total thickness of colluvial deposits is assessed as abnormal (Mitusov et al., 2013; 2014). Statistical bar charts for the thickness of colluvial deposits vary depending on the key area (Fig. 3). The bar chart of the thickness of colluvial

deposits from the key area Bornhoeved has no well expressed peak in the data. It might be caused by the location of this key area in a relatively flat valley. Thick peaks are clearly visible on the bar chart of the data from the key area Perdoel. Two main peaks within the intervals 49 – 92 cm and 145 – 176 cm are caused by the distribution of sampling points on slopes and at the bottom of the relatively steep valley. The thickness of colluvial deposits in the interval 6 – 27 cm is caused by ploughing.

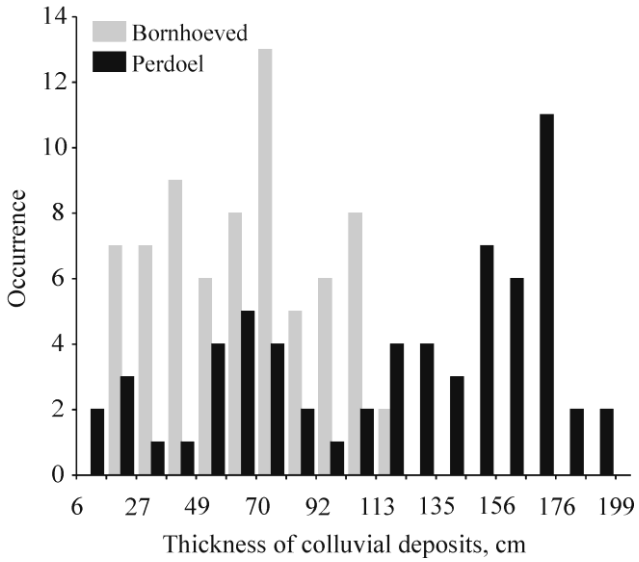

Fig. 3. Statistical distribution of the thickness of colluvial deposits.

3.2. Statistical relationships in dataset

Relationships between the thickness of colluvial deposits and *MCA* are relatively strong and positive: $r_S = 0.69$ at the key area Bornhoeved (Mitusov et al., 2013) and $r_S = 0.85$ at the key area Perdoel (Mitusov et al., 2014). Correlations between the thickness of colluvial deposits and curvatures are visualised in Fig. 4. Signatures of r_S with curvatures indicates a concentration of the thickest colluvial deposits at convergent areas ($kh < 0$) and at the zones of relative deceleration of surface flows ($kv < 0$) with a more twisted section for *kv* in comparison with *kh* ($E > 0$). These land surface portions are characterised by a tendency to concave geometry ($kmin < kmax < 0$) with a more twisted section for *kmin* in comparison with *kmax* ($H < 0$). Correlations with *K* indicate tendency of colluvial thickness increase at saddles ($K < 0$) in comparison with other landforms.

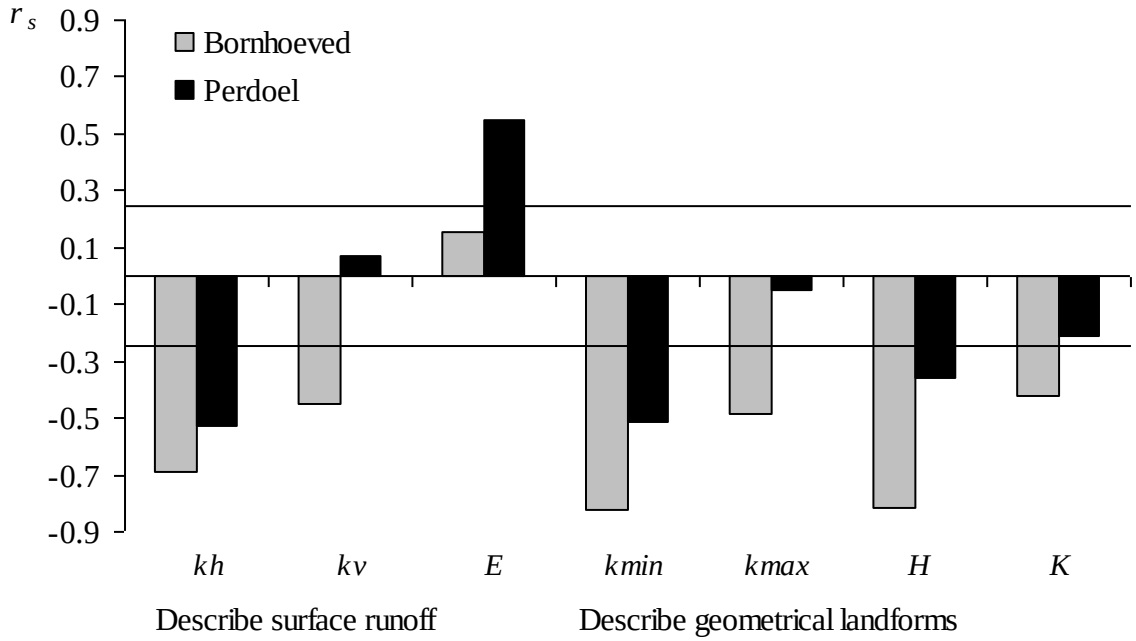

Fig. 4. Spearman correlations (r_S) between total thickness of colluvial deposits and curvatures. Based on data from Mitusov et al., (2013; 2014). The horizontal lines show $p = 0.05$.

3.3. Distribution of the thickness of colluvial deposits at main local landforms

Correlations with curvatures (Fig. 4) indicate that land surface portions with the thickest colluvial deposits can be described by negative and positive curvatures in the same time. Hence, the analysis of spatial distribution of the thickness of colluvial deposits at MLLFs was carried out (Table 3). The types of MLLFs 1, 2, 3 and 8 are characterized by relatively thick colluvial deposits. All these MLLFs have $kmin < kh < 0$. The types of MLLFs 6, 9, 10 and 12 are characterized by relatively thin colluvial deposits. All these MLLFs have $0 < kh < kmax$. These results were the same for both key areas (Table 3). At other MLLFs the thickness of colluvial deposits varies depending on the key area.

Table 3. The thickness of colluvial deposits (cm) at main local landforms.

Type of MLLFs	The key area Bornhoeved				The key area Perdoel			
	n	Q_1	Median	Q_3	*n*	Q_1	Median	Q_3
1	3	69.1	76.3	80.9	8	146.5	169.3	175.0
2	7	88.4	92.0	103.3	7	91.8	133.0	167.3
3	10	67.0	75.2	101.3	18	92.5	160.3	169.8
4	2	55.5	64.4	73.4	8	88.8	146.0	163.6
5	3	26.2	27.0	28.8	2	157.3	162.5	167.8
6	6	27.1	37.2	62.0	5	63.0	83.0	105.5
7	9	77.3	80.7	94.0	4	39.8	82.5	125.0
8	7	66.6	100.7	101.8	2	134.3	140.5	146.8
9	11	48.3	55.0	61.5	4	57.5	65.0	72.3
10	7	34.0	44.0	62.0	3	88.5	109.0	118.0
12	6	27.5	35.5	44.8	3	50.5	80.0	99.8
Entire dataset	71	44.3	67.0	88.3	64	71.1	133.0	136.9

Note: Q_1 and Q_3 – first and third quartiles.

4. Discussion

4.1. Maps of orographic structures related with potential erosion and accumulation

It is expected if colluvial deposits have a strong relationship with orographic structures, then these structures can indicated potential colluvial patterns. In conditions of the key areas, the maps of *MCA* and MLLFs can be used for these purposes. Landforms described by curvatures are not sensitive to landscape position. *MCA* as well as such regional terms as "slope" and "valley" cannot be defined on a local level. Hence, *MCA* is linked to the distribution of colluvial deposits on a regional level (Fig. 5A and C); MLLFs – on a local level (Fig. 5B and D).

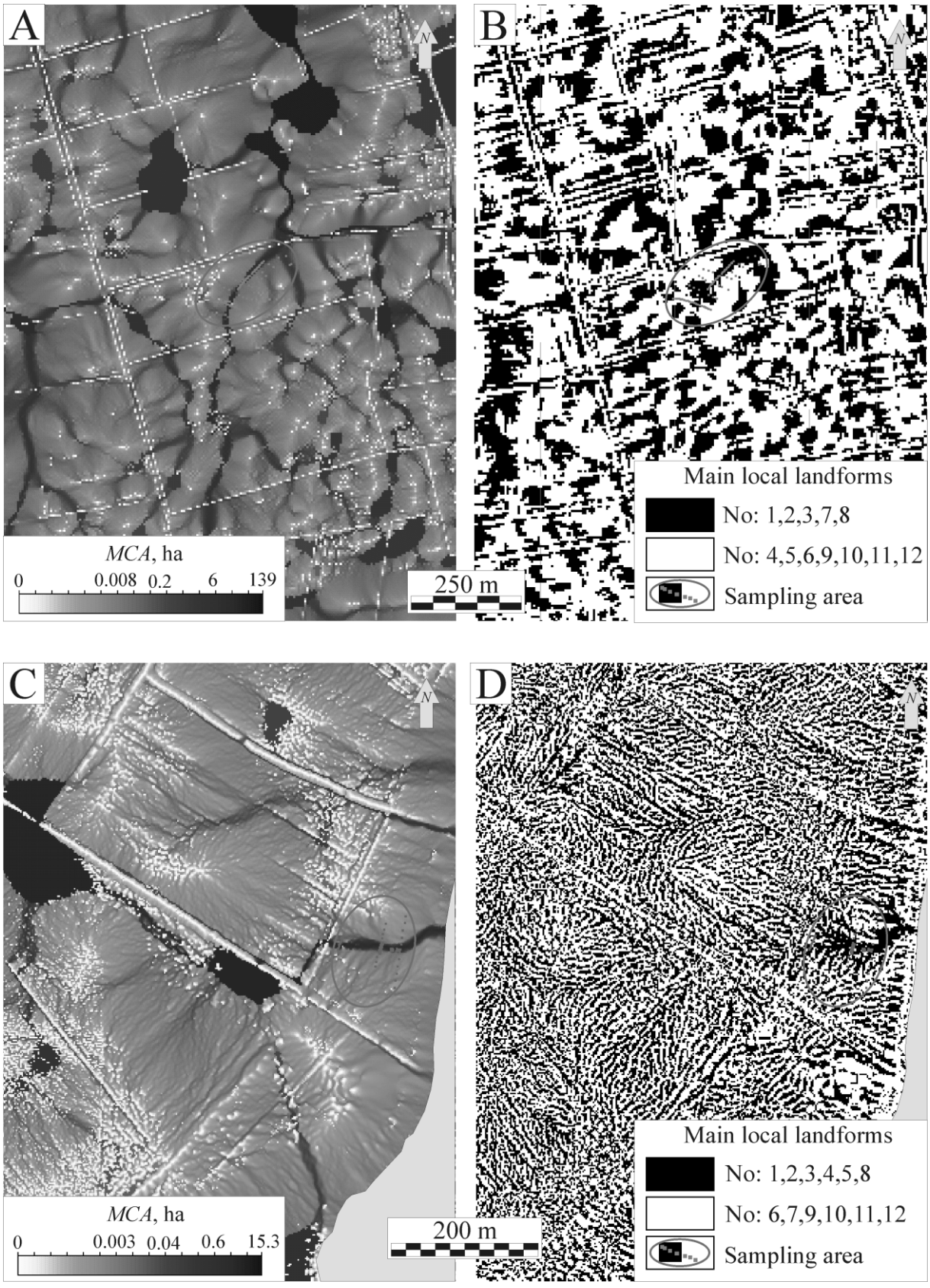

Fig. 5. Land surface portions with potential erosion (light areas) and accumulation (dark areas) on regional (maps of *MCA*) and local (maps of MLLFs) levels. A and B: The key area Bornhoeved, grid spacing 5 m. C and D: The key area Perdoel, grid spacing 1 m.

Relationships with *MCA* show that colluvial deposits are concentrated in areas with high values of *MCA*. High values of *MCA* are observed at valley bottoms and in closed depressions. Hence, light cells of the gridded map of *MCA* show areas with potential soil erosion, dark cells – potential colluvial accumulation (Fig. 5A and C). The space between these areas can be characterised as transit zones on slopes. These areas have no sharp borders because the map of *MCA* represents a continuous surface.

Correlations between colluvium and curvatures (Fig. 4) as well as the distribution of the median thickness of colluvial deposits (Table 3) show that colluvial deposits accumulate on several types of MLLFs. The size of an individual MLLF obligatory coincides with the grid spacing of a DEM. However, most of the MLLFs are incorporated into larger clusters with a systematic spatial structure (Fig. 5B and D). Light clusters indicate areas of potential erosion; dark clusters indicate potential accumulation. The clusters of MLLFs have sharp borders at certain grid spaces. This is caused by the fact that a map of MLLFs represents a discrete surface.

Applications of maps of MVs for the description of the potential pattern of colluvial deposits cannot be considered as an alternative to predictive modelling. However, the predictive properties of MVs are useful in situations of initial data lacks and large distance from samplings. It has to be marked that patterns of local and regional orographic structures coincides only approximately. It is expected because *e.g.*, similar results can be observed at comparisons between maps of *MCA* and *kh* as well. A mathematical theory for the comparison of local and regional orographic structures is not developed. This is the main reason that restricts the investigations in this direction.

4.2. Assessment of potential for erosion and accumulation from geomorphometric point of view

The material content of MLLFs (*e.g.* thickness of colluvium) reflects processes related with these MLLFs (*e.g.* erosion or accumulation). Hence, the size of an area occupied by these MLLFs and/or their occurrence frequency indicates the scale of the related processes. At both key areas several types of local landforms with a large storage of colluvial deposits ($MLLFs^M$) were identified (Table 3). Therefore, an analysis of their occurrence frequency may reflect the erosion/accumulation status of the land surface in sampling points and the surrounding terrain.

It is assumed that the occurrence of $MLLFs^M$ at the level of 50 % indicates equilibrium between potential erosion and potential accumulation. The occurrence frequency of $MLLFs^M$ at sampling points at both key areas is more than 50 % (Fig. 6). It indicates the domination of accumulative processes at sampling points on the local level. This coincides with the positive correlation between the thickness of colluvium and *MCA*, which indicates the domination of accumulative processes in sampling points on the regional level as well. The occurrence of $MLLFs^M$ in the areas around sampling points is stable at approximately 40 % and is not sensitive to the size of terrain around the key areas (Fig. 6). These results show a potential domination of erosion processes around the key areas on the local level.

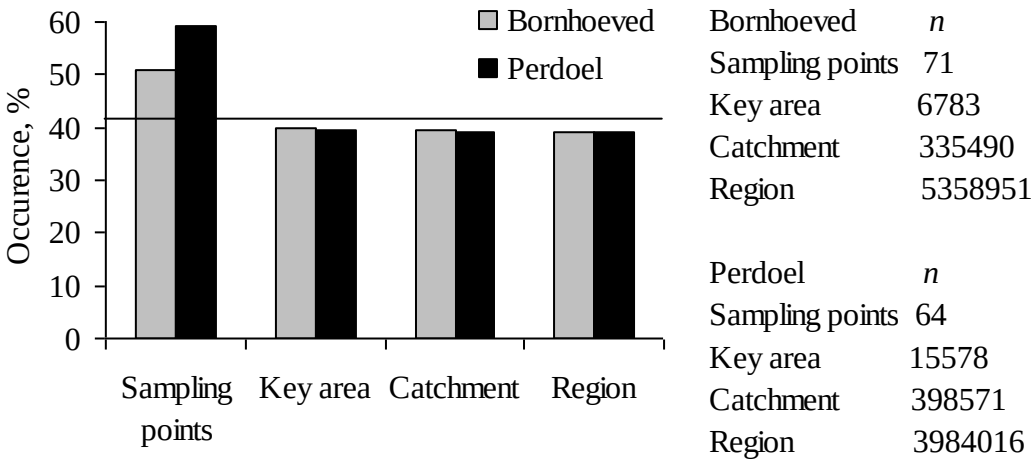

Fig. 6. The occurrence frequency of the group of main local landforms with colluvial deposits thicker than the median for a whole key area ($MLLFs^M$). The horizontal line shows the theoretical occurrence frequency of $MLLFs^M$ (= 41.67 %). *n* is the number of points in the dataset.

Based on the occurrence frequency of MLLFs it is possible to determine either potential domination of soil erosion or colluvial accumulation on large areas. However, a direct comparison of the occurrence frequency does not indicate the intensity of these processes. Therefore experimental results have to be compared with the theoretical distribution of MLLFs for a random surface. The random surface is free of traces of any systematic process. Activation of erosion or accumulation processes on such surface will increase the number of MLLFs related with the dominant process. Hence, the more the deviation between random and natural surfaces, the more intensive the backbone process is manifested.

Five types of MLLFs are related to colluvial accumulation at the key areas. The theoretical occurrence frequency of this number of MLLFs is 41.67 % (probability 5/12). The maximal difference from this level was observed for data from sampling points of Perdoel. It shows an intensive transformation of the land surface due to accumulation. At sampling points of Bornhoeved, the land surface transformation is also caused by accumulation and its intensity can be assessed as medium. For the surrounding terrains the little differences between the experimental and theoretical occurrence frequency of $MLLFs^M$ were determined. It is shown that processes of land surface transformation were caused by erosion of low intensity.

5. Conclusions

Correlations indicate that colluvium concentrates at landforms described by a complex combination of signatures of curvatures. Such landforms were quantitatively described by Shary's classification (Shary, 1995). This classification divides the land surface into twelve MLLFs. The distribution of quartiles of the thickness of colluvium divides MLLFs in two groups characterized by relatively thick and thin deposits. Thus the potential role of the MLLFs in spatial distribution of colluvial deposits was determined. In the present investigation, approximately 40 % of the terrain around the key areas is covered by $MLLFs^M$

which potentially store colluvial deposits. Other MLLFs, covering approximately 60 % of the terrain, can be considered as zones of potential erosion. This proportion reflects that a terrain around the key areas is potentially characterized by the domination of weak erosion processes. The intensity of landform modifications can be assessed according to differences between the occurrence frequency of MLLFs on natural and random surfaces.

Finally, it was shown that the occurrence frequency of MLLFs is a quantitative criterion for the assessment of domination and intensity of processes of land surface transformation. This pure geomorphometric criterion is free of any subjective manipulations and can be used for the comparison of different terrains.

Acknowledgements

The investigation was financially supported by the Graduate School "Human Development in Landscapes" of Christian-Albrechts University Kiel. I would like to thank my colleagues Stefan Dreibrodt, Hans-Rudolf Bork, Iraj Emadodin, Jann Wendt, Svetlana V. Khamnueva, and Olga E. Mitusova, for useful research discussions.

References

Ad-hoc-Arbeitsgruppe Boden (Ed.), 2005. Bodenkundliche Kartieranleitung, 5th edition. Bundesanstalt für Geowissenschaften und Rohstoffe in Zusammenarbeit mit den Staatlichen Geologischen Diensten, Hannover. 438 p.

Bork, H.-R., 1983. Die holozäne Relief- und Bodenentwicklung in Löβgebieten. Catena Suppl. 3, 1–93.

Brown, A.G., 2009. Colluvial and alluvial response to land use change in Midland England: An integrated geoarchaeological approach. Geomorphology 108, 92–106.

de Moor, J.J.W., Verstraeten, G., 2008. Alluvial and colluvial sediment storage in the Geul River catchment (The Netherlands) – Combining field and modelling data to construct a Late Holocene sediment budget. Geomorphology 95, 487–503.

Dietrich, W.E., Reiss, R., Hsu, M.-L., Montgomery, D.R., 1995. A process-based model for colluvial soil depth and shallow landsliding using digital elevation data. Hydrol. Process. 9 (3-4), 383–400.

Dotterweich, M., 2008. The history of soil erosion and fluvial deposits in small catchments of central Europe: Deciphering the long-term interaction between humans and the environment — A review. Geomorphology 101, 192–208.

Dreibrodt, S., Lubos, C., Terhorst, B., Damm, B., Bork, H.-R., 2010. Historical soil erosion by water in Germany: Scales and archives, chronology, research perspectives. Quaternary International 222, 80–95.

Dreibrodt, S., Nelle, O., Lütjens, I., Mitusov, A., Clausen, I., Bork, H.-R., 2009. Investigations on buried soils and colluvial layers around Bronze Age burial mounds at

Bornhöved (Northern Germany): an approach to test the hypothesis of "landscape openness" by the incidence of colluviation. The Holocene 19, 487–497.

Dreibrodt, S., Wiethold, J., *submitted*. Lake Belau and its catchment (northern Germany) – a northern central Europe key site of human impact on the landscape since the onset of agriculture. The Holocene.

Florinsky, I.V., Eilers, R.G., Manning, G., Fuller, L.G., 2002. Prediction of soil properties by digital terrain modelling. Environmental Modelling and Software 17, 295–311.

Follain, S., Minasny, B., McBratney, B.A., Walter, C., 2006. Simulation of soil thickness evolution in a complex agricultural landscape at fine spatial and temporal scales. Geoderma 133, 71–86.

Gauss, C.F., 1827. Disquisitiones generales circa area superficies curvas. Gott. Gel. Anz. 177, S1761–S1768 (in Latin).

Houben, P., 2012. Sediment budget for five millennia of tillage in the Rockenberg catchment (Wetterau loess basin, Germany). Quaternary Science Reviews 52, 12–23.

Landesvermessungsamt Schleswig-Holstein, 2012. http://www.schleswig-holstein.de/LVERMGEOSH/DE/LVERMGEOSH_node.html.

Lang, A., 2003. Phases of soil erosion-derived colluviation in the loess hills of South Germany. Catena 51, 209–221.

Lang, A., Hönscheidt, S., 1999. Age and source of colluvial sediments at Vaihingen–Enz, Germany. Catena 38(2), 89–107.

Mitasova, H., Mitas, L., Brown, W.M., Johnston, D., 1997. GIS tools for erosion/deposition modeling and multidimensional visualization. Part IV: Processed based erosion simulation for spatially complex conditions and its applications to installations. Part V: Impact of transport capacity and terrain structures on erosion simulations. Report for USA CERL. Urbana-Champaign: University of Illinois, 30 p. Website: http://www4.ncsu.edu/~hmitaso/gmslab/reports/cerl97/rep97.html]

Mitusov, A.V., Dreibrodt, S., Mitusova, O.E., Khamnueva, S.V., Bork, H.-R., 2013. Detection of land surface memory by correlations between colluvial deposits and morphometric variables. Geomorphology 191, 109–117.

Mitusov, A.V., Mitusova, O.E., Wendt, J., Dreibrodt, S., Bork, H.-R., 2014. Correlation of colluvial deposits with modern land surface and problem of slope profile description. Geomorphology 220, 30–40.

Shary, P.A., 1995. Land Surface in Gravity Points Classification by a Complete System of Curvatures. Mathematical Geology 27 (3), 373–390.

Shary, P.A., Sharaya, L.S., Mitusov, A.V., 2002. Fundamental quantitative methods of land surface analysis. Geoderma 107, 1–35.

Shary, P.A., Sharaya, L.S., Mitusov, A.V., 2005. The problem of scale-specific and scale-free approaches in geomorphometry. Geografia Fisica e Dinamica Quaternaria. Volume devote to 32 International Geological Congress (December, 2005). 28 (1), 81–101.

Sinai, G., Zaslavsky, D., Golany, P., 1981. The effect of soil surface curvature on moisture and yield-Beer Sheba observations. Soil Science 132, 367–375.

Spearman, C., 1904. The Proof and Measurement of Association between Two Things, The American journal of Psychology 15 (1), 72–101.

Tarboton, D.G., 1997. A new method for the determination of flow directions and upslope areas in grid digital elevation models. Water Resources Research 30, 9–17.

Troeh, F.R., 1964. Landform parameters correlated to soil drainage. Soil Science Society of America Proceedings 28, 808–812.

Walling, D.E., 1983. The sediment delivery problem. Journal of Hydrology 65, 209–237.

Wood, J., 2009. Overview of software packages used in geomorphometry. In: T. Hengl and H.I. Reuter (Eds.). Geomorphometry: Concepts, Software, Applications. Developments in Soil Science, Volume 33. Amsterdam, etc.: Elsevier, Chapter 10, pp. 257–267.